

MAX PLANCK INSTITUTE
FOR POLYMER RESEARCH



Interaction of anti-PEG antibodies with PEG and their presence in the protein corona

Dissertation

Zur Erlangung des Grades

„Doktor der Naturwissenschaften“ (Dr. rer. nat.)

im Promotionsfach Chemie

am Fachbereich Chemie, Pharmazie, Geographie und Geowissenschaften
der Johannes Gutenberg-Universität in Mainz



JOHANNES GUTENBERG
UNIVERSITÄT MAINZ

Mareike Deuker

geb. in Wiesbaden

Mainz, 2023

DekanIn:

1. GutachterIn:
2. GutachterIn

Tag der mündlichen Prüfung:

Die vorliegende Arbeit wurde im Zeitraum von Oktober 2019 bis Juni 2023 am Max-Planck-Institut für Polymerforschung in Mainz im Arbeitskreis von Prof. Dr. Katharina Landfester angefertigt. Ich versichere, die vorliegende Arbeit selbstständig angefertigt zu haben. Alle verwendeten Hilfsmittel und Quellen habe ich eindeutig als solche kenntlich gemacht. Weder die vorliegende Arbeit noch Teile davon wurden bei einer anderen Fakultät bzw. einem anderen Fachbereich als Dissertation eingereicht.

Mainz, den

Mareike Deuker

Abstract

Nanomedicine is a field of research that has gained increasing importance over the last decades. In particular, nanocarriers (NCs) are a promising approach for efficient and targeted drug delivery. One major challenge is the sufficient blood circulation time of the NCs. Once NCs enter the bloodstream, proteins accumulate on the surface, forming a so-called protein corona, and determining the further course of the NCs. The current gold standard for reducing unspecific protein adsorption and prolonging circulation time in the body is the attachment of poly(ethylene glycol) (PEG). The polymer provides a stealth effect so that the NC is recognized less by the immune system and can circulate for a longer time. However, antibodies specifically directed against PEG were identified in recent years. An increasing prevalence of these anti-PEG antibodies was described and their presence correlated with reduced efficacy and, in some cases, severe allergic reactions to PEGylated therapeutics. Nevertheless, the presence of anti-PEG antibodies in the protein corona and their effect on the cellular uptake of PEGylated NCs have not been investigated yet. Therefore, we studied the pre-existing anti-PEG antibodies in healthy individuals, their accumulation in the protein corona of PEGylated NCs, and their impact on cellular uptake behavior.

First, we examined the distribution of the antibodies in the German population and revealed a high prevalence across all age groups. Afterwards, the binding behavior of anti-PEG antibodies was investigated. The analysis revealed strong and specific binding to long-chain PEG, with the binding strength decreasing with decreasing chain length. Characterization of the protein corona of different NC systems showed a significant accumulation of anti-PEG antibodies on the surface of PEGylated NCs compared to non-PEGylated. Finally, we monitored the cellular uptake of PEGylated NCs in macrophages. With increasing anti-PEG antibody concentration in the protein corona, the cellular uptake increased steadily.

In conclusion, the anti-PEG antibodies in the protein corona could mitigate the stealth effect of PEG, leading to accelerated blood clearance and undesirable side effects. Following our results, the existence of anti-PEG antibodies in patients' blood needs to be accounted for when designing new nanocarrier-based therapies.

Zusammenfassung

Die Nanomedizin ist ein Forschungsgebiet, das in den letzten Jahrzehnten zunehmend an Bedeutung gewonnen hat. Insbesondere Nanocarrier (NC) sind ein vielversprechender Ansatz für die effiziente und gezielte Verabreichung von Wirkstoffen. Eine große Herausforderung ist die ausreichende Blut-Zirkulationszeit der NC. Sobald die NC in den Blutkreislauf gelangen, reichern sich Proteine auf der Oberfläche an und bilden eine sogenannte Proteinkorona, die das weitere Schicksal der NC bestimmt. Der derzeitige Goldstandard zur Verringerung unspezifischer Proteinadsorption und zur Verlängerung der Zirkulationszeit ist die Anbringung von Poly(ethylenglykol) (PEG). Das Polymer sorgt für einen sogenannten „Stealth“-Effekt, so dass der NC vom Immunsystem weniger erkannt wird und besser im Körper zirkulieren kann. Allerdings wurden in den letzten Jahren Antikörper identifiziert, die spezifisch gegen PEG gerichtet sind. Eine zunehmende Prävalenz dieser anti-PEG-Antikörper wurde beschrieben und ihr Vorhandensein mit einer verminderten Wirksamkeit und teilweise schweren allergischen Reaktionen auf PEGylierte Therapeutika in Verbindung gebracht. Trotzdem wurde das Vorhandensein von anti-PEG-Antikörpern in der Proteinkorona und deren Auswirkung auf die zelluläre Aufnahme von PEGylierten NC noch nicht untersucht. Daher wurden die bereits existierenden anti-PEG-Antikörper bei gesunden Personen, ihre Anreicherung in der Proteinkorona von PEGylierten NC und ihre Auswirkungen auf das zelluläre Aufnahmeverhalten untersucht. Zunächst wurde die Verteilung der Antikörper in der deutschen Bevölkerung ermittelt, wobei eine hohe Prävalenz in allen Altersgruppen festgestellt wurde. Anschließend wurde das Bindungsverhalten der Anti-PEG-Antikörper bestimmt. Die Analyse ergab eine starke und spezifische Bindung an langkettiges PEG, wobei die Bindungsstärke mit abnehmender Kettenlänge abnahm. Die Charakterisierung der Proteinkorona verschiedener NC-Systeme zeigte eine signifikante Anreicherung von Anti-PEG-Antikörpern auf der Oberfläche von PEGylierten NC. Schließlich wurde die Aufnahme von PEGylierten NC in Makrophagen untersucht. Mit steigender Anti-PEG-Antikörperkonzentration in der Proteinkorona nahm die zelluläre Aufnahme stetig zu. Folglich könnten die anti-PEG-Antikörper in der Proteinkorona den Stealth-Effekt von PEG abschwächen, was zu einer beschleunigten Ausscheidung im Blutkreislauf und unerwünschten Nebenwirkungen führt. Nach unseren Ergebnissen muss die Existenz von Anti-PEG-Antikörpern im Blut von Patienten bei der Entwicklung neuer Therapien auf der Basis von NC berücksichtigt werden.

Table of Contents

Abstract	i
Zusammenfassung	iii
1 Motivation	9
2 State of the Art	11
2.1 Nanocarriers for biomedical applications	11
2.2 Interaction with blood	12
2.3 PEGylation	16
2.4 Immune system and anti-PEG antibodies	18
3 Methods	25
3.1 Enzyme-linked immunosorbent assay.....	25
3.2 Microscale thermophoresis	27
3.3 Pierce assay	29
3.4 Liquid chromatography-mass spectrometry.....	29
4 Results and Discussion	31
4.1 Anti-PEG antibody quantification.....	31
4.1.1 ELISA development and optimization.....	32
4.1.2 Plasma screening among the German population	34
4.1.3 Conclusion	38
4.2 Binding characterization of anti-PEG antibody to soluble PEG.....	39
4.2.1 Competitive ELISA	39
4.2.2 Microscale thermophoresis	40
4.2.3 Fluorescence correlation spectroscopy	43

4.2.4	Conclusion	45
4.3	Detection of anti-PEG antibodies in the protein corona	46
4.3.1	NC properties	47
4.3.2	Protein corona analysis	49
4.3.3	Anti-PEG antibody quantification	53
4.3.4	Conclusion	57
4.4	Effect of anti-PEG antibodies in the protein corona on cell uptake.....	58
4.4.1	Defined protein corona	58
4.4.2	Uptake in RAW macrophages and THP-1 cells	59
4.4.3	Conclusion	64
5	Experimental.....	65
5.1	Materials.....	65
5.1.1	Proteins and cell uptake reagents	65
5.1.2	Other reagents	66
5.2	Methods and Instrumentation.....	67
5.2.1	Enzyme linked immunosorbent assay (ELISA).....	67
5.2.2	Microscale thermophoresis	68
5.2.3	Fluorescence correlation spectroscopy	68
5.2.4	Dynamic light scattering (DLS).....	69
5.2.5	Transmission electron microscopy (TEM)	69
5.2.6	Zeta potential measurements.....	69
5.2.7	Pierce assay	70
5.2.8	Liquid chromatography-mass spectrometry (LC-MS).....	70
5.2.9	Flow cytometry	71
5.3	Anti-PEG antibody quantification by ELISA	71
5.4	Binding characterization of anti-PEG antibody to soluble PEG.....	72
5.4.1	Competitive ELISA	72
5.4.2	Microscale thermophoresis	72
5.4.3	Fluorescence correlation spectroscopy	72

5.5	Detection of anti-PEG antibodies in the protein corona	73
5.5.1	Synthesis of silica nanocapsules (SiNCs)	73
5.5.2	Synthesis of polystyrene nanoparticles (PS-NPs).....	74
5.5.3	Protein corona analysis	74
5.5.4	FACS for protein corona analysis.....	75
5.5.5	ELISA protein corona	75
5.6	Effect of anti-PEG antibodies in the protein corona on cell uptake.....	76
5.6.1	Protein corona preparation.....	76
5.6.2	Cell culture.....	76
5.6.3	THP-1 macrophage differentiation	76
5.6.4	Cell uptake experiments and flow cytometry measurements	77
5.6.5	Cell blocking experiments with antibodies.....	77
5.6.6	Cytokine assay	77
6	Summary and Outlook.....	79
7	List of Abbreviations	83
8	References.....	85
	Appendix.....	v
	Acknowledgments.....	v
	Curriculum Vitae.....	vii

1 Motivation

The idea of using nanomaterials for diagnoses and treating diseases has driven biomedical research for decades. When fighting severe diseases like cancer, finding the right drug is not the only challenge. Systemic exposure to toxic drugs often causes many unwanted side effects. Additionally, to ensure appropriate dosage in the target area, often high amounts of the drug need to be administered.¹

To overcome these challenges, drug delivery is a promising approach. Nanotechnology has revolutionized conventional therapeutic and diagnostic procedures by taking advantage of the unique physicochemical properties of nanocarriers (NCs) such as their small size and large surface area.^{2,3} By incorporating drugs into NCs, several advantages can be achieved. The drug and the body are protected from each other, preventing degradation of the drug by metabolism and systemic exposure to the drug to minimize side effects.⁴ Additionally, when specific targeting is realized, it ensures that the full dosage can reach the target side.⁵

Despite the great properties and potential, only a few NC systems have been approved by the FDA and are available on the market. Nanomedicine still faces many challenges in the process of clinical translation. Besides the active targeting, the circulation time of the NC is crucial for its successful therapy. When a NC enters the blood stream, proteins and biomolecules adsorb on the surface and form the so-called protein corona.^{6,7} The protein corona shapes the biological identity of the NC and determines the fate *in vivo*. Depending on which type of proteins adsorb, they can both increase the circulation time or accelerate the blood clearance. One common method to enhance the circulation time is the attachment of a specific polymer named poly(ethylene glycol) (PEG) to the NC.^{8,9} PEG ensures that mainly proteins of the dysopsonin class bind to the NC surface, which provide a so-called stealth effect. They “mask” the NC by reduction of unspecific protein adsorption so that it is not recognized by the immune system as a foreign compound and can circulate unimpeded.¹⁰

PEGylation was considered the gold standard for improving the circulation time. However new challenges are emerging. Even though PEG is considered highly biocompatible, antibodies specifically directed against PEG exist.¹¹ Those so-called anti-PEG antibodies were first described in 1983, but were considered to be of no clinical significance due to

their low observed prevalence.¹² Still in 2005, many researchers were not convinced of the relevance of anti-PEG antibodies and claimed that “no one has ever reported the generation of antibodies to PEG under routine clinical administration of PEGylated proteins.”¹³ Nevertheless, increasing prevalence of anti-PEG antibodies in the general population as well as the structure of the antibody-PEG complex were described in the last years.¹⁴⁻¹⁹ This increased prevalence might be due to the ubiquitous use of PEG in consumer products like cosmetics and processed food.²⁰ Additionally, the Pfizer-BioNTech or Moderna COVID-19 vaccines contain mRNA loaded into lipid nanoparticles (LNP), which are stabilized by PEGylated lipids.²¹ Thus, the generation of anti-PEG antibodies might become even more relevant now after the COVID-19 pandemic and the widespread administration of PEGylated vaccines.

The presence of anti-PEG antibodies has been correlated with the reduced efficacy of PEGylated therapeutics in clinical trials. Various research groups observed that the administration of repeated doses of PEGylated NCs led to an accelerated blood clearance and weakened efficacy of PEGylated therapeutics.²²⁻²⁴ Additionally, acute severe allergic reactions were observed in some cases.

Regardless of the potentially serious consequences of circulating anti-PEG antibodies, their impact on the effect of NC therapeutics and related side effects remains uncertain up to now. Neither the prevalence nor the concentration of pre-existing anti-PEG antibodies among the general population are well known so far.¹¹ Furthermore, anti-PEG antibodies could potentially become enriched in the protein corona of PEGylated NCs depending on their presence in blood plasma, and induce unwanted side effects as described earlier. Accordingly, anti-PEG antibodies in the protein corona are likely to be an important factor for the fate of the NCs *in vivo*.²⁵ To address this question, we investigated the prevalence of anti-PEG antibodies in healthy individuals, examined their presence in the protein corona of PEGylated NCs, and studied their influence on cellular uptake.

2 State of the Art

2.1 Nanocarriers for biomedical applications

The National Nanotechnology Initiative of the U.S. Government (NNI) defines nanotechnology as research and development at the atomic, molecular, or macromolecular scale.²⁶ Nanomaterials are developed in different forms and shapes with dimensions on a scale of 1-100 nm and exhibit novel properties compared to the bulk material because of their small size.

NCs are a potentially useful tool for medical applications because they could interact at the cellular level in a controlled way. One promising approach in the field of nanomedicine is the use for diagnostic purposes for example as an imaging agent.^{27, 28} Furthermore, the idea of NCs as drug delivery system was already investigated in the 70s.^{29, 30} First, single macromolecules were used to couple drugs covalently, now larger colloidal systems of assembled polymers or crosslinked materials are being established.

Colloidal drug delivery systems are most commonly developed to guide drugs to the desired location in the body while avoiding systemic side effects. By encapsulating, the drug is likewise protected from degradation before it reaches the target location and the circulation time in the blood stream can be prolonged.⁴ Sufficient circulation time *in vivo* is necessary for efficient targeting and high bioavailability. For example, highly lipophilic drugs and drugs that are not stable in biological environments like proteins or nucleic acids can be delivered via encapsulation.³¹ Additionally, potentially toxic drugs can be incorporated into the nanomaterial to avoid unwanted interactions with the organism during the transport in the body and therefore minimize systemic side effects.

For guiding the NCs to a specific location, passive or active targeting strategies can be used. Passive targeting relies on the enhanced-permeation-and-retention (EPR) effect in tumor tissues whereas active targeting requires a certain functional structure attached to the carrier, which “addresses” a recognizing structure in the body.⁵ The idea of active targeting was already predicted by Paul Ehrlich over 100 years ago. He described a “magic bullet”

concept where in theory drugs go straight to their intended cell-structural targets yet remain harmless in healthy tissues.³²

Nowadays many different NCs are developed, each exhibiting advantages and disadvantages. The transported drug can be dissolved, entrapped, encapsulated, or attached to a NC matrix depending on the method of preparation.³³ Overall, the use of colloidal drug delivery systems can improve the performance of conventional drugs, prolong the circulation time, guide the drug to a specific location, protect the cargo, and suppress unspecific interactions with cellular components.

2.2 Interaction with blood

Once NCs are administrated into the body, they are modified by the interaction with the biological environment. In more detail, due to the high surface energy of the NCs, plasma proteins and other biomolecules adsorb on the surface and form a so-called protein corona.^{6, 7} The protein corona influences the properties and behavior of the NCs within the body tremendously. The NCs' former chemical identity is substituted by a biological identity.^{34, 35}

Size, shape, surface charge, and functionalization as well as polymer material and stabilization agent determine the chemical identity of the carrier.¹⁰ These surface properties in turn affect the type and binding affinity of the proteins. The relevant forces for the interactions are Van der Waals forces, hydrogen bonds, hydrophobic and electrostatic interactions. These forces influence the interaction of the proteins with the surface and can lead to conformational changes or denaturation and consequently change the activity and recognition of the proteins.³⁶ The new biological identity given by the adsorbed proteins determines the fate and physiological response of the NC *in vivo* (**Figure 1**).

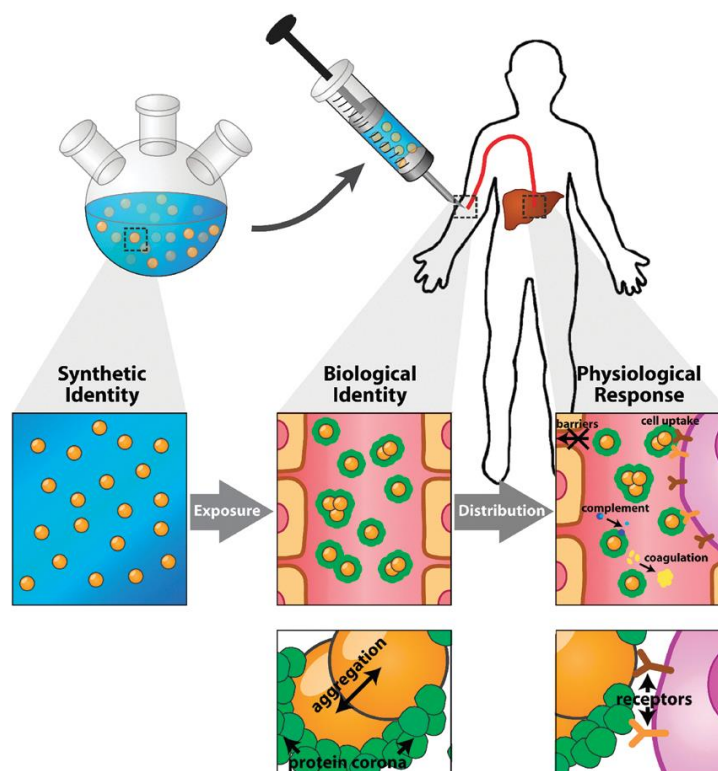


Figure 1. The chemical identity of the NC is replaced by a biological identity due to the adsorbed proteins. The formed protein corona is accountable for the physiological response. Reprinted with permission from reference ³⁴. Published by The Royal Society of Chemistry. Copyright © 2012.

The process of protein corona formation is a competition between different proteins. Upon first contact with blood plasma, highly abundant proteins predominately surround the NCs and adsorb onto their surface. However, these proteins do not necessarily show the highest affinity to the material. Over time, less abundant proteins with a higher affinity are likely to substitute the initially adsorbed proteins with lower affinity. This dynamic competitive adsorption is known as the “Vroman Effect”.³⁷ It is a kinetically driven effect and describes why the abundance of certain proteins in the protein corona is not necessarily proportional to their abundance in the blood.³⁸ The result is a dynamic cloud of proteins around the NC with more tightly bound proteins near the surface (“hard protein corona”) and loosely bound proteins in the outer layer (“soft protein corona”).³⁴ These proteins near the surface are considered irreversibly bound and are stable enough to not be interrupted during experimental procedures like centrifugation.^{39, 40}

The protein coronas on different nanomaterials can be complex and variable. The complete plasma proteome is expected to contain as many as 3700 proteins. Approximately 50 have been identified in association with various nanoparticles.^{10,41} An important class of proteins are opsonins. They include extracellular proteins such as complement factors or immunoglobulins (Ig) that trigger an immune response. Opsonins act as markers that identify objects to be "eaten" by macrophages.⁴² In contrast, dysopsonins such as human serum albumin and various apolipoproteins promote prolonged circulation in the bloodstream.^{10, 43}

The types and amount of proteins that form the protein corona strongly depend on the NC. Material parameters like size, surface chemistry, or charge influence the protein binding as well as environmental parameters like incubation time or temperature and pH value (**Figure 2**). For example, hydrophobic NCs attract more proteins than hydrophilic ones. In addition, lipophilic proteins like most dysopsonins tend to be highly present in the protein corona of hydrophobic NCs.^{44,45} An example of the influence on opsonins is the interaction with immunoglobulins. NCs with a neutral surface charge exhibit less unfavorable interactions with immunoglobulins compared to cationic ones.⁴⁶ Moreover, adsorption of IgG on charged NCs results in significant aggregation.⁴⁷ Furthermore, a high concentration of IgG in plasma leads to a significantly higher fraction of IgG in the respective protein corona, resulting in an increased uptake in human and murine macrophages *via* F_c-receptor mediated endocytosis. This enrichment can be overcome by pre-coating the NC with high-affinity stealth proteins like clusterin.⁴⁸

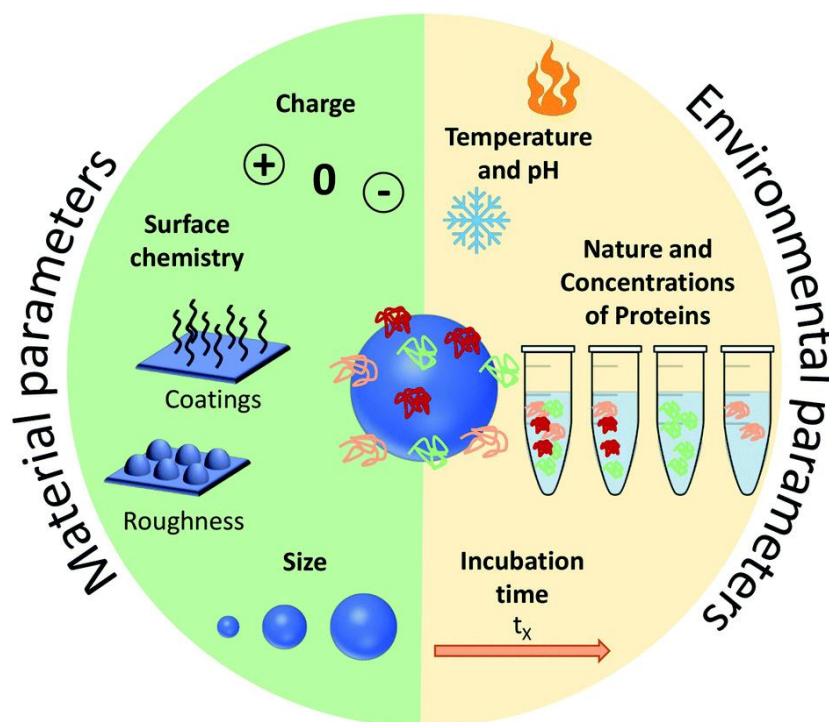


Figure 2. Schematic representation of the main parameters influencing the protein corona formation. Reprinted with permission from reference ⁴⁹. Published by The Royal Society of Chemistry. Copyright © 2021. This open access article is licensed under CC-BY-3.0.

Sufficient circulation time in the bloodstream is crucial for successful NC therapy, enabling efficient targeting and high bioavailability. However, when administered into the blood, NCs can be rapidly opsonized and degraded by phagocytic cells before reaching their target site. Despite the great advantages of drug delivery systems and the wide variety of applicable NCs, a major limitation is still that proteins are adsorbed upon contact with the biological environment, altering their synthetic identity and affecting their final fate and efficacy at the target site. It has been proposed to modify the surface of NCs to prevent interaction with plasma proteins, but protein adsorption cannot be completely suppressed.⁵⁰ The interaction between NCs and individual proteins may be reduced or promoted based on the design of the NC. For a prolonged circulation time, the goal is to reduce opsonin adsorption and therefore prevent unspecific uptake in macrophages. This is usually referred to as the ‘stealth’ effect, i.e. being almost undetectable by the immune system.⁵¹ The attachment of poly(ethylene glycol) chains is a common method to reduce overall protein adsorption and prolong the circulation time in blood. PEG is an attractive material to reduce

opsonization because it is uncharged, hydrophilic, and non-immunogenic.⁸ Accordingly, PEGylated drugs and NCs show longer blood half-lives and less non-specific cellular uptake compared to unmodified drugs.^{52, 53} PEGylation can be achieved via adsorption, grafting, or entrapment methods. It has become the means of choice for improving the stealth effect of NCs.³¹

2.3 PEGylation

Poly(ethylene glycol) can be formed by a process of linking repeating units of ethylene glycol to form polymers with linear or branched shapes of different molecular masses.¹³ A variety of chemical modifications can be used to prepare PEG derivatives. The end-group is especially important to insert functional groups to modify further reactivity.

PEGylation is the process by which PEG chains are attached to proteins, peptide drugs, or NCs.⁵⁴ PEGylation of NCs can be achieved in different ways: (1) PEG physically adsorbs on the NC by electrostatic or hydrophobic interaction; (2) PEG is covalently grafted onto the surface by forming a covalent bond; (3) PEG can be conjugated with hydrophobic chains and thus be applied as a surfactant or for the formation of self-assembled carriers.⁵⁵ For our NC systems we achieved PEGylation via the non-covalent approach with a PEG-based surfactant Lutensol®. It is based on a C₁₆-C₁₈ fatty alcohol as lipophilic part and PEG as hydrophilic part (**Figure 3(3)**).

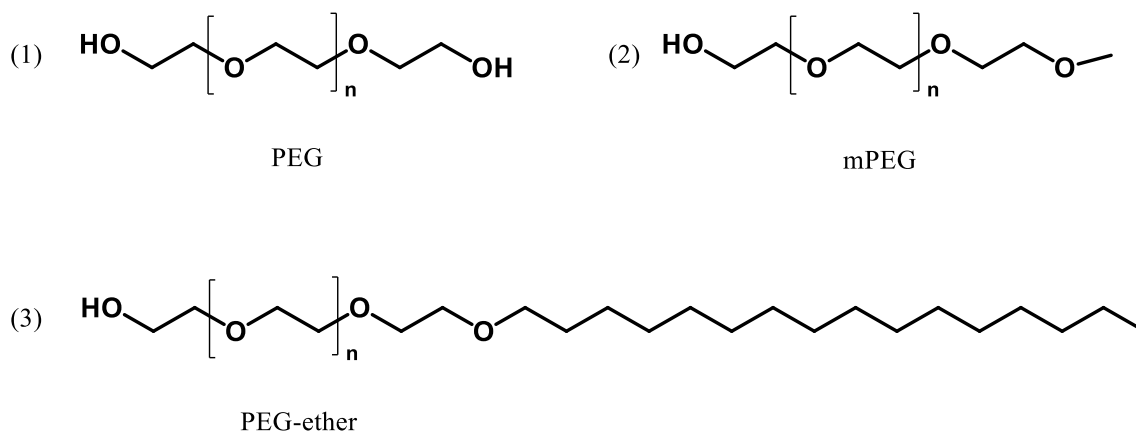


Figure 3. Typical PEG structures applied for PEGylation.

In the late 1970s, Abuchowski *et al.* were the first to report the coupling of PEG to a protein.⁵⁶ They demonstrated the improved pharmacokinetic and pharmacodynamic properties of PEGylated albumin by an extension in the blood circulation time. PEGylation of polypeptide drugs can increase their water solubility while renal clearance and toxicity can be reduced.⁵⁷ As kidneys filter substances basically according to size, by making the molecule larger through PEGylation renal clearance can be reduced.⁵⁸ Studies on PEG in solution revealed that each ethylene glycol subunit is associated with two or three water molecules. This binding of water molecules makes PEGylated compounds five to ten times larger than their unmodified version.⁵⁹ After polymers as drug-delivery vehicles were introduced in the 1970s, Kabanov *et al.* were the first to propose the use of PEG as a hydrophilic part of linear block copolymers for micellization in 1989.⁶⁰ Through PEGylation of the NC, both inhibition of opsonization and enhancement of water solubility can be achieved. Furthermore, PEG reduces the tendency of particles to aggregate by steric stabilization, thereby producing formulations with increased stability during storage and application.⁹ In 1990, pegademase (Adagen®) was the first PEGylated protein drug approved by the FDA. It is used for the treatment of severe combined immunodeficiency (SCID), a disease associated with an inherited deficiency of adenosine deaminase.⁶¹ Up to now, the FDA has approved around 30 PEGylated drugs and more are undergoing clinical investigation.⁶²

In addition, PEG is not only used to optimize drug delivery but also in everyday products. PEG and their derivatives are widely used in cosmetics such as surfactants, cleansing agents, emulsifiers, skin conditioners, and humectants. They comprise a class of compounds varying in molecular weights between 200 and over 10,000 g mol⁻¹. The most common uses include toothpaste, skin lotions, deodorant sticks, shaving creams, hand creams, face makeup, bath products, and hair care products.²⁰

One major disadvantage of PEG is its non-biodegradability.⁹ Oligomers with a molar mass below 400 g mol⁻¹ were found to be toxic in humans as a result of sequential oxidation into diacid and hydroxy acid metabolites by alcohol and aldehyde dehydrogenase. The oxidative degradation significantly decreases with increasing molar mass. Therefore, a molar mass well above 400 g mol⁻¹ should be used.⁶³ On the other hand, the molar mass should not

exceed the renal clearance threshold. Accordingly, a molar mass limit of 20-60 kg mol⁻¹ is reported for nondegradable polymers.^{20, 52}

PEG is considered the gold standard polymer with a high stealth effect and low intrinsic toxicity. However, in some cases it was observed that PEGylation resulted in an enrichment of opsonins such as immunoglobulins, promoting unspecific cell uptake.⁶⁴ This could be related to PEG-binding antibodies.⁶⁵ More details on antibodies and their specific binding to PEG are described below in chapter 2.4.

2.4 Immune system and anti-PEG antibodies

The immune system has the main function to protect the body from foreign compounds. It can be divided into the innate and adaptive immune system. The innate immune system provides an immediate, but non-specific response. Its major functions are to recruit immune cells to the infection site, activate the complement cascade, and stimulate the adaptive immune system. When a pathogen enters the body, the immune cells start to fight it. Granulocytes, monocytes/macrophages, and dendritic cells exhibit pattern recognition receptors (PRRs). They can destroy the pathogen itself by ingestion and digestion (phagocytosis) or control the immune response of the organism by releasing inflammatory mediators like cytokines or chemokines and attracting other defense cells to the site of inflammation. The adaptive immune responses are highly specific to the particular pathogen that induced them. The adaptive immune system creates an immunological memory and can provide long-lasting protection. Any substance capable of eliciting an adaptive immune response is referred to as an antigen (*antibody generator*).⁶⁶ There are two response classes of the adaptive immune system: antibody responses and cell-mediated immune responses, which are carried out by different classes of lymphocytes (B cells and T cells, respectively). Regarding the antibody responses, B cells are activated to secrete antibodies, which are proteins called immunoglobulins. The antibodies circulate in the blood stream and bind specifically to the foreign antigen causing it to inactivate. Antibody binding also marks the invading pathogens for destruction, mainly by making it easier for phagocytic cells of the innate immune system to ingest them (**Figure 4**).

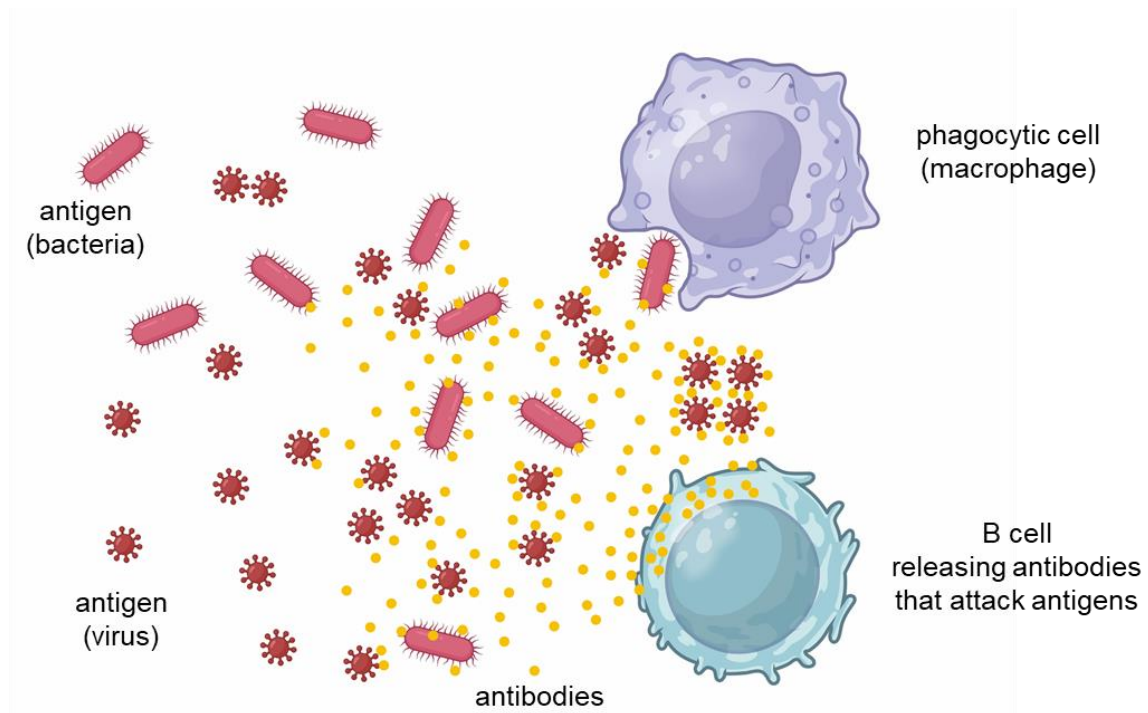


Figure 4. B cells produce antibodies that bind to antigens, inactivate them and mark them for phagocytic cells. Phagocytic cells destroy antigens by phagocytosis.

Igs are categorized into five classes for humans and most mammals: IgA, IgD, IgE, IgG, and IgM (**Figure 5**). All Igs share the same monomeric Y-shaped structure that consists of two heavy chains (50 kDa for IgG, 55 kDa for IgA, and 70 kDa for IgM) and two light chains (25 kDa), which are linked via disulfide bonds. The two arms of the Y-structure carry the binding sites for the antigens at their ends. Those antigen-binding fragments (F_{ab} -fragments) are highly variable and it is estimated that each person has at least 10^7 different antibody specificities.⁶⁷ The stem mediates the effector functions and is called crystallizable fragment (F_c -fragment) (**Figure 6**).

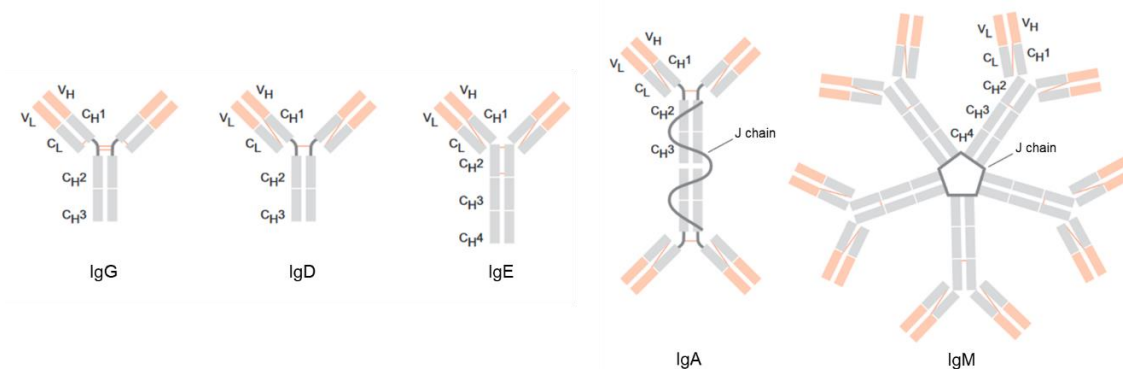


Figure 5. The five main classes of antibodies (immunoglobulins): IgG, IgA, IgD, and IgE. Adapted with permission from reference ⁶⁷. Published by Springer-Verlag GmbH Deutschland. Copyright © 2019.

The Ig classes differ in structure, distribution in the organism, and their effector functions: Antibodies of the IgM class account for about 10% of all Igs. They are pentamers and consist of five identical subunits of 180 kD each. All naïve B cells carry IgM as a B cell receptor on their surface. Accordingly, IgM is the first Ig secreted in the course of an immune reaction. After the acute phase, the IgM concentration in the blood plasma decreases and IgG levels rise for a long-term "memory" effect of the immune system against the pathogen. In terms of quantity, IgG is the dominant Ig class in serum, where it accounts for approximately 10 g L⁻¹ and about 75% of all serum immunoglobulins. IgA exists in three forms: as a monomer, as a dimer with J-chain, and as secretory IgA. It is mainly located in secretory substances, such as tears, and forms a barrier at the mucous membranes to prevent pathogens from entering further into the body. IgE occurs only in extremely small amounts in the serum. The vast majority of IgE is present cell-bound on eosinophils, basophils, and mast cells. Its reaction with an antigen causes the release of mediators of the anaphylactic reaction.

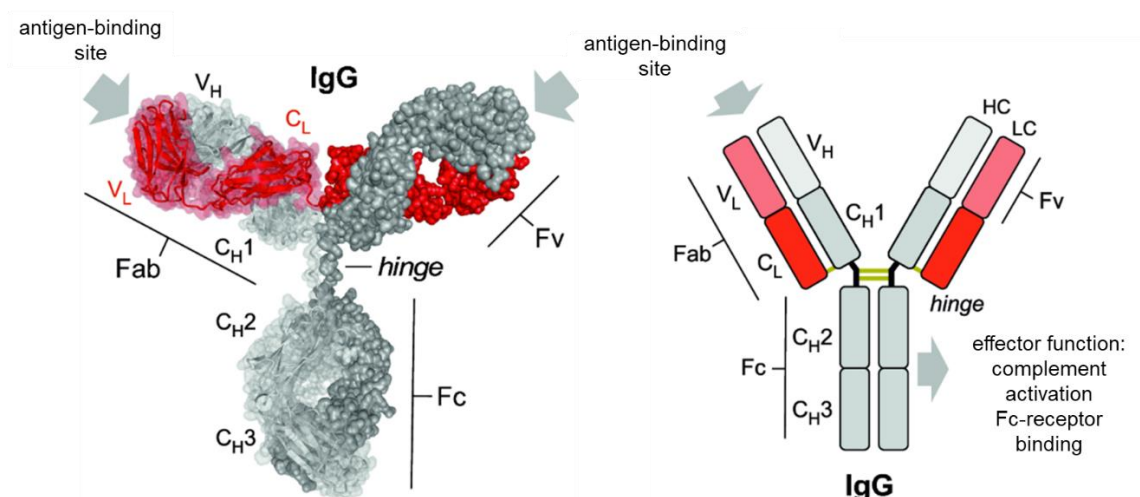


Figure 6. X-ray crystal structure and schematic representation of an IgG. Heavy chains are shown in gray and light chains in red. Adapted with permission from reference ⁶⁸. Published by Springer-Verlag GmbH Deutschland. Copyright © 2019.

NCs can be recognized as foreign compounds by the body or alter the protein physiological functions and thereby trigger the action of the immune system, causing inflammatory reactions. To shield the NCs from the immune system, PEGylation is typically used to decrease unspecific protein adsorption and enrich certain proteins with stealth properties on their surface. However, nowadays antibodies that specifically bind to PEG have emerged. Those anti-PEG antibodies were first described by Richter *et al.* in 1983.¹² They were only observed in approximately 0.2% of healthy blood donors, which at that time was considered to be of no clinical significance and probably not to interfere with the clinical use of PEGylated therapeutics.⁶⁹ Later on, various research groups observed that the administration of repeated doses of PEGylated NCs led to an accelerated blood clearance and weakened efficacy of PEGylated therapeutics.²² Additionally, for example, Doxil, a PEGylated liposome formulation, caused immediate hypersensitivity reactions upon first injection in some patients.²⁴ Acute severe allergic reactions to pegnivacogin, a PEGylated aptamer, were observed exclusively in patients with pre-existing anti-PEG antibodies and were associated with complement activation and tryptase release.²³ In animal models, repeated injection of PEGylated liposomes induced the formation of anti-PEG IgM and enhanced clearance of a second dose. Cheng *et al.* raised the assumption that the ethylene oxide repeating unit in PEGylated NCs acts as a TI-2 (thymus independent) antigen and

could be an immunogenetic epitope of PEG and a binding site for anti-PEG IgM. TI-2 antigens can induce an immunological response by cross-linking the cell surface immunoglobulins of specific B cells (marginal zone B cells), resulting in the secretion of IgG and IgM from the B cells.⁷⁰ Binding of IgM can trigger opsonization of complement factors that subsequently promote phagocytosis by Kupffer cells (**Figure 7**).⁷¹

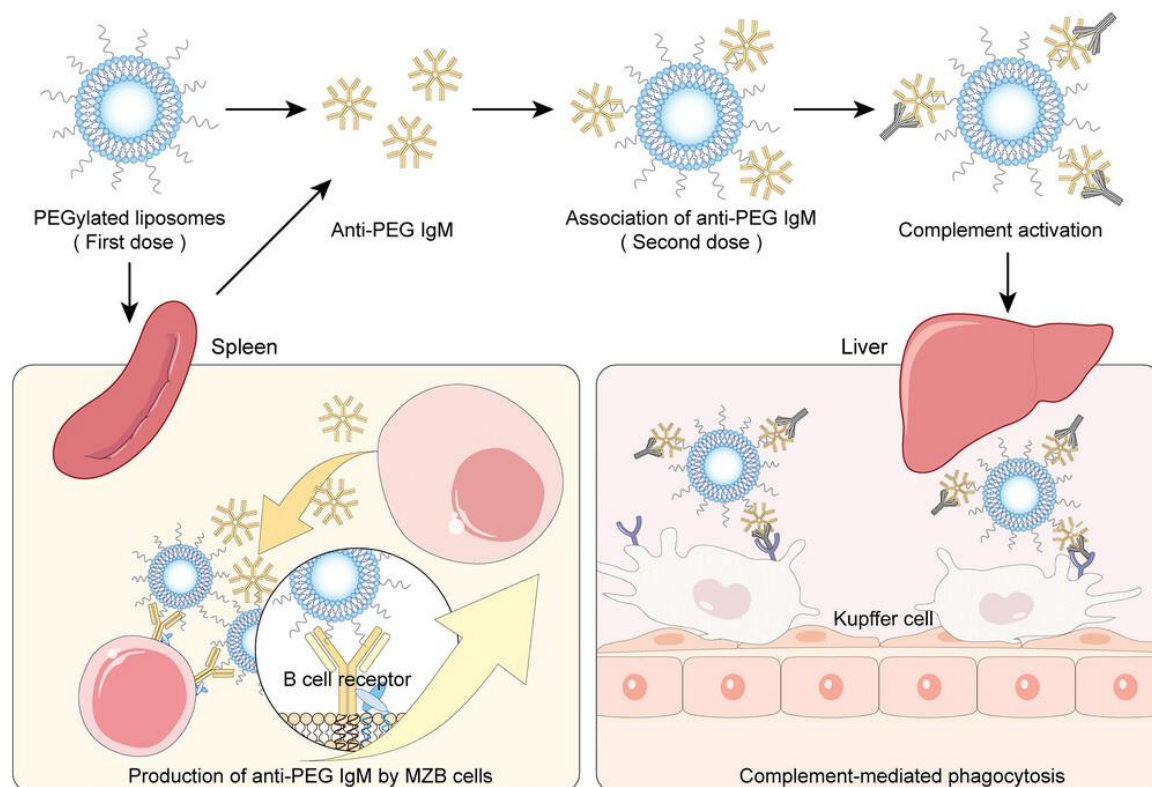


Figure 7. Representation of the sequence of events leading from anti-PEG IgM induction in marginal zone B cells (MZB cells) to accelerated clearance of PEGylated liposomes and complement activation. Reprinted with permission from reference ⁷². Published by Wiley-VCH GmbH. Copyright © 2023. This open access article is licensed under CC-BY-4.0.

In contrast to most antidrug antibodies, anti-PEG antibodies were observed in both PEGylated therapeutics-treated patients and healthy (treatment-naïve) individuals. In 2016, Chen *et al.* reported pre-existing anti-PEG antibodies in healthy Han Chinese and found that 44.3% of participants tested positive for anti-PEG IgG and IgM antibodies.¹⁷ Yang *et al.* found detectable anti-PEG antibodies in as much as 72% of the samples (18% IgG, 25% IgM, and 30% both).¹⁸ One reason for the high prevalence throughout the population might

be the abundance of PEG in everyday products such as cosmetics and processed food.²⁰ Casual exposure to PEG compounds may induce anti-PEG antibodies.⁷³

It was controversial how antibodies could recognize a flexible and unspecific structure like PEG.⁷⁴ A recent study by Huckaby *et al.* characterized the anti-PEG antibody structure in complexes with PEG chains by X-ray crystallography.¹⁹ They demonstrated how antibodies could bind highly flexible repeating structures like PEG between two anti-PEG F_{ab} fragments in an open ring-like sub-structure, whereby the PEG backbone is likely to be captured and stabilized via Van der Waals interactions. They reported the PEG size of the PEG antigen epitope to consist of roughly ~16 repeating units, suggesting that a PEG chain would have to be >700 g mol⁻¹ to be able to interact with the antibodies (**Figure 8**).

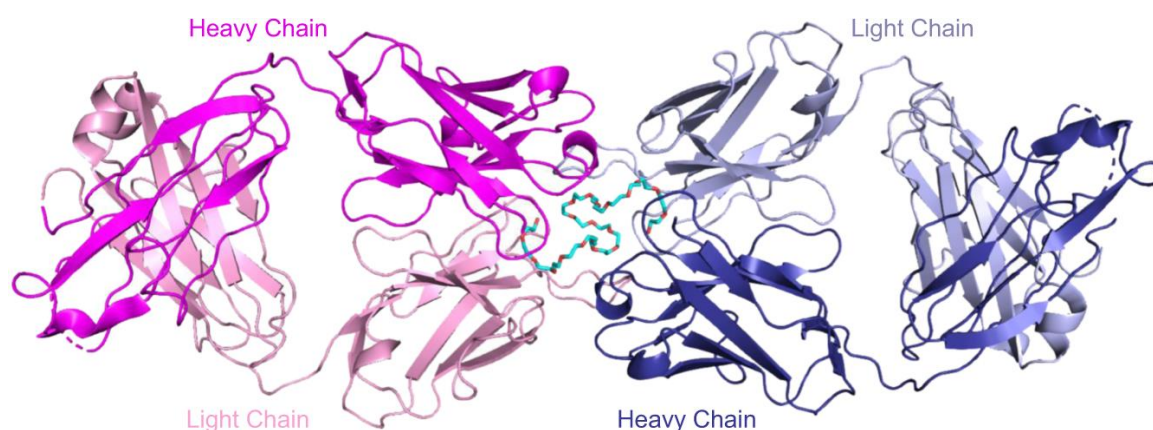


Figure 8. Crystal structure of two anti-PEG antibody F_{ab} fragments forming a dimer complex with a single PEG chain. Color to denote heavy and light chain pairings of each F_{ab} monomer (heavy chain 1, magenta + light chain 1, pink; heavy chain 2, deep blue + light chain 2, light blue). Reprinted with permission of m reference¹⁹. Published by Springer Nature. Copyright © 2020. This open access article is licensed under CC-BY-4.0.

Subsequently, anti-PEG antibodies could interact with PEGylated NCs and counteract the stealth effect of PEG, leading to accelerated blood clearance and possible severe allergic reactions. Their impact on the effect of NC therapeutics and related side effects remains uncertain up to now.

3 Methods

3.1 Enzyme-linked immunosorbent assay

An enzyme-linked immunosorbent assay (ELISA) can be used to determine the concentration of a compound, usually a protein. It is based on the specific interaction between an antibody and its antigen and is normally executed in microtiter plates. The antigen can be immobilized directly in the well via unspecific adsorption (direct ELISA) or it can be captured with an antibody (sandwich ELISA). After several washing steps, a specific detection antibody binds to the immobilized antigen. An enzyme is covalently linked to the detection antibody and can be quantified in a colorimetric reaction.^{75,76} In this work, ELISA was used for the quantification of PEG binding to IgG and IgM. Anti-PEG IgG and IgM (although technically antibodies) are here considered to be the antigens. To detect anti-PEG antibodies specifically, PEG chains were adsorbed to the surface of the well. Only anti-PEG antibodies bound to the immobilized PEG chains and any unbound proteins were washed away. Subsequently, an antibody specifically binding to the F_c domain of human IgG was used for the detection of anti-PEG IgG. Horseradish peroxidase (HRP) was linked to the secondary antibody and catalyzed the oxidation of 2,2'-azino-bis(3-ethylbenzothiazoline-6-sulfonic acid (ABTS) in the presence of hydrogen peroxide (**Figure 9**). The stable radical cation, which is the reaction product, has an absorption maximum at 405 nm and can be quantified photometrically after 30 min reaction time. The concentration can be determined by comparing to a serial dilution of a standard.

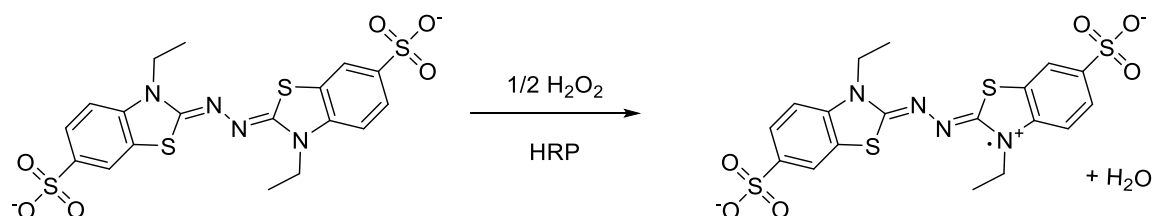


Figure 9. Oxidation of ABTS for photometric quantification in an ELISA.

3.1 Enzyme-linked immunosorbent assay

To analyze the specific binding, a competition assay can be performed. Therefore, soluble PEG chains were added before incubation with the biological sample. Anti-PEG antibodies subsequently interact with immobilized and free PEG chains and after several washing steps, the concentration of the competition assay will be decreased. **Figure 10** displays a schematic overview of the assay.

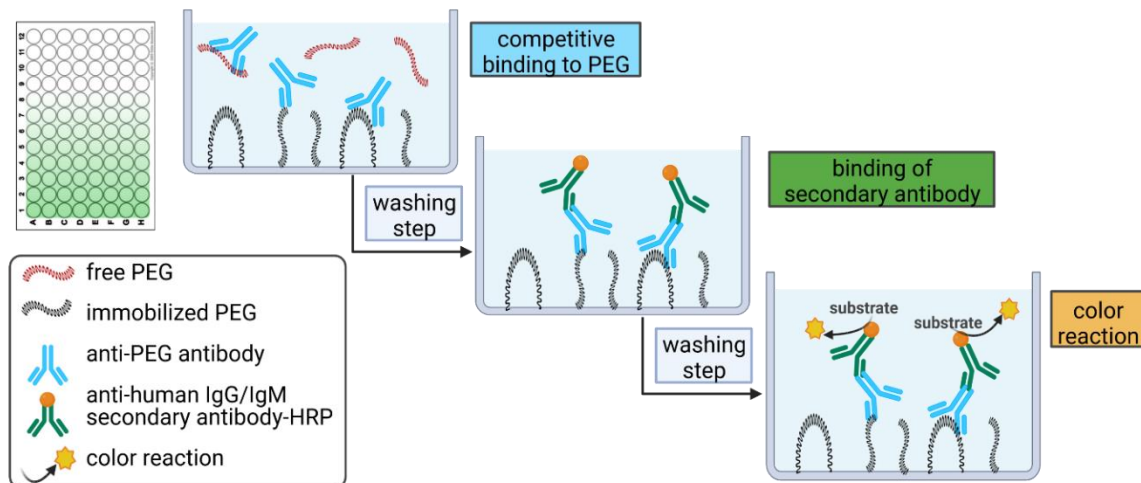


Figure 10. Schematic setup of the ELISA test.

3.2 Microscale thermophoresis

Microscale thermophoresis (MST) is a biophysical technique that measures the strength of interaction between two molecules by detecting variations in fluorescence intensity because of an infrared (IR) laser-induced temperature change. The strength of the interaction between the binding partners is represented by the dissociation constant K_d . It represents the likelihood that the interaction between the molecules will break apart. One requirement is a fluorescent binding partner. A fluorophore re-emits light upon light excitation, depending on the structure and its chemical environment. **Figure 11** displays the MST setup. Heating a small volume in a capillary with an IR laser induces a rapid temperature change. This induces both a temperature related intensity change (TRIC) and thermophoresis. TRIC describes how the fluorescence intensity of a fluorophore depends on the local temperature of the solution. The extent of the temperature dependence is strongly related to the chemical environment of the fluorophore. Thermophoresis describes the movement of molecules along temperature gradients, which results in a quantifiable change in the local concentration of the target molecules. Initially, the molecules are homogeneously distributed and a constant “initial fluorescence” is detected. Within the first second after activation of the IR laser, a rapid change in fluorophore properties occur due to the fast temperature change and subsequently thermophoretic movement out of the heated sample volume. After deactivation of the IR-Laser “backdiffusion” of molecules occurs **Figure 11C**). The change in fluorescence is recorded as a function of temperature as well as concentration of its ligand. The range of the variation in the fluorescence signal correlates with the binding of a ligand to the fluorescent target (**Figure 11D**).⁷⁷⁻⁷⁹ A concentration series of the non-fluorescent ligand, in our case anti-PEG IgG, was prepared and the fluorescent target (FITC-labelled PEG) was added. By comparing the fluorescent signal at a low concentration (unbound state) with a high concentration (bound state), the dissociation constant can be determined. Therefore, the change in the fluorescence signal is plotted against the concentration of the non-fluorescent ligand to yield a binding curve, which can be fitted to derive binding constants.

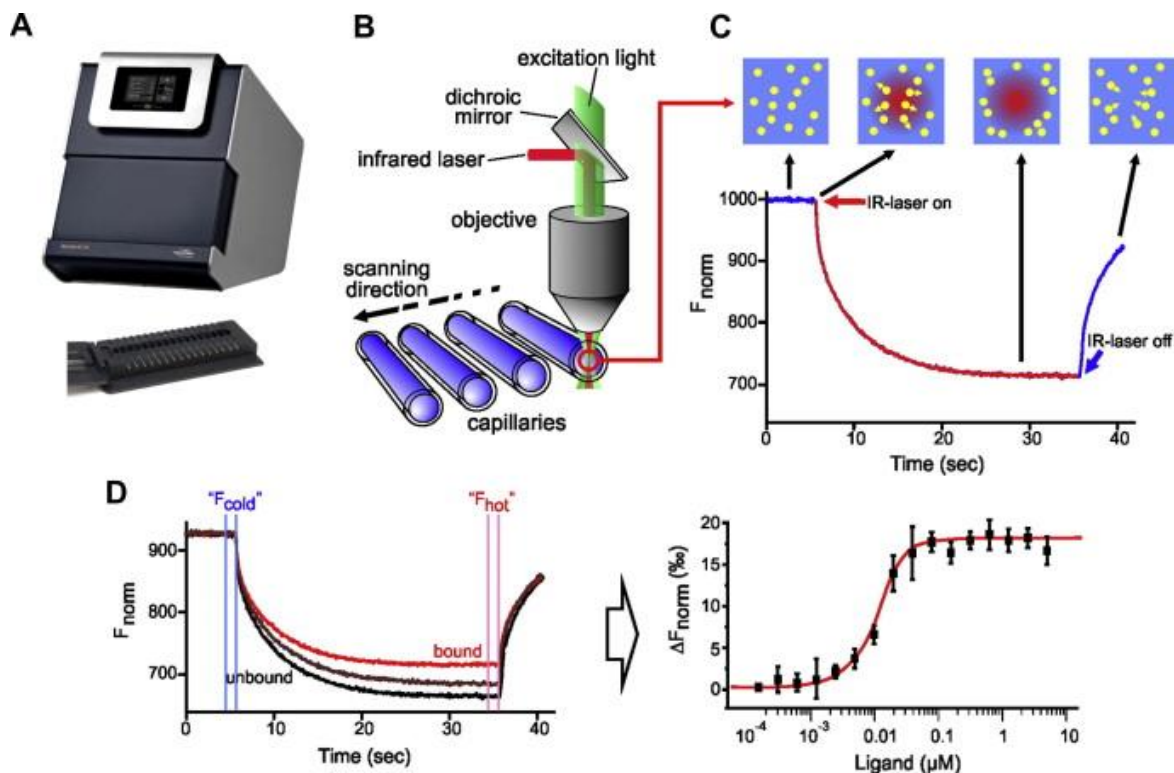


Figure 11. MST setup and experiments. (A) The Monolith NT.115 from NanoTemper Technologies GmbH with capillary tray. (B) Schematic representation of MST optics. (C) Typical signal of an MST experiment. (D) Typical binding experiment. Black trace: unbound state, red trace: bound state. Plot of ΔF_{norm} at different ligand concentrations yields in a binding curve and can be fitted to derive binding. Reprinted with permission from reference ⁷⁹. Published by Elsevier B.V. Copyright © 2014. This open access article is licensed under CC-BY-3.0.

3.3 Pierce assay

The protein quantification of desorbed corona proteins is the first step in the analysis of the protein corona. The Pierce 660 nm assay is based on the formation of a metal complex with proteins in acidic media. The dye-metal complex is a polyhydroxybenzenesulfonephthalein-type dye and a transition metal binding to mainly basic amino acid residues in proteins such as histidine, arginine, and lysine.⁸⁰ The dye-metal complex is reddish-brown and changes to green upon protein binding. The color change is produced by deprotonation of the dye at low pH value facilitated by interactions with positively charged amino acid groups in proteins and can be detected by measuring the absorbance at 660 nm. The protein concentration can be determined by comparing the absorbance to a serial dilution of bovine serum albumin (BSA) as standard.

3.4 Liquid chromatography-mass spectrometry

For the identification of proteins, analysis by liquid chromatography-mass spectrometry (LC-MS) is performed. Before the actual analysis, the proteins must be digested with trypsin to obtain smaller fragments (peptides) with detectable mass/charge (m/z) ratios. Trypsin cleaves proteins behind the C-terminus of lysine and arginine, which results in peptides of about 14 amino acids. These smaller peptides can then be separated by high-performance liquid chromatography (HPLC) according to their polarity. Subsequently, the peptides must be ionized via electrospray ionization (ESI) in a positive ionization mode. After analysis via MS, the measured m/z signals of the peptides are matched to a database in a so-called “peptide-mass fingerprinting” process. Since the same peptide fragments may appear in multiple proteins, careful analysis of MS experiments regarding proteins is required and only proteins with at least 2 unique peptides found are considered identified successfully.⁸¹⁻⁸³

4 Results and Discussion

4.1 Anti-PEG antibody quantification

The following chapter 4.1.2 is based on the submitted manuscript “Anti-PEG antibodies enriched in the protein corona of PEGylated nanocarriers impact the cell uptake”. For the thesis, this chapter was extended with additional experiments and details.

In 1983, Richter *et al.* first reported the potential immunogenicity of PEG itself.¹² They observed anti-PEG antibodies (mainly IgM isotype) in approximately 0.2% of healthy blood donors. Subsequent studies verified the presence of pre-existing anti-PEG antibodies but observed a wide range of positive frequencies. In individual studies, between 22-72% of the samples were found positive for anti-PEG antibodies.¹⁴⁻¹⁸

One explanation for the discrepancy in the reported prevalence of anti-PEG antibodies may be the multiple assay systems used. Results obtained with different methods are usually incomparable, and some of them are only qualitative rather than quantitative. It was also criticized that many assays for anti-PEG antibodies are flawed and lack specificity.⁷⁴ Early methods such as passive hemagglutination are not specific enough and are now mostly obsolete. Currently, the standard method is ELISA. It can simultaneously provide high sensitivity and rapid screening of multiple samples. However, anti-PEG antibody specificity was not always thoroughly confirmed and detergents like Tween® could interfere with the antibody binding.⁸⁴ Without a commercially available human anti-PEG antibody standard, only relative amounts of anti-PEG antibodies can be estimated, which makes the comparison of different studies difficult.⁶⁵ Consequently, a validated ELISA protocol is critically needed.

Chen *et al.* engineered chimeric monoclonal anti-PEG antibodies (IgM and IgG) generated by combining mouse F_{ab} with human F_c fragments and analyzed anti-PEG IgG and IgM antibodies by direct ELISA.¹⁷ Those antibodies were used as standards to analyze the anti-PEG antibody prevalence among the German population.

4.1.1 ELISA development and optimization

As mentioned above, the ELISA protocol is based on the development by Chen *et al.*¹⁷ In the assay, anti-PEG antibodies in the plasma samples bound to poly(ethylene glycol) diamine immobilized on the plates. An enzyme-linked secondary antibody then specifically detected anti-human IgG or IgM antibodies. The relative concentrations of anti-PEG IgG or IgM antibodies in the plasma samples were determined by comparison to standard curves obtained from a serial dilution of chimeric anti-PEG antibodies c3.3-IgG or cAGP4-IgM.⁸⁵ The schematic setup of the ELISA is shown in **Figure 10** (chapter 3.1).

First, the capabilities of the herein used ELISA method were investigated by determining the method's limit of detection (LOD) and limit of quantification (LOQ) in accordance with DIN 32645. For this, ten blank samples were analyzed according to the protocol described in chapter 5.3. LOD was calculated as the mean background absorbance of the blank samples plus three times its standard deviation and LOQ was calculated as the mean background absorbance plus ten times its standard deviation. As a result, LOQ was determined to be an absorbance of $A_{LOQ} = 0.27$. This determines the lower limit of quantifiable concentration to be $0.5 \mu\text{g mL}^{-1}$. IgM naturally occurs in a lower concentration than IgG; hence a higher sensitivity is necessary. To detect the lower concentration of anti-PEG IgM a peroxidase substrate with a higher sensitivity was used. QuantaBlu® Fluorogenic Peroxidase Substrate is a soluble fluorogenic substrate for the detection of peroxidase activity. It produces a blue fluorescent product that can be quantitated by fluorometry. With this, a quantification down to a concentration of $0.05 \mu\text{g mL}^{-1}$ is possible.

For optimal quantification, the standard needs to be in a linear range. For anti-PEG c3.3-IgG the curve was linear for a concentration range between $0.5 - 8.0 \mu\text{g mL}^{-1}$ with $R^2 > 0.985$. For anti-PEG cAGP4-IgM the curve was linear in a log-log plot for a concentration range between $0.05 - 6.5 \mu\text{g mL}^{-1}$ with $R^2 > 0.978$. For each well plate used in an ELISA experiment a separate calibration was performed. **Figure 12** displays the standard curves performed on several days to highlight the reproducibility.

Additionally, we performed a competition assay to confirm that anti-PEG antibodies specifically bind to PEG and did not randomly adsorb on the plates. For the competition assay, free PEG was added to the plasma samples to compete with the immobilized PEG

chains. This reduced the number of detectable antibodies. Consequently, the sample was considered positive for anti-PEG antibodies if the color reaction was reduced by at least 35% compared to the reading without adding free PEG.

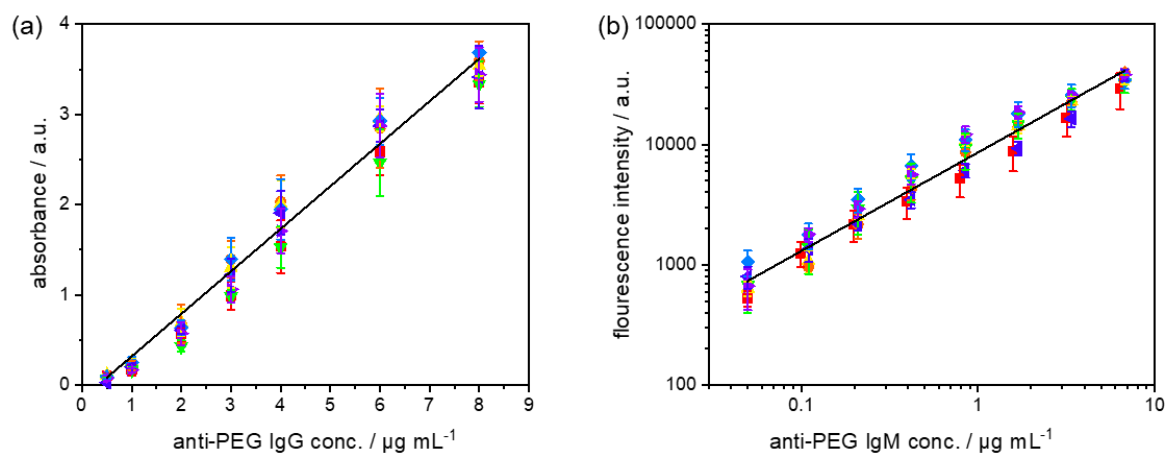


Figure 12. Chimeric antibody standard curve. Eight individual standard curves were performed on several separate days over one month. Error bars represent standard deviation from triplicates. Linear regression based on mean values of all eight standard curves. (a) Linear range of the calibration curve with c.3.3-IgG as standard and ABTS. (b) Calibration curve with cAGP4-IgM and QuantaBlu® in a log-log plot.

4.1.2 Plasma screening among the German population

As mentioned earlier, an increasing number of studies report pre-existing anti-PEG antibodies in Chinese and North American populations.^{17, 18, 65} We performed plasma screening to evaluate the prevalence of the anti-PEG antibodies among the German population. To this end, we received 500 plasma samples from healthy blood donors, representing the plasma source we typically use for protein corona studies. The samples were chosen randomly and collected together with information about the donor's age (year of birth) and gender. **Figure 13** shows the age distribution of all collected plasma samples. It is important to note that the plasma samples were collected in early 2019 before PEGylated Covid-19 vaccines were approved and applied. We analyzed the anti-PEG antibody prevalence and concentration in plasma samples using a modified ELISA test as described in chapter 4.1.1.

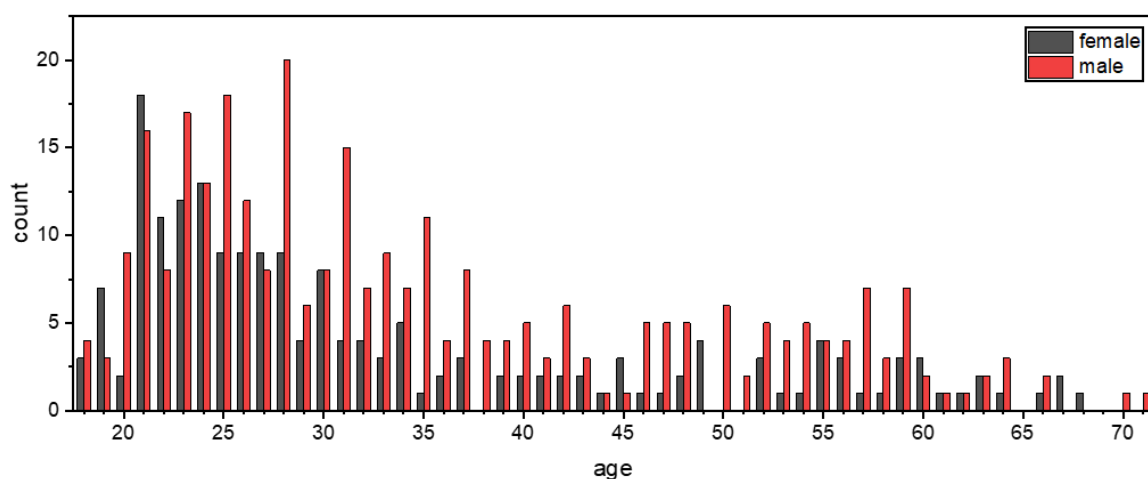


Figure 13. Age distribution of all collected plasma samples (black: female, red: male samples).

As indicated in **Figure 14**, anti-PEG antibodies were present in the majority of the samples with minor differences between male and female donors. 82% of the female donors were positive for anti-PEG IgG, and 55% were positive for anti-PEG IgM. The male donors showed a slightly lower prevalence of 74% for anti-PEG IgG and 54% for anti-PEG IgM. Overall, 49% of all donors were positive for both IgG and IgM and in only 17% no anti-PEG antibodies could be detected. This means that in ~83% of all donor samples anti-PEG

antibodies were found. In general, anti-PEG IgG was more prevalent than IgM, while both followed a similar trend, as shown in **Figure 14d**. The prevalence of anti-PEG IgG and IgM is shown depending on donor age. Samples were grouped into 10-year time intervals and groups of <20 and >60 years of age. Here, it can be seen that anti-PEG prevalence roughly followed a linear trend and decreased with age for both immunoglobulin isotypes.

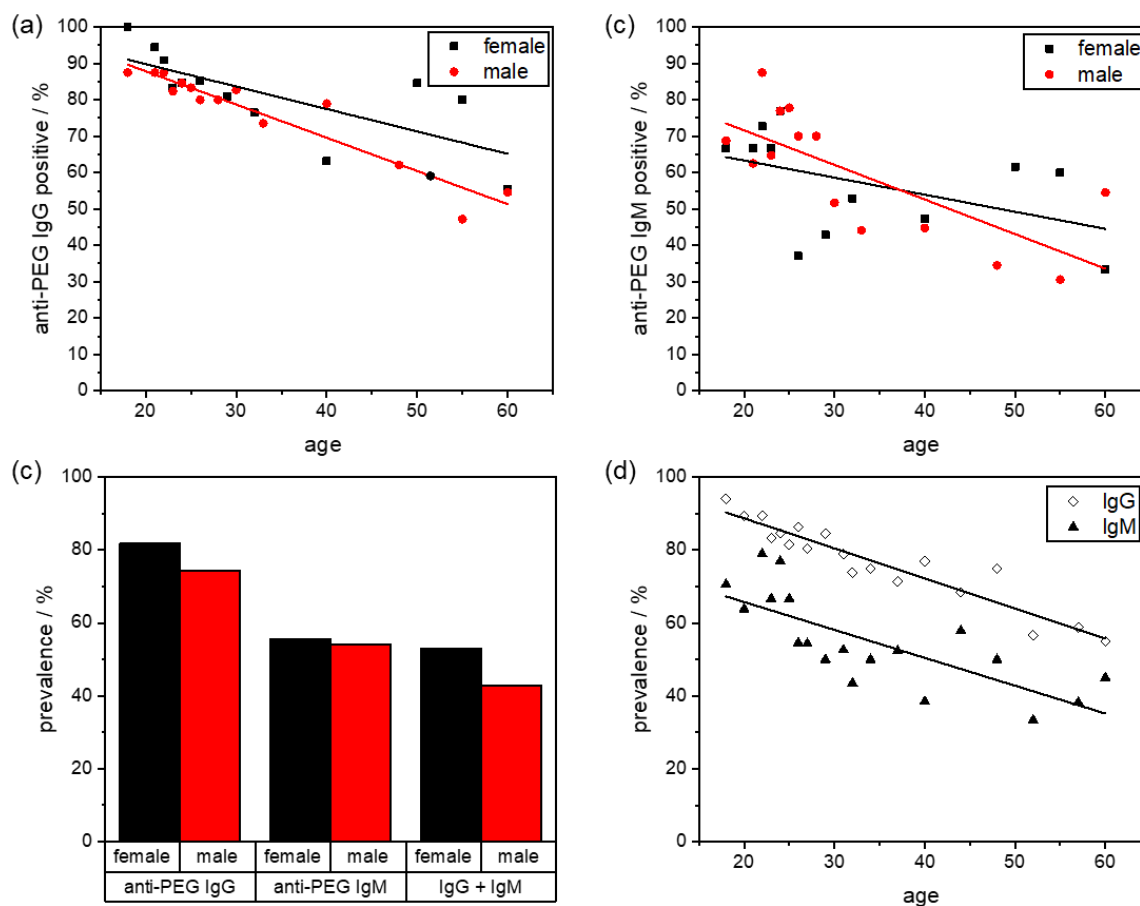


Figure 14. (a, b) Prevalence of anti-PEG IgG and IgM antibody distribution depending on age and separated by gender (black: female, red: male samples). (c) Mean prevalence of anti-PEG IgG and IgM antibodies (black: female, red: male samples). (d) Overall prevalence distribution depending on age.

4.1 Anti-PEG antibody quantification

Figure 15 displays the anti-PEG IgG and IgM concentrations for all measured samples depending on age and gender. Additionally, samples were grouped into 10-year time intervals and groups of <20 and >60 years of age. Both immunoglobulin isotypes varied the most and showed the highest absolute concentrations in the age group between 21-30 years. The outliers and mean values of antibody concentration slightly decreased with increasing age, more prominently for anti-PEG IgG than for IgM.

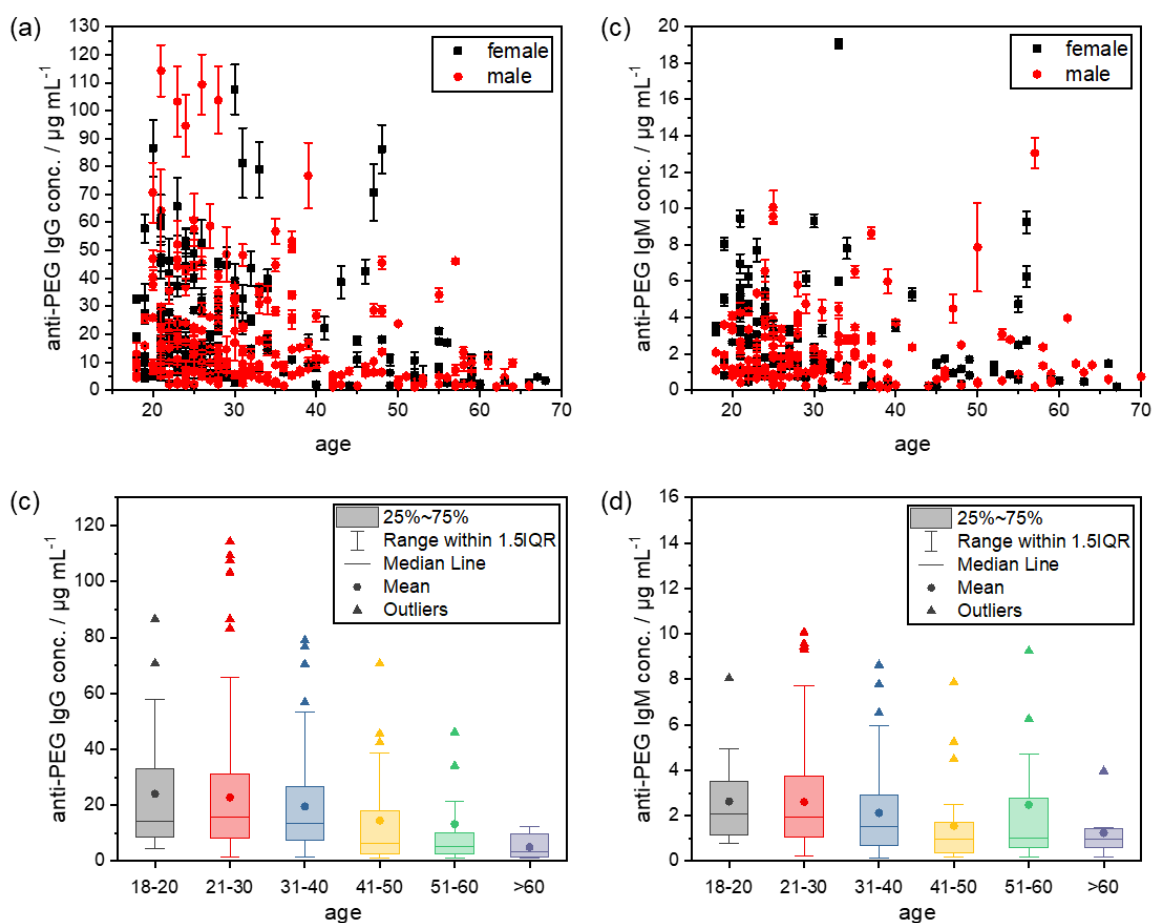


Figure 15. (a, b) Concentration of anti-PEG IgG and IgM antibodies of all measured samples depending on age. Error bars represent standard deviation from triplicates. (c, d) Concentration of anti-PEG IgG and IgM antibodies in age groups.

These results agree with findings from previous studies. Chen *et al.* reported anti-PEG IgG and IgM antibodies in 44.3% of healthy donors, and Yang *et al.* found detectable anti-PEG antibodies in as much as 72% of the samples (18% IgG, 25% IgM, and 30% both).^{17, 18}

Here, it is also important to compare the results with regard to the thresholds of minimum ELISA sensitivity among the different studies. Chen *et al.* reported LOQs of $0.3 \mu\text{g mL}^{-1}$ for IgG and $0.1 \mu\text{g mL}^{-1}$ for IgM. Yang *et al.* investigated their samples using different minimum cutoff values of either 0.5 or $0.1 \mu\text{g mL}^{-1}$ for both classes. In our experiments, LOQ was determined to be $0.5 \mu\text{g mL}^{-1}$ for IgG and $0.05 \mu\text{g mL}^{-1}$. Notably, for anti-PEG IgM there were no samples with a concentration between $0.05 - 0.1 \mu\text{g mL}^{-1}$. Thus, the detection sensitivity applied to our experiments to obtain results in terms of prevalence (% positive samples) was comparable to the previously mentioned studies.

One reason for the high prevalence throughout the population might be the abundance of PEG in everyday products such as cosmetics and processed food.²⁰ Casual exposure to PEG compounds may induce anti-PEG antibodies.⁷³ Yang *et al.* postulated the following mechanism: The skin is always exposed to external stimuli, which can cause an inflammatory response and the recruitment of immune cells. Upon exposure to PEG in daily use of cosmetics, PEG is likely to come into close proximity with highly activated immune cells, which might result in the induction of anti-PEG antibodies. Accordingly, daily exposure to for example cosmetics, toothpaste, or shampoos, that contain some forms of PEG, might contribute to the increase in the prevalence of pre-existing anti-PEG antibodies. Subsequent exposure to PEGylated therapeutics may further induce a robust memory immune response to PEG.¹⁶ The higher prevalence of anti-PEG antibodies in younger individuals might be due to the more widespread use of PEG in convenience products and cosmetics in recent years and changes in general consumer behavior. Additionally, a diminished immune response in older individuals could play a role.⁸⁶

4.1.3 Conclusion

Several studies report pre-existing anti-PEG antibodies in a wide range of positive frequencies (0.2-72%).¹⁴⁻¹⁸ The increased anti-PEG antibody prevalence might be due to an improved method and limit of detection over time but also greater exposure to PEG in everyday products. Small protocol differences like antigen coating, incubation time, agents, etc. can significantly affect final readings, which makes it difficult to compare results from different experiments directly.⁸⁷ We based our ELISA measurements on the development by Chen *et al.* and just slightly modified the protocol to adapt to the properties of our samples. The standard curves displayed in **Figure 12** highlight the reproducibility and the low LOQ ($0.5 \mu\text{g mL}^{-1}$ for anti-PEG IgG and $0.05 \mu\text{g mL}^{-1}$ for anti-PEG IgM) of our method.

The plasma screening revealed a high prevalence of anti-PEG antibodies in the German population. 83% of the plasma samples were found to be positive for anti-PEG IgG or IgM. Interestingly, the prevalence inversely correlates with age. The same trend could be observed for the concentration. The highest absolute concentration and most variation were detected in the age group between 21-30 years. This high prevalence might well be due to casual exposure to PEG compounds in everyday products.

4.2 Binding characterization of anti-PEG antibody to soluble PEG

The following chapter 4.2.2 is based on the submitted manuscript “Anti-PEG antibodies enriched in the protein corona of PEGylated nanocarriers impact the cell uptake”. For the thesis, this chapter was extended with additional experiments and details.

A few studies exist that discuss the binding behavior of anti-PEG antibodies. The cross-reactivity of anti-PEG antibodies toward other polymers with a C-C-O backbone or the specific binding to the PEG backbone versus the end-group were analyzed by competitive ELISA test.^{88, 89} Additionally, X-ray crystallography studies offer insight into the structural basis of PEG recognition by the anti-PEG antibody as described in chapter 2.4.^{19, 90, 91} A correlation between PEG molecular weight and anti-PEG IgG binding was analyzed by determining the EC₅₀ values by applying ELISA.¹⁷ However, no study on the direct binding affinity of monospecific anti-PEG antibodies to PEG with different chain lengths exists so far.

As a preliminary study, we used a competitive ELISA to compare the binding of anti-PEG IgG to PEG with different chain lengths and end-groups. To quantify the strength of the interaction between anti-PEG antibodies and PEG, we performed microscale thermophoresis (MST) measurements. Additionally, we used fluorescence correlation spectroscopy (FCS) to confirm our results.

4.2.1 Competitive ELISA

We used a competitive ELISA to compare the binding behavior of anti-PEG IgG to PEG with different chain lengths. The wells were coated with PEG_{10k}-diamine. PEG with a chain length between 2,000 and 10,000 g mol⁻¹ and with hydroxy or methoxy end-group was used for competition. A dilution series of the competitor was analyzed to compare the concentration. The stronger the binding is, the lower the concentration is needed for the same competition (reduction of the initial signal). More details on the method are described in chapter 5.4.1. The competition achieved by the different PEG variants is displayed in **Figure 16**. The maximum competition seemed to be reached for all samples at a concentration of ~ 0.1 µg mL⁻¹, which refers to 1.25 µg PEG per well. No change in the competition behavior can be seen between PEG_{10k}, mPEG_{10k}, and mPEG_{5k}. The samples

that showed the most significant difference are PEG_{10k} and PEG_{2k}, which are displayed again for better visibility in **Figure 16b**. The relevant concentration range is marked with a red frame. For the same concentration, a higher competition is achieved with PEG_{10k} compared to PEG_{2k}, referring to a higher binding. If PEG_{2k} is used as a competitor, the antibodies tended to bind more to the PEG_{10k}-diamine in the well than PEG_{2k} in the solution. This quick and easy method revealed a stronger binding of anti-PEG IgG to PEG_{10k} than to PEG_{2k} and is in good agreement with previous studies.¹⁷ Competitive ELISA can be used for a quick comparison but for more detailed analysis, especially direct binding affinities, a different method is necessary.

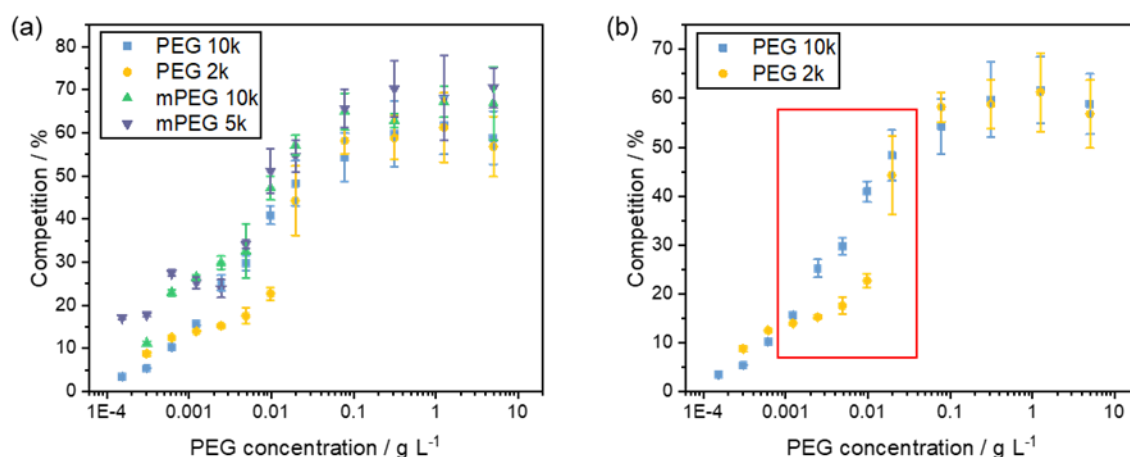


Figure 16. ELISA competition assay. (a) Dilution series of PEG_{10k}, PEG_{2k}, mPEG_{10k} and mPEG_{5k} competitor. (b) Comparison between PEG_{10k} and PEG_{2k}. Red frame indicates the relevant concentration range with the most significant difference.

4.2.2 Microscale thermophoresis

No study on the direct binding affinity of anti-PEG antibodies to PEG with different chain lengths exists so far. We performed microscale thermophoresis (MST) measurements to quantify the strength of the interaction between anti-PEG antibodies and PEG. The technique is based on a temperature-induced fluorescence change of a labeled target as a function of the concentration of a non-fluorescent ligand.⁷⁷ We used FITC-conjugated mPEG (methoxy-terminated PEG) as a target. Varying the PEG chain length gave us an insight into how the chain length influences the binding affinity to anti-PEG IgG,

represented by the dissociation constant (K_d). As a negative control, we used FITC-conjugated dextran. In **Table 1** details on the used settings can be found. The obtained results are listed in **Table 2** and the corresponding binding curves are shown in **Figure 17**. The binding of anti-PEG IgG to mPEG with a molecular weight of 10,000 or 20,000 g mol⁻¹ yielded the lowest K_d values (28 – 44 nM), which indicates the highest binding affinity. The difference between the two K_d values is not significant, but for lower PEG molecular weights the obtained K_d values were considerably higher. This means that binding strength decreased with decreasing PEG chain length. As expected, no binding could be observed in the negative control.

Table 1. Settings used for microscale thermophoresis analysis. Target: methoxy-terminated poly(ethylene glycol) (mPEG) with different chain lengths, ligand: anti-PEG IgG. Highlighted in gray are the settings plotted in Figure 17.

target	target concentration/ nM	ligand concentration/ μ M	excitation power/ %
mPEG20k-FITC	20	2.5	100
mPEG20k-FITC	20	1	80
mPEG10k-FITC	25	0.75	60
mPEG10k-FITC	25	0.75	80
mPEG10k-FITC	25	0.75	100
mPEG10k-FITC	20	1	60
mPEG10k-FITC	20	4	40
mPEG5k-FITC	50	1.65	20
mPEG2k-FITC	50	4	40
dextran-FITC (neg. control)	50	1.65	80

4.2 Binding characterization of anti-PEG antibody to soluble PEG

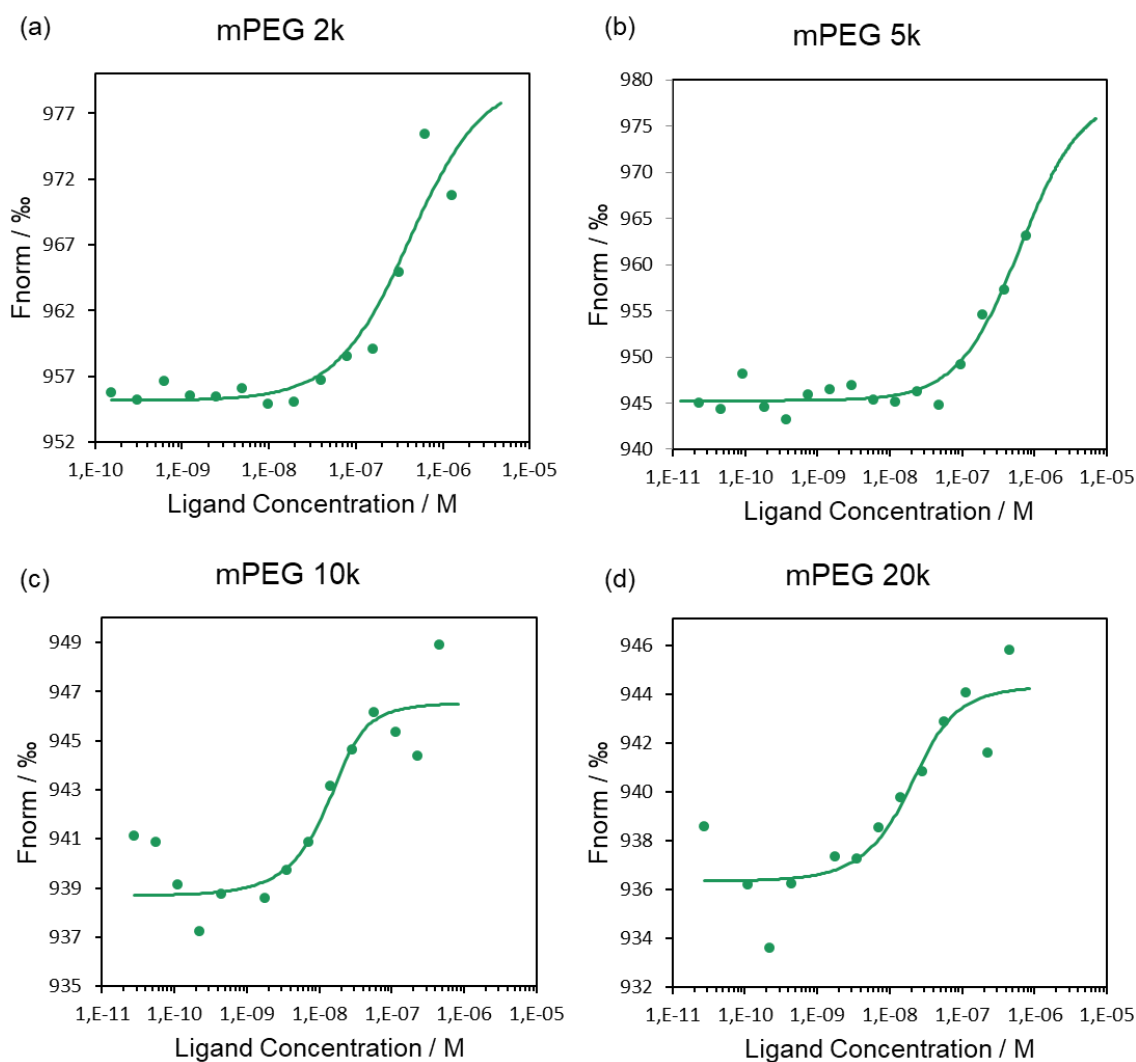


Figure 17. Microscale thermophoresis data analysis. Plot of the normalized fluorescence F_{norm} (%) vs the concentration of anti-PEG IgG as ligand. The target FITC conjugated mPEG with different chain lengths: mPEG20k-FITC (a), mPEG10k-FITC (b), mPEG5k-FITC (c), mPEG2k-FITC (d) was incubated with increasing concentration of anti-PEG IgG as ligand. The settings of the measurements can be seen in the table above, highlighted in gray are the used settings (Table S1). The MST traces are fitted according to the law of mass action to obtain K_d values.

These results indicate a strong and specific binding of anti-PEG IgG to mPEG and agree with previous studies. Chen *et al.* analyzed the binding of anti-PEG IgG to immobilized mPEG ranging in size from $30,000 \text{ g mol}^{-1}$ to $2,000 \text{ g mol}^{-1}$ and observed better binding (characterized by EC_{50} values) for longer chains of mPEG.¹⁷ Additionally, the same group investigated the binding of bispecific PEG engagers to mPEG_{5k} with MST. They observed a strong binding with a K_d value of 7.6 nM .⁹² Furthermore, Huckaby *et al.* reported the PEG

size of the PEG antigen epitope consists of roughly ~16 repeating units, suggesting that a PEG chain would have to be $>700 \text{ g mol}^{-1}$ to be able to interact with the antibodies.¹⁹ This confirms our results that a certain chain length is necessary for sufficient binding and a longer PEG chain leads to stronger binding of anti-PEG antibodies.

Table 2. Microscale thermophoresis analysis to quantify interaction strength (dissociation constant K_d) between anti-PEG IgG and FITC-labeled mPEG or dextran as a negative control.

target	polymer molecular weight/ g mol^{-1}	K_d / nM
mPEG _{20k} -FITC	20,000	44 ± 25
mPEG _{10k} -FITC	10,000	24 ± 12
mPEG _{5k} -FITC	5,000	249 ± 51
mPEG _{2k} -FITC	2,000	2690 ± 946
dextran-FITC (neg. control)	10,000	no binding

4.2.3 Fluorescence correlation spectroscopy

Fluorescence correlation spectroscopy (FCS) is a very sensitive method to determine fluctuations in fluorescence intensity. Based on this, information about the diffusion constant, concentration, and binding behavior can be obtained. We used FCS to confirm our analysis with MST for one exemplary PEG chain length (mPEG_{5k}). The experiments were performed by Dr. Kaloian Koynov (MPI-P).

In **Figure 18a**, the autocorrelation curves for FITC-labeled mPEG_{5k} with three different concentrations of anti-PEG IgG are shown. The anti-PEG IgG concentrations were based on the results of the MST analysis to cover the relevant range from no binding to full binding. The black squares display the autocorrelation curve for mPEG_{5k}. A shift of the autocorrelation curve toward higher lag times refers to a slower diffusion coefficient and therefore larger hydrodynamic radius (R_h). By applying a fit to the autocorrelation curves using a sum of exponential decays, the change in the average diffusion coefficient after binding can be extracted. With the addition of $0.5 \mu\text{M}$ anti-PEG IgG, the fit is almost the same as for the pure polymer ($R_h = 2.4 \pm 0.2 \text{ nm}$ compared to $R_h = 2.1 \pm 0.2 \text{ nm}$ for the

polymer). This means at a low antibody concentration nearly no interactions between anti-PEG antibodies and PEG could be seen. With a higher concentration of 2.5 μM anti-PEG IgG, the curve shifted towards higher lag times and the size of the fluorescent species increased to an R_h of about 60 ± 6 nm. For the highest concentration of 5.0 μM anti-PEG IgG, the curve shifted further and the size of the fluorescent species increased even more to an R_h of about 117 ± 12 nm. Additionally, confocal laser scanning microscopy (cLSM) images were taken from the bottom of the chamber (**Figure 18b-d**). Comparing the images, an increased aggregation can be observed with increasing anti-PEG IgG concentration. This correlates with the measured increasing R_h .

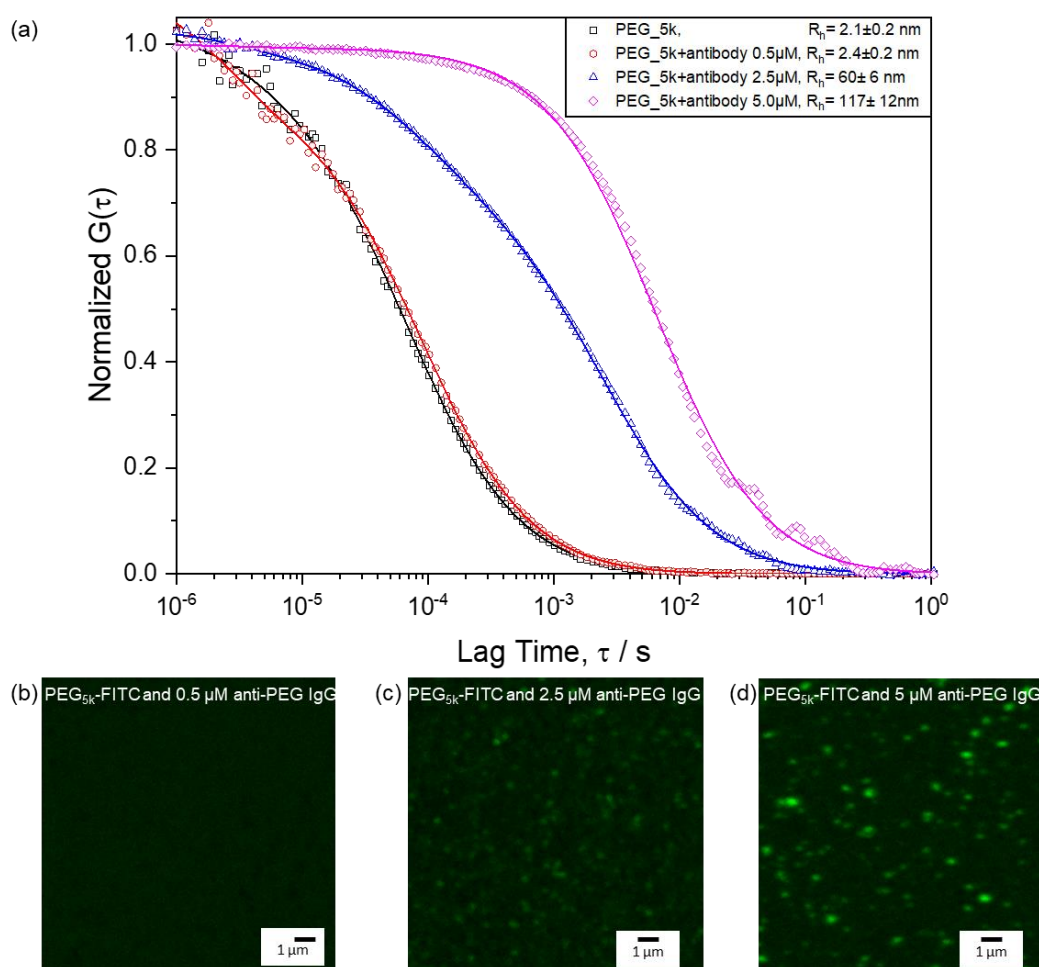


Figure 18. (a) FCS autocorrelation curves and corresponding fits of PEG_{5k}-FITC with different amounts of anti-PEG IgG. Pure PEG_{5k}-FITC (black squares), PEG_{5k}-FITC and 0.5 μM anti-PEG IgG (red circles), PEG_{5k}-FITC and 2.5 μM anti-PEG IgG (blue triangles), PEG_{5k}-FITC and 5.5 μM anti-PEG IgG (pink diamonds). CLSM images of the bottom of the chamber (b) PEG_{5k}-FITC and 0.5 μM anti-PEG IgG, (c) PEG_{5k}-FITC and 2.5 μM anti-PEG IgG, (d) PEG_{5k}-FITC and 5.0 μM anti-PEG IgG.

PEG_{5k} has a molecular weight of 5,000 g mol⁻¹ and around 113 repeating units. For IgG, an R_h of about 6 nm was reported.⁹³ Imagining the polymer chain as a completely stretched chain, where always two antibodies interact with ~16 repeating units, a maximum of 14 antibodies could theoretically bind to the PEG chain. This would correspond to an R_h of about 100 nm. The actual structure in solution is likely different but the theoretical maximum fits well with the observed binding results.

Overall, the shift in the autocorrelation curves indicates a higher extent of binding with an increase in the antibody concentration. For a more detailed analysis on the binding behavior, further investigation is still needed in the future. Nevertheless, the analysis confirms the results obtained by MST.

4.2.4 Conclusion

Competitive ELISA can be used for a qualitative comparison of the binding behavior of anti-PEG antibodies to PEG with different chain lengths and end-groups. Our analysis revealed no difference regarding the end-group, but a stronger binding to PEG_{10k} compared to PEG_{2k} could be observed. Microscale thermophoresis was used for a more detailed analysis and to quantify the binding strength of anti-PEG IgG. The analysis revealed a clear trend that binding strength decreased with decreasing PEG chain length, which is in good agreement with other studies.^{17, 19} Additionally, the binding behavior for anti-PEG IgG to mPEG_{5k} was confirmed by FCS measurements.

4.3 Detection of anti-PEG antibodies in the protein corona

Parts of the following chapters are based on the submitted manuscript “Anti-PEG antibodies enriched in the protein corona of PEGylated nanocarriers impact the cell uptake”. For the thesis, this chapter was extended with additional experiments and details.

PEGylation is widely used and an important approach to both stabilize and prolong the circulation time of colloidal NCs. As soon as NCs enter the bloodstream, the NC surface interacts with proteins to form the so-called “protein corona”, depending on the physico-chemical properties of the material. The protein corona is the biological coating of the NC that creates its biological identity as recognized by cells.^{7, 94} The presence of PEG strongly determines the composition of the protein corona of PEGylated NCs. It decreases unspecific protein adsorption and enriches stealth proteins like clusterin, which in combination reduces macrophage uptake.^{50, 95} However, due to the high abundance of anti-PEG antibodies in the plasma, they could potentially become enriched in the protein corona of PEGylated NCs and induce unwanted side effects. Accordingly, anti-PEG antibodies in the protein corona are likely to be an important factor for the fate of the NCs.²⁵

To study the antibody presence in the protein corona, silica nanocarriers (SiNCs) and polystyrene nanoparticles (PS-NPs) were synthesized and non-covalently PEGylated. Subsequently, the protein corona was formed using undiluted pooled human plasma. The protein corona was analyzed regarding the overall protein content and composition and specifically the anti-PEG IgG concentration. Only anti-PEG IgG was monitored because it is usually present in a higher concentration than anti-PEG IgM and therefore easier to analyze and detect small changes. ELISA was already proven to be a highly sensitive method and was therefore used to analyze anti-PEG IgG in the protein corona.

4.3.1 NC properties

SiNC and PS-NPs were synthesized and PEGylated using the non-covalent PEG-based surfactant Lutensol®.⁹⁶ Via this approach, it is feasible to compare the same NC batch with or without PEGylation and vary the PEG chain length and density systematically without influencing any other physicochemical parameters. For all NCs, the PEG chain molecular weights varied between $\sim 1,000 - 4,000 \text{ g mol}^{-1}$. We chose this particular chain length as it is a typical one used for nanocarrier stabilization ($2,000 - 3,000 \text{ g mol}^{-1}$), yielding an ideal steric stabilization. For example, the currently applied COVID-19 vaccines exhibit PEG chains of this length.²¹ **Table 3** shows transmission electron microscopy (TEM) micrographs and physicochemical characterization data for all SiNC samples investigated in this study. The NC size (hydrodynamic diameter D_h) was determined from multiangle dynamic light scattering (DLS) and ranges between 148 and 212 nm for all SiNCs. **Table 4** shows physicochemical characterization data for all PS-NP samples. The PS-NP size determined from DLS ranges between 171 and 187 nm. The zeta potential is related to the net surface charge of the NCs. As expected, the zeta potential for all PEGylated NCs was slightly negative, while SiNCs with CTMA-Cl exhibited a positive zeta potential.

4.3 Detection of anti-PEG antibodies in the protein corona

Table 3. Characterization of silica nanocarrier systems regarding morphology and physicochemical properties.

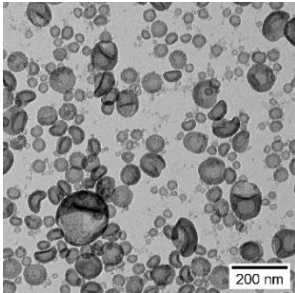
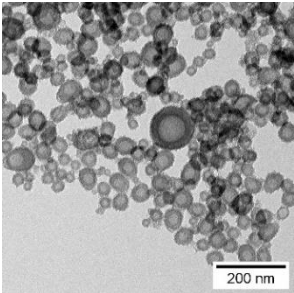
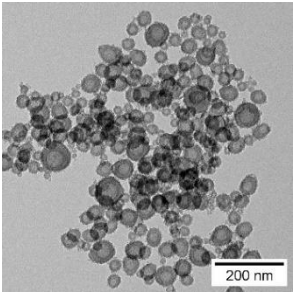
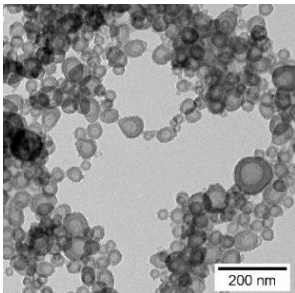
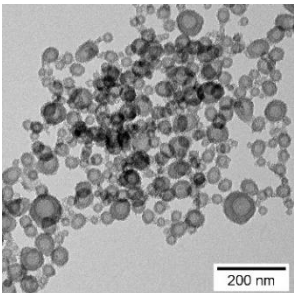
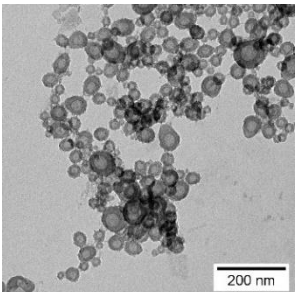
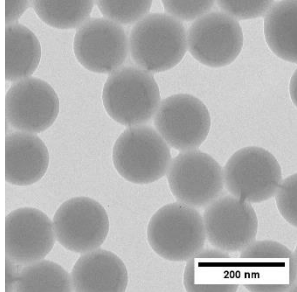
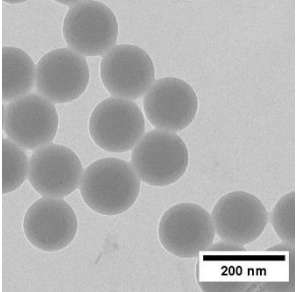
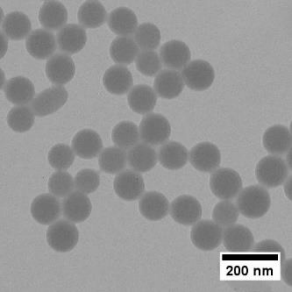
	SiNC-CTMA-Cl	SiNC PEG n=25 medium	SiNC PEG n=50 low
			
Surfactant	Cetyltrimethylammonium chloride (CTMA-Cl)	Lutensol® AT25	Lutensol® AT50
n(Lutensol®) / mol		2.85×10^{-5}	1.42×10^{-5}
M_w PEG / g mol ⁻¹		1,230	2,460
D_h (PDI) / nm	262 ± 65 (0.13)	231 ± 39 (0.14)	153 ± 3 (0.11)
Zeta potential/ mV	$+13 \pm 1$	-2 ± 1	-5 ± 1
	SiNC PEG n=50 medium	SiNC PEG n=50 high	SiNC PEG n=80 medium
			
Surfactant	Lutensol® AT50	Lutensol® AT50	Lutensol® AT80
n(Lutensol®) / mol	2.85×10^{-5}	5.70×10^{-5}	2.85×10^{-5}
M_w PEG / g mol ⁻¹	2,460	2,460	3,940
D_h (PDI) / nm	212 ± 47 (0.25)	164 ± 8 (0.23)	207 ± 34 (0.35)
Zeta potential / mV	-7 ± 1	-9 ± 1	-7 ± 1

Table 4. Characterization of polystyrene nanoparticle systems regarding morphology and physicochemical properties.

	PS-NP PEG n=25	PS-NP PEG n=50	PS-NP PEG n=80
			
Surfactant	Lutensol® AT25	Lutensol® AT50	Lutensol® AT80
n(Lutensol®) / mol	2.85×10^{-5}	2.85×10^{-5}	1.42×10^{-5}
M_w PEG / g mol ⁻¹	1,230	2,460	3,940
D_h / nm	171 ± 11	174 ± 11	187 ± 16
Zeta potential/ mV	-5 ± 1	-5 ± 1	-4 ± 1

4.3.2 Protein corona analysis

We prepared the protein corona using undiluted pooled human plasma and determined the anti-PEG antibody level in this plasma batch by ELISA. The detected anti-PEG IgG concentration was $9.6 \pm 0.8 \mu\text{g mL}^{-1}$, which corresponds to 0.06% of the total immunoglobulins found in this plasma batch (**Table 5**). We analyzed the protein corona using different methods to establish the overall protein concentration by Pierce assay and the detailed protein composition in the protein corona by LC-MS. Results for SiNCs can be found in **Table 5** and **Figure 19** and results for PS-NPs in **Table 6** and **Figure 20**.

All PEGylated NCs show a similar protein composition with lipoproteins as their most abundant protein, especially apolipoprotein A1 for the SiNCs and clusterin for the PS-NPs were enriched. Those are known as stealth proteins and are often enriched on PEGylated NCs.^{97,98}

4.3 Detection of anti-PEG antibodies in the protein corona

Table 5. LC-MS identification of proteins found on SiNCs with different stabilization. Proteins were grouped according to function and pure pooled citrate plasma is shown as a reference. Values are represented in % based on all identified proteins. The protein group with the highest abundance was highlighted in grey. LC-MS analysis was performed by R. da Costa Marques.

	plasma (reference)	CTMA-Cl	PEG n=50 low	PEG n=50 medium	PEG n=50 high	PEG n=25 medium	PEG n=80 medium
Acute Phase	6.03	0.01	0.06	0.13	0.21	0.09	0.04
Coagulation	4.39	79.62	7.58	13.63	13.74	6.18	10.52
Complement	4.54	2.65	1.33	2.58	1.84	2.87	2.54
Immunoglobulins	25.28	1.87	2.41	2.44	2.70	1.34	2.52
Lipoproteins	1.57	8.99	56.12	67.35	63.95	79.72	72.25
Other Plasma Components	7.84	1.63	5.53	2.95	3.63	1.36	2.53
Serum Albumin	50.06	1.14	14.61	1.24	1.70	0.29	0.79
Tissue Leakage	0.30	4.10	12.36	9.67	12.24	8.16	8.81

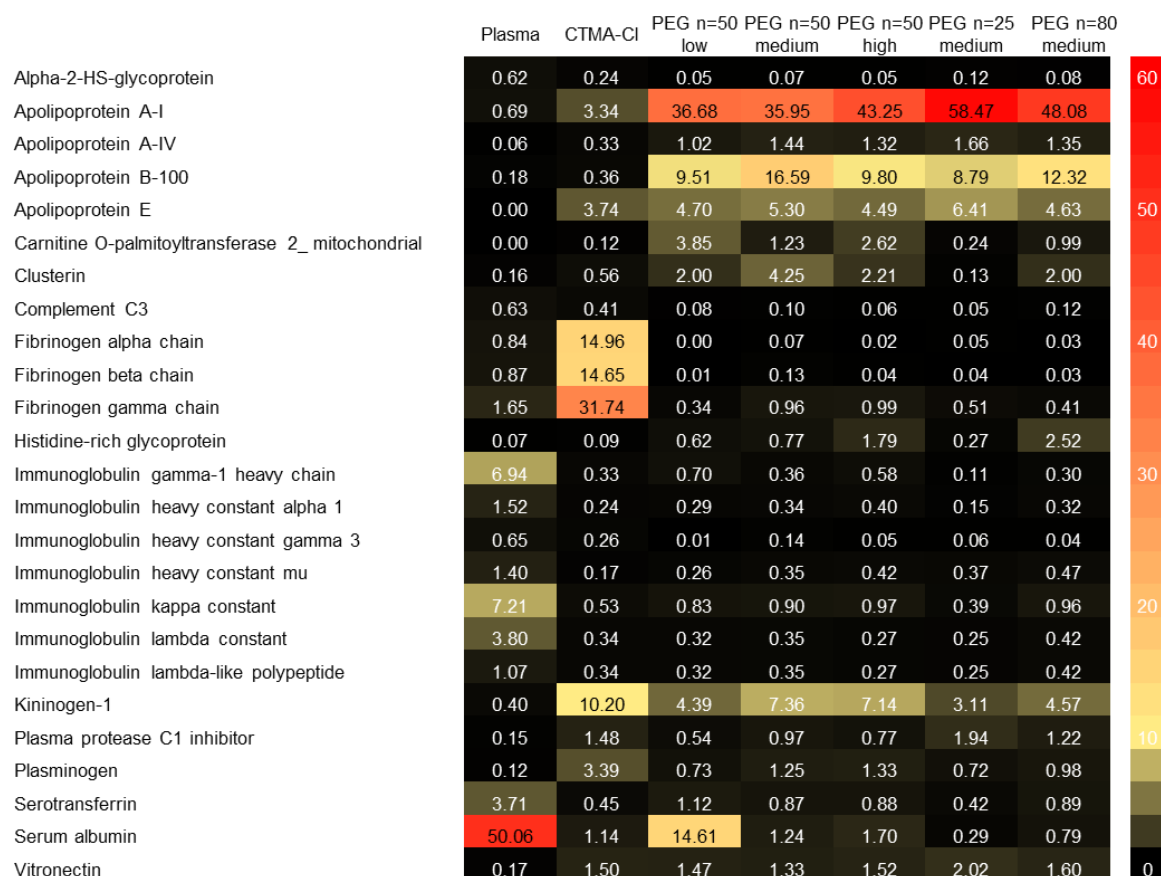


Figure 19. LC-MS identification of proteins found on SiNCs with different stabilization. Heatmap indicating the most abundant proteins (Top 25) in the pure plasma (reference) and protein corona. Values are represented in % based on all identified proteins. LC-MS analysis was performed by R. da Costa Marques.

4.3 Detection of anti-PEG antibodies in the protein corona

Table 6. LC-MS identification of proteins found on PS-NP with different stabilization. Proteins were grouped according to function and pure pooled citrate plasma is shown as a reference. Values are represented in % based on all identified proteins. The protein group with the highest abundance was highlighted in grey. LC-MS analysis was performed by R. da Costa Marques.

	plasma (reference)	PEG n=25	PEG n=50	PEG n=80
Acute Phase	6.03	0.34	0.48	0.49
Coagulation	4.39	0.55	0.60	0.94
Complement	4.54	0.22	0.26	0.61
Immunoglobulins	25.28	1.80	1.84	3.48
Lipoproteins	1.57	64.04	63.66	74.86
Other Plasma Components	7.84	0.23	0.50	0.66
Serum Albumin	50.06	0.87	0.75	1.55
Tissue Leakage	0.30	31.95	31.92	17.40

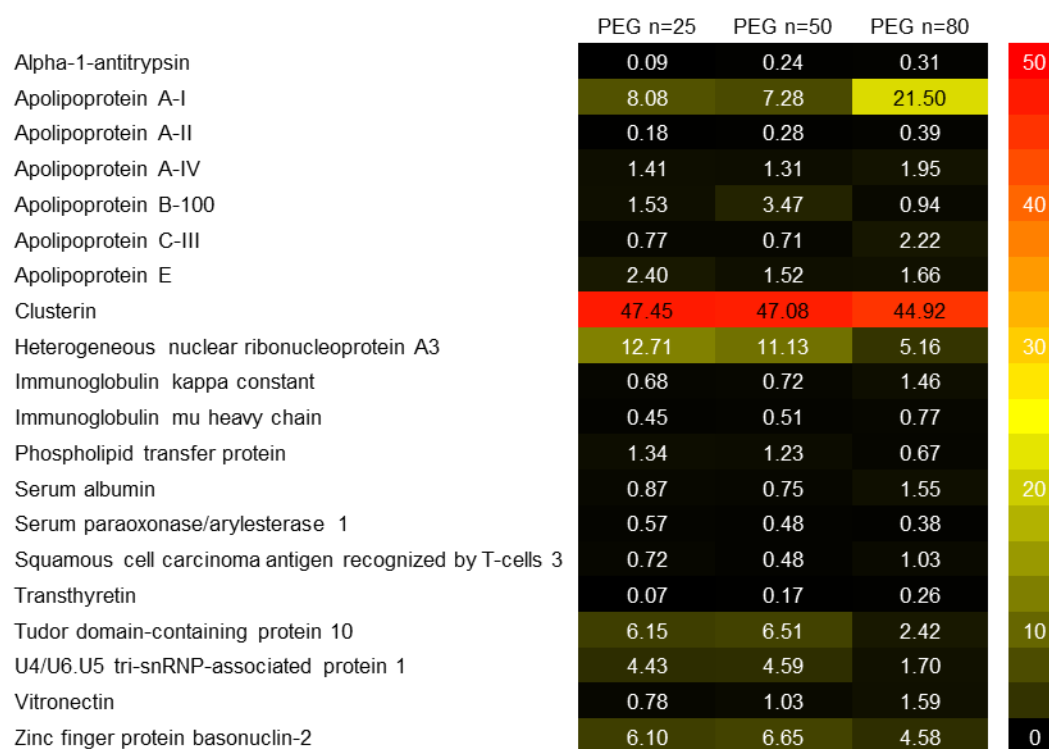


Figure 20. LC-MS identification of proteins found on PS-NP with different stabilization. Heatmap indicating the most abundant proteins (Top 20) in the protein corona. Values are represented in % based on all identified proteins. LC-MS analysis was performed by R. da Costa Marques.

4.3.3 Anti-PEG antibody quantification

We used flow cytometry as the first method to detect changes in anti-PEG IgG concentration in the protein corona. A secondary antibody binds to the F_c part of anti-PEG IgG in the protein corona and can be fluorescently quantified with flow cytometry. The detailed method is described in chapter 5.5.4 and the median fluorescence intensity (MFI) and percent of fluorescence positive events can be seen in **Figure 21**. The protein corona was formed using plasma samples with a low, medium, and high anti-PEG IgG concentration, the same samples were used for the cell uptake and are explained in more detail in chapter 4.4.1. Additionally, two different amounts of secondary antibody were tested. To detect anti-PEG IgG in the protein corona a fluorescently labeled secondary anti-human IgG antibody was used. This secondary antibody is not specific to anti-PEG IgG in the protein corona but to all IgG. Still, increasing IgG concentrations could be detected with this method, which also correlates to an increasing anti-PEG IgG concentration in the protein corona. Overall, there was more IgG detected in the sample with high anti-PEG IgG concentration. Nevertheless, it is only a qualitative measurement. It cannot be used to quantify anti-PEG IgG concentration in the protein corona but it was possible to see a trend. A different method is necessary to quantify anti-PEG antibody concentration in protein corona.

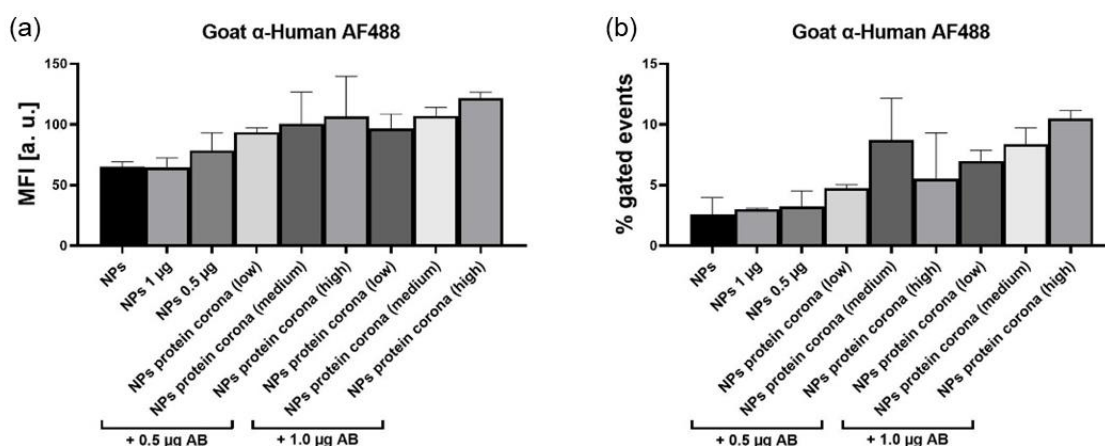


Figure 21. Flow cytometry results to analyze anti-PEG IgG in the protein corona on SiNCs (NPs). Protein corona was prepared with different amounts of anti-PEG IgG in the plasma (low, medium, and high) and two different amounts of secondary antibody (AB). (a) Median fluorescence intensity (MFI), (b) percent of fluorescence positive events.

Next, ELISA was used to measure the anti-PEG IgG concentration in the protein corona samples. **Figure 22** shows the scheme of protein corona analysis and the corresponding results of SiNCs. For a more detailed comparison, the fraction of anti-PEG IgG antibodies of the total immunoglobulin concentration is displayed in **Figure 22c**.

The overall determined protein amount was similar for all PEGylated SiNCs, as expected from the general effect of PEGylation, while SiNC-CTMA-Cl showed a significantly higher number of adsorbed proteins. Additionally, we detected a slightly higher concentration of immunoglobulins in the protein corona of CTMA-Cl stabilized NCs. In contrast, PEGylated NCs exhibited the highest concentration and fraction of anti-PEG IgG in the protein corona. We observed no significant difference in anti-PEG IgG fraction in the protein corona derived from NCs with a PEG chain length of $n=50$ or $n=80$ PEG repeating units and a medium or high surface density. In contrast, a lower surface density of PEG led to a slight decrease of anti-PEG IgG fraction in the protein corona. This was even more noticeable when a shorter PEG chain length ($n=25$ repeating units) was present on the NC surface.

This trend agrees with the determined binding affinities as mentioned before, which increased with longer PEG chains. In general, anti-PEG IgG is enriched in the protein corona of PEGylated NCs compared to non-PEGylated NCs or human plasma. Our results indicate that a certain density and chain length was necessary for a “saturation” of the protein corona with anti-PEG antibodies. Afterwards, higher density or longer chain length did not lead to increased binding of anti-PEG antibodies.

Interestingly, even the CTMA-Cl NCs showed a slight enrichment of anti-PEG IgG compared to plasma levels. It is not clear what the reason for this enrichment is, but it might be related to the charge of the NCs. It is known that especially charged surfaces induce interactions with immunoglobulins, but so far this effect was not investigated on the level of specific antibodies.^{47, 99}

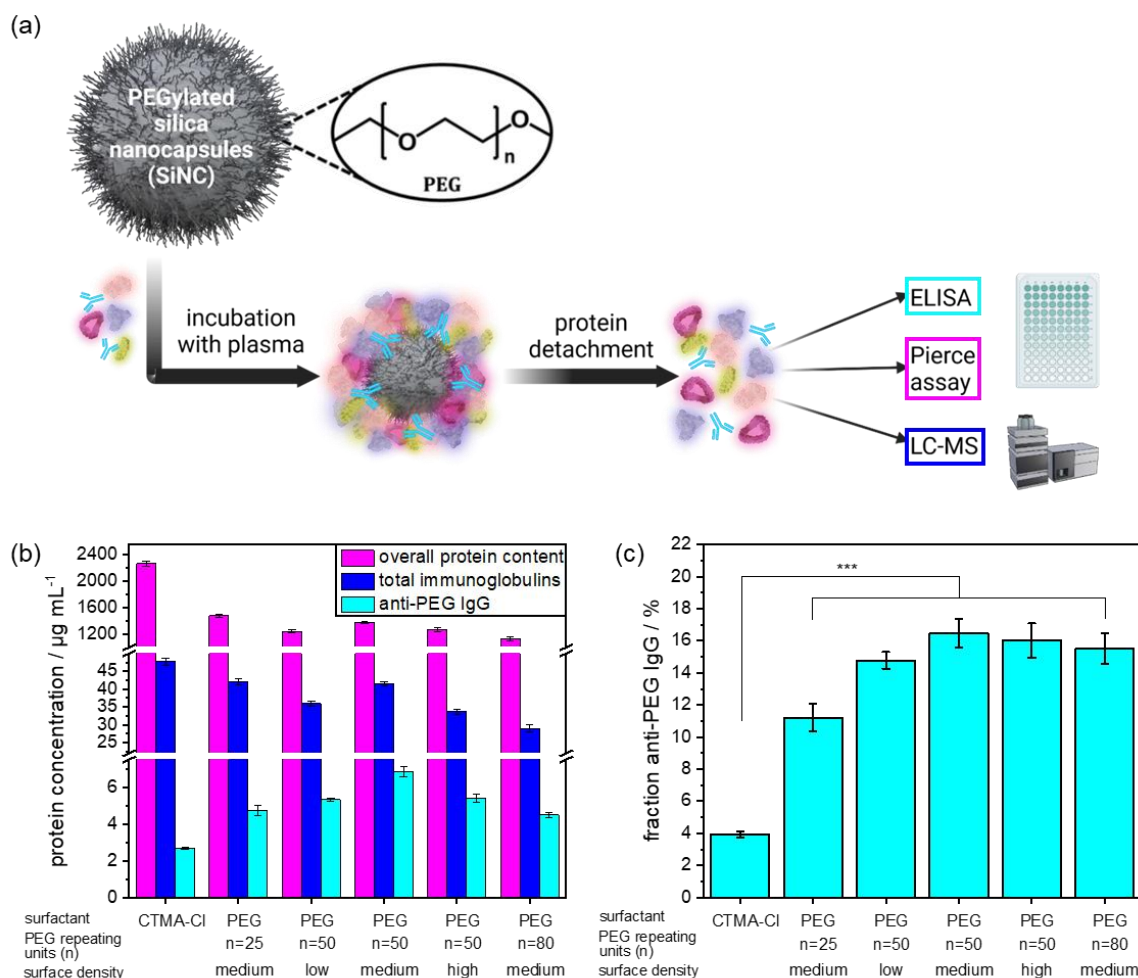


Figure 22. Investigation of anti-PEG IgG presence in the protein corona of SiNCs. Values are mean values with a standard deviation of three replicates. (a) Scheme of protein corona preparation and analysis (b) Protein concentration in the protein corona depending on the presence of PEG on the SiNC surface, for a normalized NC surface area of 0.05 m² per sample. Purple: overall protein concentration of all plasma proteins as analyzed by a Pierce assay, blue: total immunoglobulin concentration as analyzed with LC-MS (percentage of total proteins converted to concentration based on Pierce assay), cyan: anti-PEG IgG concentration analyzed by ELISA. (c) Fraction of anti-PEG IgG concentration compared to the total concentration of immunoglobulins. The analysis of variance (ANOVA) one-way test was used for statistical analysis yielding *** $p < 0.001$, corresponding to the difference between CTMA-Cl and PEG-stabilized NCs.

The protein corona of PS-NPs was analyzed the same way. However, the detached protein corona could not be examined regarding the anti-PEG IgG concentration as before. The samples showed a generally low absorbance (around LOQ) and low competition (<35%). The competition needs to be >35% to confirm specific binding and exclude random absorbance.

4.3 Detection of anti-PEG antibodies in the protein corona

Multiple variables were changed to optimize the measurement as it can be seen in **Table 7**. First, we suspected the anti-PEG IgG concentration to be too low to measure. Therefore, we used higher concentrated protein corona samples. The protein concentration did not seem to be the issue, but other substances might have been influencing the analysis. To examine the influence of the detergents like sodium dodecyl sulfate (SDS) and Lutensol®, SDS was removed before the ELISA analysis. Additionally, an alternative protein detachment with urea/thiourea was tested. Potentially free Lutensol® was removed by centrifugation before protein corona preparation. After excluding SDS and Lutensol® from the suspect list, we tested covalently PEGylated PS-NPs. The absorbance in the ELISA measurement was above LOQ and therefore sufficient to analyze, but the competition was still below 35%. Lastly, we spiked the protein corona samples with a known amount of anti-PEG IgG right before the ELISA analysis. The results can be seen in **Figure 23a**. Still, no increase in absorbance could be detected. In comparison, the expected increase in the absorbance could be seen for the protein corona of SiNCs, when spiking with anti-PEG IgG was performed (**Figure 23b**). We also treated pure plasma the same as the protein corona formation (centrifugation, addition of SDS, heating) but it was still possible to analyze and the spiking with anti-PEG standard showed an increase in absorbance.

In summary, PS-NPs seem to behave differently than SiNCs and affect the protein corona more than expected. Maybe PS residues prohibited the ELISA measurement. Further analysis is necessary, also with different particle systems, to obtain a better understanding of how the NP material influences the protein corona and subsequent ELISA measurement.

Table 7. Changed variables to optimize ELISA measurements for the analysis of anti-PEG IgG after protein detachment on PS-NPs. X means tested and failed.

	Absorbance below LOQ	Competition <35%
Higher concentrated protein corona samples	X	X
SDS removal before ELISA	X	X
Alternative detachment with urea/thiourea	X	X
Removal of potentially free Lutensol® before protein corona preparation	X	X
Covalently PEGylated PS-NPs		X

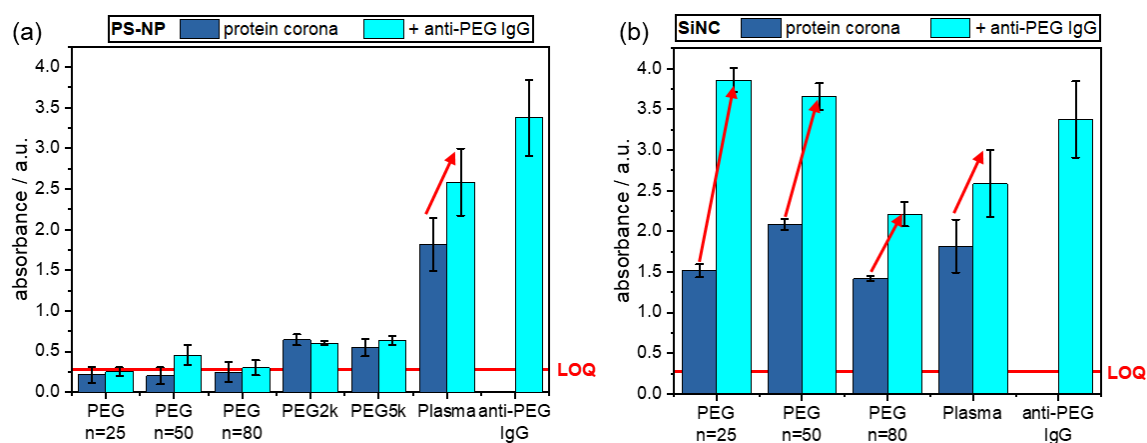


Figure 23. ELISA measurements of the protein corona. Normal protein corona samples and addition of anti-PEG IgG standard directly before the ELISA measurement. (a) Protein corona on non-covalently PEGylated PS-NPs (PEG n=25, 50 and 80) and covalently PEGylated PS-NPs (PEG2k and PEG5k) (b) protein corona non-covalently PEGylated SiNCs. Red arrows indicate increase in absorbance with the addition of anti-PEG IgG standard.

4.3.4 Conclusion

To study the anti-PEG antibody presence in the protein corona of PEGylated particles, SiNCs, and PS-NPs were synthesized. They were PEGylated with the non-covalent PEG-based surfactant Lutensol® to compare the same NC batch with or without PEGylation and vary the PEG chain length and density systematically.

The protein corona was analyzed using a Pierce assay and LC-MS to determine the overall protein content and composition. As expected, the PEGylated NCs showed an enrichment in stealth proteins like apolipoprotein A1 (SiNCs) and clusterin (PS-NPs).

It was possible to analyze the protein corona regarding the anti-PEG antibody content with flow cytometry, but this is only a qualitative measurement. ELISA can be used to quantify the anti-PEG antibody concentration in the detached protein corona. The analysis of the protein corona on SiNCs revealed an enrichment of anti-PEG IgG on PEGylated SiNCs compared to non-PEGylated. In the protein corona of PS-NPs anti-PEG IgG could not be detected with ELISA. Here, further investigation into the influence of the NC material is still needed.

4.4 Effect of anti-PEG antibodies in the protein corona on cell uptake

The following chapter 4.4.2 is based on the submitted manuscript “Anti-PEG antibodies enriched in the protein corona of PEGylated nanocarriers impact the cell uptake”. For the thesis, this chapter was extended with additional experiments and details.

PEGylation in general often leads to a decrease of unspecific protein adsorption and enrichment of stealth proteins like clusterin, which in combination helps to reduce unspecific cellular uptake.⁵⁰ The results of the protein corona analysis revealed that anti-PEG IgG was enriched in the protein corona of PEGylated SiNCs, which was not yet reported for any NC system. We monitored the cellular uptake in RAW 264.7 (murine) and THP-1 (human) macrophages of PEGylated SiNCs with varying amounts of adsorbed anti-PEG antibodies to further investigate the consequences of anti-PEG antibodies in the protein corona. We only used SiNCs to monitor the cell uptake because the protein corona on PS-NP was not possible to characterize with ELISA (see chapter 4.3.3), but we expect a similar behavior for both NC systems.

4.4.1 Defined protein corona

To analyze the effect of anti-PEG antibodies in the protein corona on cell uptake, we chose one NC system and varied the anti-PEG antibody concentration in the protein corona. We used SiNCs with a medium PEG chain length ($n=50$) and density because they showed the highest fraction of anti-PEG antibodies in the protein corona compared to non-PEGylated SiNCs. Plasma samples from the plasma screening were selected and pooled to obtain plasma batches with systematically pre-determined anti-PEG IgG concentrations. We pooled 5 plasma samples each with a resulting low ($<0.5 \mu\text{g mL}^{-1}$), medium ($9.6 \mu\text{g mL}^{-1}$), and high ($110.5 \mu\text{g mL}^{-1}$) anti-PEG IgG concentration. We used these pooled plasma samples to form the protein corona with a varied presence of anti-PEG IgG together with a sample containing the protein corona formed from pure anti-PEG IgG as a positive control. For anti-PEG IgG, a protein concentration roughly equivalent to the “high” anti-PEG IgG concentration ($120 \mu\text{g mL}^{-1}$) was chosen for incubation.

4.4.2 Uptake in RAW macrophages and THP-1 cells

After protein corona formation, the SiNCs were incubated with both macrophage cell lines. The schematic setup for the protein corona formation and cell uptake can be seen in **Figure 24a**. We investigated their cellular uptake in terms of percent of fluorescence positive cells (**Figure 24b, d**) and median fluorescence intensity (MFI) (**Figure 24c, e**). The results from the MFI measurement show a trend similar to the fluorescence positive cells although not as noticeable.

In RAW 264.7 macrophages, the cellular uptake steadily increased with increasing anti-PEG IgG concentration in the protein corona, referring to the fraction of fluorescence positive cells. In particular, the uptake of NCs with only anti-PEG IgG in the protein corona was significantly higher than those NCs with very little anti-PEG IgG present. The general uptake in human THP-1 macrophages was similar to RAW 264.7. The uptake of NCs with pooled plasma containing different concentrations of anti-PEG IgG displayed only a very slight increase with anti-PEG IgG concentration; whereas the uptake doubled when the protein corona was formed only from anti-PEG IgG. These results are in good agreement with the generally increased uptake in macrophages of NCs with a high concentration of immunoglobulins in the protein corona. It is known that IgG enrichment in the protein corona can lead to significantly increased uptake in macrophages via F_c -receptor-mediated endocytosis.⁴⁸ Therefore, we performed F_c -receptor blocking experiments to evaluate this uptake mechanism. Anti-CD16, anti-CD 32, and/or anti-CD 64 were added before incubation of cells with NCs (**Figure 25**). The receptors CD16/32 (binding aggregated IgG with low affinity for the ligand¹⁰⁰) and CD 64 (binding monomeric IgG with high affinity for the ligand¹⁰¹) were either blocked individually or all three were blocked at the same time. In RAW 264.7 macrophages, blocking all F_c -receptors led to significantly lower uptake of NCs with high anti-PEG IgG concentration or only anti-PEG IgG in the protein corona. In THP-1 cells, the uptake after blocking was slightly decreased, especially when CD64 was blocked. This agrees with previous studies including F_c blocking in THP-1 cells, highlighting that human macrophages are more complex than mouse macrophages and various uptake mechanisms are probably involved.⁴⁸ Further investigations together with the examination of other human cell lines and in vivo experiments will be necessary in the future to evaluate the uptake mechanisms.

4.4 Effect of anti-PEG antibodies in the protein corona on cell uptake

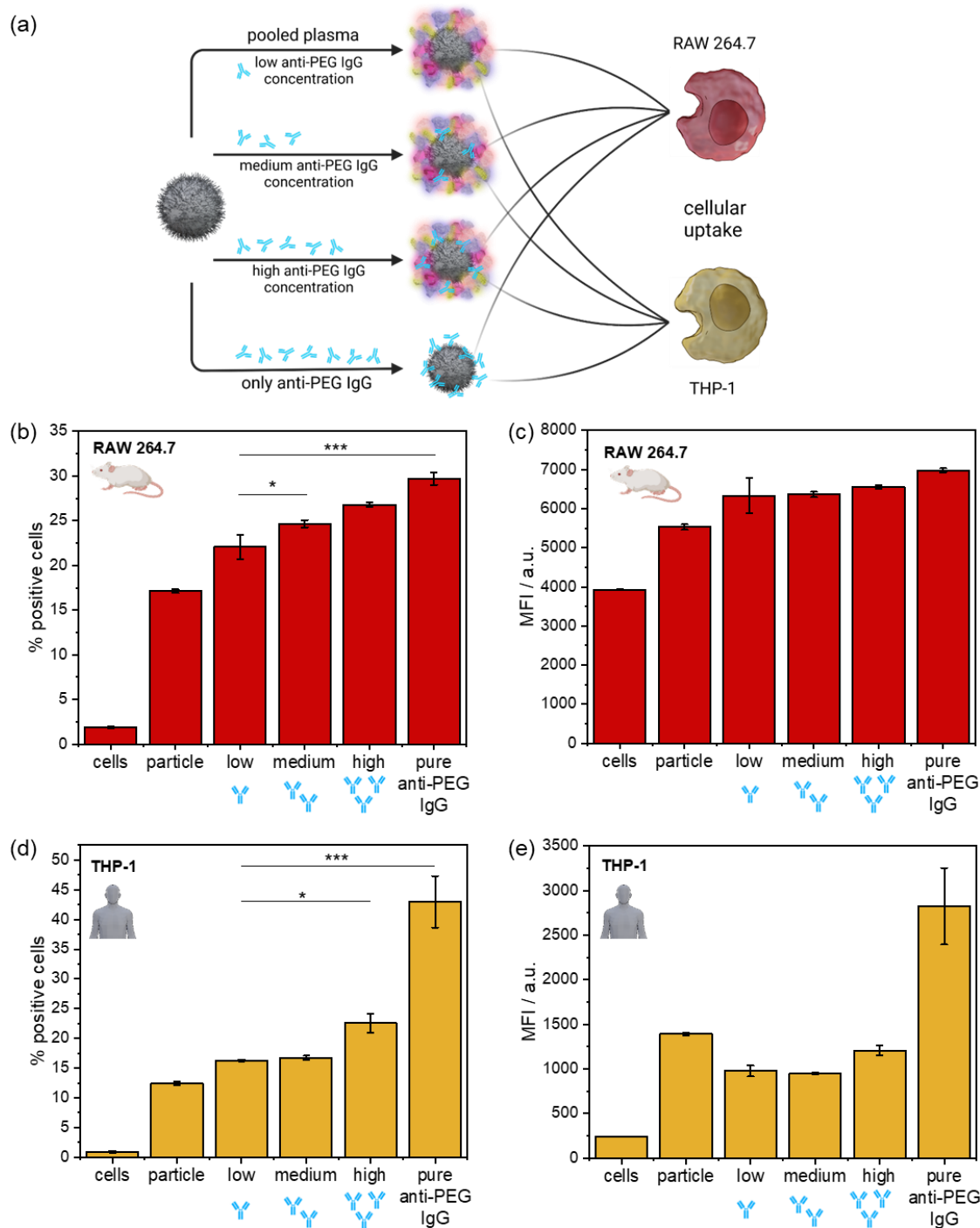


Figure 24: Cellular uptake of SiNCs coated with proteins including an increasing concentration of anti-PEG IgG. Values are mean values with standard deviation of three biological replicates. The analysis of variance (ANOVA) two-way test was used for statistical analysis yielding * $p < 0.05$, *** $p < 0.001$, corresponding to the individual types of protein corona. (a) Schematic overview of the experimental scheme. (b, c) Uptake in murine RAW264.7 macrophages, displayed in % of fluorescence positive cells and median fluorescence intensity (MFI). (d, e) Uptake in human THP-1 macrophages, displayed in % of fluorescence positive cells and median fluorescence intensity (MFI). For the negative control, only cells without any addition of NCs were measured.

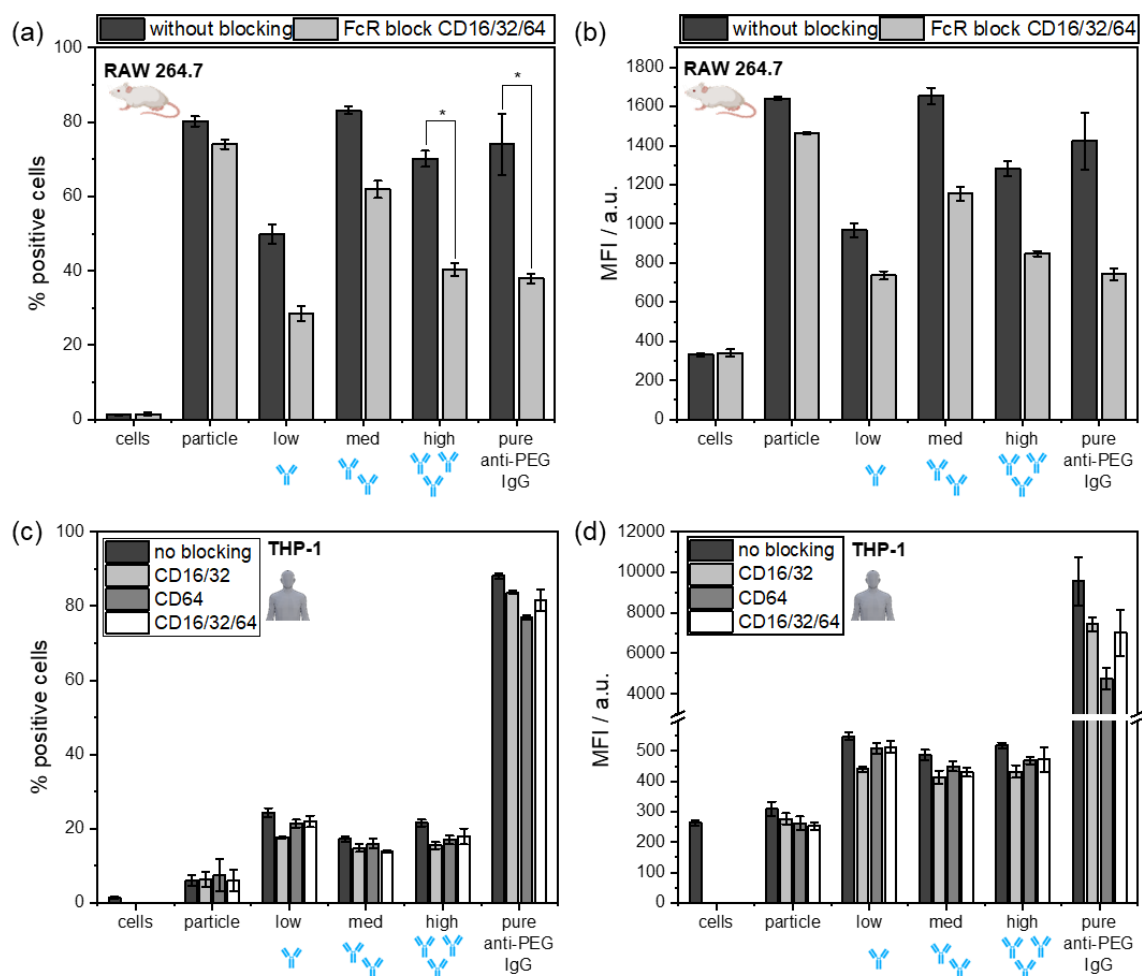


Figure 25: Fc blocking experiments of SiNCs with protein corona including an increasing concentration of anti-PEG IgG. Plasma samples with a low ($<0.5 \mu\text{g mL}^{-1}$), medium ($9.6 \mu\text{g mL}^{-1}$), and high ($110.5 \mu\text{g mL}^{-1}$) anti-PEG IgG concentration were used for the protein corona preparation. Additionally, pure anti-PEG IgG was used as a positive control. For the negative control, only cells without any addition of NCs were measured. CD16/CD32 (binding aggregated IgG with low affinity for the ligand) and CD64 (binding monomeric IgG with high affinity for the ligand) receptors were either blocked individually or all three at the same time. Uptake at 4°C in murine RAW264.7 macrophages, displayed in % positive cells (a) and median fluorescence intensity (MFI) (b). Uptake at 4°C in human THP-1 macrophages, displayed in % positive cells (c) and median fluorescence intensity (MFI) (d). Values are mean values with standard deviation of three biological replicates. The analysis of variance (ANOVA) two-way test was used for statistical analysis yielding $*p < 0.05$ corresponding to blocked/unblocked receptors.

4.4 Effect of anti-PEG antibodies in the protein corona on cell uptake

Further, we evaluated the cytokine response in RAW 264.7 (**Figure 26**). Cytokine testing was performed by Dr. Michael Fichter (MPI-P/University Medical Center). Cytokines are soluble polypeptides and play an important role in immunological reactions and in inflammatory processes. They are distinguished between pro- and anti-inflammatory cytokines.¹⁰² All SiNC systems showed a similar, low cytokine response, especially when compared to the positive control. The most important cytokine for macrophage activation is IFN- γ produced by TH1 cells.¹⁰³ This exhibited a low secretion throughout all samples.

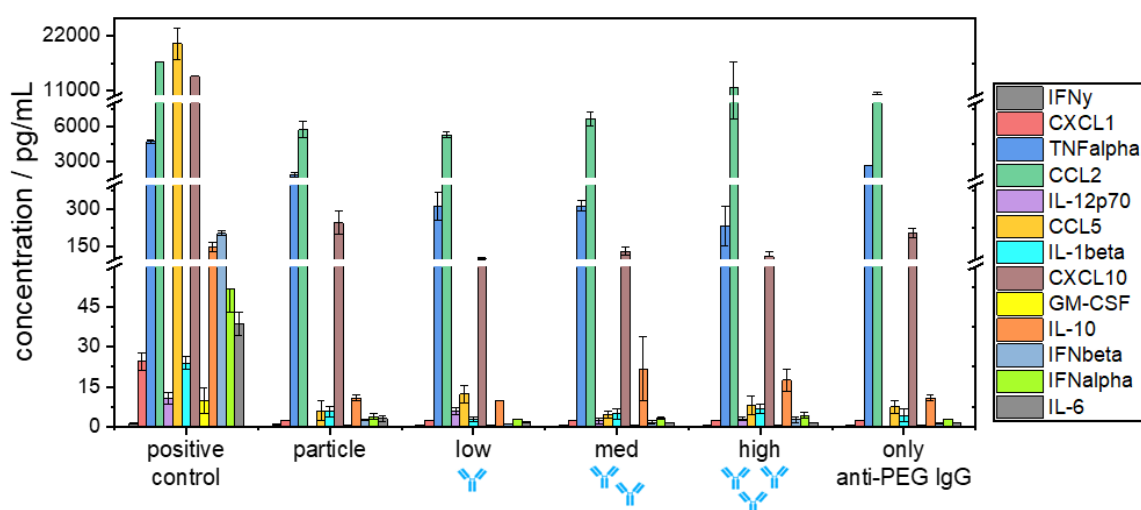


Figure 26: Quantification of cytokine secretion by RAW 264.7 macrophages. Cell culture supernatants were collected 2 h following coincubation with $75 \mu\text{g mL}^{-1}$ NC and $5 \mu\text{L}$ per sample was used for cytokine quantification performed using a multiplex protein quantification assay.

Overall, as anti-PEG quantities increased in the corona, an enhanced cell uptake in mouse and human macrophages was detected. In general, IgG acts as an opsonin, meaning when present in the corona it promotes the internalization of NCs into phagocytosing cells.¹⁰⁴ Accordingly, our observed increased uptake in macrophages might not be anti-PEG antibody specific, but a general result of an increased presence of immunoglobulins in the protein corona. Due to sensitivity reasons, we were not able to analyze the presence of IgM in the protein corona and its consequences for cellular uptake. However, we expect a similar trend but with generally lower concentrations. Many studies reported that anti-PEG antibodies can be elicited by PEGylated drugs or drug delivery systems and are therefore

likely to be responsible for accelerated blood clearance.¹⁰⁵⁻¹⁰⁷ This described anti-PEG antibody response was found to be predominately IgM related for empty PEGylated liposomes and IgG related for PEGylated proteins or lipid NCs with encapsulated nucleotides.¹⁰⁸⁻¹¹⁰ Both antibody classes can efficiently activate the complement system via different pathways and subsequently promote phagocytosis and clearance.^{16, 71} As already mentioned, rare cases of anaphylaxis following COVID-19 vaccine administration have been reported.¹¹¹ In contrast to complement system activation, anaphylaxis is usually IgE-mediated.¹¹² Zhou *et al.* recently developed a bead assay to determine anti-PEG IgG, IgM, and IgE.¹¹³ They reported PEGylated drug-associated anaphylaxis was due to specific anti-PEG IgE-mediated type 1 hypersensitivity. Due to the low concentration of anti-PEG IgE in the plasma and the limitation of the ELISA setup, it has not been possible to analyze anti-PEG IgE concentration so far. In the future, it would be extremely interesting to examine also IgE plasma levels and evaluate the interaction of IgE with PEGylated NCs.

Following our results, the existence of anti-PEG antibodies in the bloodstream needs to be considered when designing NCs. Their presence in the protein corona of PEGylated NCs may well mitigate the stealth effect of PEG, leading to higher uptake in macrophages and additionally inducing unwanted side effects as mentioned above.

The composition of the protein corona depends on various factors - primarily the physico-chemical properties of the NCs. Many researchers attempt controlling the composition of the proteins adsorbed to NCs to prevent clearance by immune cells.¹¹⁴ To obtain further insight into the role of anti-PEG antibodies and generalize their effect, additional PEGylated and unPEGylated NC systems need to be investigated. Due to the high concentration of anti-PEG antibodies in the blood stream, they might also accumulate non-specifically in the protein corona. Thus, it is also of great interest to explore more widely which antibody types are found among the immunoglobulins in the protein corona.

4.4.3 Conclusion

We monitored the cellular uptake in RAW 264.7 (murine) and THP-1 (human) macrophages of PEGylated SiNCs to analyze the effect of anti-PEG antibodies in the protein corona on cell uptake. In RAW 264.7 macrophages, the cellular uptake steadily increased with increasing anti-PEG IgG concentration in the protein corona. The uptake in human THP-1 macrophages was similar to RAW 264.7, especially the uptake doubled when the protein corona was formed only from anti-PEG IgG.

The F_c-receptor blocking experiments revealed a significantly lower uptake of NCs with high anti-PEG IgG concentration in the protein corona. This effect was more prominent in RAW 264.7 than in THP-1 macrophages.

5 Experimental

5.1 Materials

All plasma samples were obtained from the Transfusion Medicine Department at the University Medical Centre of the Johannes Gutenberg University Mainz. Blood samples for the plasma screening were collected from 500 healthy donors after obtaining informed consent. All experiments containing human blood plasma from these donors were approved by the ethics committee of the Landesärztekammer Rheinland-Pfalz, Mainz No. 2019-14748. To obtain pooled plasma for protein corona formation, blood was taken from 10 healthy donors after obtaining informed consent and pooled subsequently. All experiments containing human blood plasma from these donors were approved by the ethics committee of the Landesärztekammer Rheinland-Pfalz, Mainz No. 837.439.12 (8540-F). Accordingly, all experiments involving human material were performed in compliance with all relevant laws and guidelines.

After collection, the citrate plasma (either individual samples or pooled plasma) was centrifuged at 20,000 g for 1 h at room temperature to remove residual protein precipitates and stored at -80 °C until further use.

5.1.1 Proteins and cell uptake reagents

Chimeric human anti-PEG IgG (clone no. c3.3 IgG) and chimeric human anti-PEG IgM (clone no. cAGP4-IgM) were purchased from IBMS Academia Sinica (Taipei, Taiwan) and used without further purification. Anti-Human IgG (F_c specific) – peroxidase antibody, HRP-conjugated goat F(ab')₂ antihuman IgM Fc_{5μ}, For the cell uptake, Dulbecco Modified Eagle Medium (DMEM, Gibco, USA), Roswell Park Memorial Institute (RPMI)-1640 (Gibco, Germany), fetal bovine serum (FBS, Gibco, Germany), penicillin (Gibco, Germany), streptomycin (Gibco, Germany), glutamine (Gibco, Germany), phorbol-12-myristate-13-acetate (PMA) (Sigma-Aldrich, Germany), trypsin (Gibco, Germany), Zombie Aqua (BioLegend, USA), anti-CD64, CD16, and/or CD32 (BioLegend, USA) were used. Sodium dodecyl sulfate (SDS, SERVA Electrophoresis GmbH, Germany),

tris(hydroxymethyl)aminomethane hydrochloride (Tris*HCl), Pierce 660 nm Assay (Thermo Scientific, Germany), bovine serum albumin (BSA, Serva, Germany) were used as received for protein corona experiments.

5.1.2 Other reagents

Poly(ethylene glycol) diamine (average $M_n = 10,000 \text{ g mol}^{-1}$) and poly(ethylene glycol) (average $M_n = 10,000 \text{ g mol}^{-1}$) were acquired from Sigma-Aldrich, USA. Dulbecco's phosphate buffered saline (PBS, Thermo Fisher Scientific, USA), skim milk powder (VWR International, USA), 3-[(3-Cholamidopropyl)dimethylammonio]-1-propanesulfonate (CHAPS, Merck, Germany), 2,2'-Azino-bis(3-ethylbenzthiazoline-6-sulfonic acid) (ABTS, Merck, Germany) and QuantaBlu Fluorogenic Peroxidase Substrate Kit (Thermo Fisher Scientific, Waltham, USA) were further used for assay experiments. Methoxy-terminated poly(ethylene glycol)-fluorescein (2k, 5k, 10k, 20k) (Creative PEGWorks, USA) and fluorescein isothiocyanate-dextran (Sigma-Aldrich, USA) were purchased for binding studies. Tetraethoxysilane (TEOS, 98%, Alfa Aesar, Germany), hexadecane (98%, TCI, Germany), olive oil (highly refined, low acidity, Sigma-Aldrich, USA), and cetyltrimethylammonium chloride (CTMA-Cl, Acros Organics, 99%), (3-aminopropyl)triethoxysilane (APTES, 99%, Sigma-Aldrich, USA), amine-reactive fluorescent dye Cyanine5 NHS ester (Cy5-NHS, Lumiprobe GmbH, Germany), Lutensol® AT50 (poly(ethylene glycol)-hexadecyl ether) (BASF SE, Germany), Lutensol® AT25 (BASF SE, Germany) and Lutensol® AT80 (BASF SE, Germany), 2,20-azobis(2-methylbutyronitrile) (V59, Wako Chemicals), freshly distilled styrene (Acros Organics, USA) were used for NC synthesis.

5.2 Methods and Instrumentation

5.2.1 Enzyme linked immunosorbent assay (ELISA)

The ELISA experiments were performed based on a previously published procedure from Chen *et al.*¹⁷ Chimeric human anti-PEG IgG (clone no. c3.3 IgG) was used as a standard. Maxisorp 96-well microplates (Thermo Fisher Scientific, Waltham, USA) were coated with 0.5 μg $\text{NH}_2\text{-PEG}_{10000}\text{-NH}_2$ in 50 μL 0.1 M $\text{NaHCO}_3/\text{Na}_2\text{CO}_3$ buffer (adjusted to pH 9.5) per well overnight at 4 °C. Afterwards, the content of the wells was discarded and the well blocked with 200 μL of 5% (w/v) skim milk powder in Dulbecco's phosphate-buffered saline (PBS, Thermo Fisher Scientific) per well at room temperature for 2 h. Plates were washed once with 100 μL PBS per well immediately before use. In wells where no competition took place, 50 μL of 2% (w/v) skim milk in PBS was added. The wells were incubated for 30 min at room temperature. For each sample (including standards), 60 μL of the sample were diluted with 120 μL of 2% (w/v) skim milk in PBS (33%-dilution). 50 μL of these 33%-diluted samples were added to the respective well and incubated for 1 h at room temperature. Unbound antibodies were removed by washing the plates twice with 0.1% 3-[(3-cholamidopropyl)-dimethylammonio]-1-propanesulfonate (CHAPS) in PBS and once with pure PBS. Afterwards, 50 μL of anti-human IgG-peroxidase antibody (0.25 mg L^{-1} in 2% (w/v) skim milk in PBS, F_c -specific) was added to each well and incubated for 1 h at room temperature. The content of the wells was discarded, and each well was washed four times with 100 μL 0.1% (w/v) CHAPS in PBS and once with 100 μL pure PBS. Then, 100 μL ABTS substrate was added per well and incubated for 30 min in the dark. The absorbance was measured at $\lambda = 405$ nm in a microplate reader (Tecan infinite M1000 plate reader, Switzerland).

For the competition experiment, the well plate was prepared as described. After blocking with skim milk for 2 h, 50 μL of poly(ethylene glycol) (5 g L^{-1} in 2% (w/v) skim milk in PBS) was added to the wells and incubated for 30 min. Afterwards, the same procedure was followed.

The analysis of anti-PEG IgM was performed accordingly. Chimeric human anti-PEG IgM (clone no. cAGP4-IgM) was used as a standard in black maxisorp 96-well microplates.

(HRP)-conjugated goat F(ab')₂ antihuman IgM Fc_{5μ} was used as secondary antibody. QuantaBlu Fluorogenic Peroxidase Substrate Kit (Thermo Fisher Scientific, Waltham, USA) was used according to the manufacturer's instructions, and the fluorescence measured at $\lambda = 325/420$ nm in a microplate reader (Tecan infinite M1000 plate reader).

For the determination of the assay's limit of detection (LOD) and limit of quantification (LOQ), ten blank samples (2% (w/v) skim milk in PBS) were measured. LOD was calculated as the mean background absorbance of the blank samples plus three times its standard deviation and LOQ was calculated as the mean background absorbance plus ten times its standard deviation according to DIN 32645.

Positive responses were defined as samples with absorbance values greater than LOQ. The relative concentrations of anti-PEG IgG or IgM in positive samples were calculated by comparison with c3.3-IgG or cAGP4-IgM standard curves, respectively. Additionally, the absorbance reading after the addition of PEG_{10k} (competition experiment) needed to be reduced by at least 35% as compared to the reading without the addition of PEG_{10k} to confirm specific binding.

5.2.2 Microscale thermophoresis

The MST measurements were performed using a Nanotemper Monolith NT.115 (Nanotemper, Germany). The samples were analyzed in premium coated capillaries with a blue excitation laser and medium MST power.

5.2.3 Fluorescence correlation spectroscopy

The FCS measurements were performed together with Dr. Kaloian Koynov at the Max Planck Institute for Polymer Research (MPI-P, Mainz, Germany). The FCS measurements were performed on a commercial setup (Carl Zeiss, Germany) consisting of the modules LSM510, ConfoCor 2, and an inverted microscope model Axiovert 200 with a C-Apochromat 40 \times , NA 1.2 water immersion objective. Either argon laser (488 nm excitation wavelength) or HeNe laser (543 nm excitation wavelength) were used for excitation and the emission was collected after filtering respectively with a BP500-550 or BP560-615 long

pass filters. 8-well, polystyrene chambered cover glasses (Laboratory-Tek, Nalge Nunc International) were used as sample cells. For each sample series of 15 measurements with a total duration of 5 min were performed. As the radial dimension r_0 of the confocal probing volume is not known a priori it was determined by performing calibration experiments using a fluorophore with a known diffusion coefficient in water, i.e. Alexa 488 or Rh6G.

5.2.4 Dynamic light scattering (DLS)

DLS measurements of SiNCs and PS-NPs were performed using an instrument from ALV (Langen, Germany) consisting of an electronically controlled goniometer and an ALV-5000 multiple τ full-digital correlator with 320 channels having a measurement range between 10^{-7} s and 10^3 s. A helium-neon laser (Type 1145 P) from JDS Uniphase (Milpitas, USA) of 632.8 nm wavelength and 25 mW output power was used as a source of light. Before measurements, samples were filtered into quartz cuvettes for light scattering from Hellma (Müllheim, Germany) with an inner radius of 9 mm. Millex-SV filters (Merck

5.2.5 Transmission electron microscopy (TEM)

TEM micrographs were taken on an FEI Tecnai F20 transmission electron microscope operated at 200 kV. Micrographs were taken using a 2k charge-coupled device camera from Gatan (Type: Ultrascan 1000).

5.2.6 Zeta potential measurements

Zeta potential measurements were performed using a Nano Z Zetasizer (Malvern Instruments GmbH, Herrenberg, Germany). 20 μ L of the sample were diluted with 1 mL of a 1 mM KCl solution and measured at 25 °C after two minutes of equilibration. Each measurement was repeated in triplicate and mean values as well as standard deviations were calculated.

Millipore, Billerica, USA) with 5 μ m pore size were used for filtration. Before use, the quartz cuvettes were cleaned with acetone using a Thurmond apparatus.

5.2.7 Pierce assay

The protein quantification of desorbed corona proteins was quantified with a Pierce 660 nm Assay (Thermo Scientific, Germany) according to the manufacturer's instructions. Bovine serum albumin (BSA) was used as a standard (Serva, Germany). The absorption was measured at 660 nm with a Tecan infinite M1000 plate reader.

5.2.8 Liquid chromatography-mass spectrometry (LC-MS)

Proteomic analysis was carried out as previously described.¹¹⁵ Briefly, SDS was removed from the protein samples via Pierce Detergent Removal Spin Columns (Thermo Fisher). Further, proteins were precipitated using a ProteoExtract protein precipitation kit (CalBioChem, Merck, Germany) overnight. Afterwards, the protein pellets were isolated via centrifugation (14 000 g, 10 min, 4 °C) and resuspended with RapiGest SF (Waters) in ammonium bicarbonate buffer (50 mM). The protein solution was reduced with dithiothreitol (Sigma-Aldrich) at a concentration of 5 mM for 45 min at 56 °C and alkylated with 15 mM idoacetoamide (Sigma-Aldrich) for 1 h in the dark. Tryptic digestion (protein : trypsin ratio 50:1) was carried out for 18 h at 37 °C. Afterwards, the reaction was quenched with 2 µL hydrochloric acid (0.1 vol%, (Sigma Aldrich).

Tryptic peptides were diluted with 0.1% formic acid spiked with 50 fmol µL⁻¹ Hi3 *E. coli* (Waters) for absolute protein quantification. The peptide solution was injected into a nanoACQUITY UPLC system coupled to a Synapt G2-Si mass spectrometer. The system was operated in resolution mode, with a NanoLockSpray source in positive ion mode. Data-independent acquisition (MSE) experiments were performed, and data was analyzed with MassLynx 4.1.

Proteins were identified with Progenesis GI (2.0) using a reviewed human database downloaded from Uniprot. For analysis, the following criteria were chosen: max. protein mass 600 kDa, one missed cleavage, fixed modifications for carbamidomethyl and cysteine, variable oxidation for methionine, and a false discovery rate of 4%. Peptide identification required three identified fragments and for protein identification, five identified fragments and two peptides were needed. Based on the TOP3/Hi3 quantification, the amount of each protein in fmol is provided.

5.2.9 Flow cytometry

For flow cytometry experiments were performed on the Attune Nxt cytometer (Invitrogen, Germany) with a 670 nm laser for excitation of Cy5-NHS-Ester (Cy5). The viability of the cells was measured by staining with the viability dye Zombie Aqua (BioLegend, USA) according to the manufacturer's instructions, before the flow cytometry measurements. The 405 nm laser was used for the excitation of the Zombie Aqua dye.

5.3 Anti-PEG antibody quantification by ELISA

Human plasma samples were pre-diluted to 20%, 50%, 80%, or no dilution in 2% (w/v) skim milk in PBS. Serial dilutions of chimeric anti-PEG antibodies c3.3-IgG in 2% (w/v) skim milk powder in PBS were prepared starting from 8 $\mu\text{g mL}^{-1}$ to 0.5 $\mu\text{g mL}^{-1}$. Serial dilutions of chimeric anti-PEG antibodies cAGP4-IgM in 2% (w/v) skim milk powder in PBS were prepared starting from 5 $\mu\text{g mL}^{-1}$ to 0.05 $\mu\text{g mL}^{-1}$.

5.4 Binding characterization of anti-PEG antibody to soluble PEG

5.4.1 Competitive ELISA

For the competition experiment, the well plate was prepared as described above. After blocking with skim milk for 2 h, a dilution series of the competitor was added. PEG_{10k}, PEG_{2k}, mPEG_{10k}, and mPEG_{5k} were used, each starting with a concentration of 5 g L⁻¹ to 1.5×10⁻⁴ g L⁻¹ in 2% (w/v) skim milk in PBS. 50 μL was added to the wells and incubated for 30 min. Afterwards, the same procedure was followed.

5.4.2 Microscale thermophoresis

For the MST measurements, a target solution (methoxy-terminated poly(ethylene glycol)-fluorescein (mPEG-FITC)) and a ligand solution (anti-PEG IgG) were prepared in PBS buffer. The target was prediluted to twice the concentration used in the measurement (**Table 2**). The obtained ligand concentration varied with a maximum concentration of 1500 μg mL⁻¹ (10 μM). The used ligand concentration in the measurement can be seen in **Table 2**. A serial dilution of the ligand was prepared by mixing 10 μL PBS buffer with 10 μL ligand solution. This was repeated 15 times to obtain 16 different concentrations. 10 μL of target solution was added to each of the 16 samples and mixed by pipetting. The solutions were transferred into premium-coated capillaries and analyzed with a blue excitation laser and medium MST power.

5.4.3 Fluorescence correlation spectroscopy

For the FCS experiment, a stock solution of mPEG_{5k}-FITC in 50 nM was prepared. Anti-PEG c3.3-IgG was prepared in three concentrations (5 μM, 2.5 μM and 0.5 μM) 25 μL of mPEG_{5k}-FITC and anti-PEG c3.3-IgG were mixed and analyzed. Additionally, the single components were measured.

5.5 Detection of anti-PEG antibodies in the protein corona

5.5.1 Synthesis of silica nanocapsules (SiNCs)

SiNCs were synthesized by Dr. Shuai Jiang and Katja Klein (MPI-P) according to the previously described procedure in an oil-in-water miniemulsion by using the surface of oil nanodroplets as a template for the hydrolysis and condensation of alkoxy silanes.⁹⁶ Specifically, 2.0 g (9.6 mmol) of TEOS was first mixed with 125 mg of hexadecane and 1 g of olive oil to form the oil phase. In the second step, 30 mL of a 0.77 mg mL⁻¹ aqueous solution of CTMA-Cl was poured into the oil mixture while stirring. After a pre-emulsification step by stirring at 1,000 rpm for 1 h, the obtained emulsion was sonicated by using a Branson 450 W sonifier with a 1/2" tip at 70% amplitude for 180 s (30 s of sonication, 10 s of pause) with ice cooling. The resulting miniemulsion was stirred at 1,000 rpm for 12 h at room temperature to obtain an aqueous dispersion of SiNCs. For the fluorescent labeling of SiNCs, Cy5-NHS was first coupled with APTES at a molar ratio of 1:1.1 to obtain fluorescently labeled silica precursors. The APTES-Cy5 conjugates were then mixed with TEOS as the silica source. The molar ratio of Cy5 with TEOS was 1:14,000.

SiNCs were PEGylated by replacing the templating surfactant CTMA-Cl with the nonionic surfactant Lutensol® AT25, AT50, or AT80. Specifically, 35 mg, 70 mg, or 140 mg of Lutensol® AT50 were added to 2 mL of SiNCs dispersion to obtain different PEG densities. Accordingly, 39 mg Lutensol® AT25 or 108 mg Lutensol® AT80 was added to 2 mL of SiNCs dispersion. The dispersion was stirred at 1,000 rpm for 2 h and then dialyzed against MilliQ water in a dialysis tube with a MWCO of 1,000 g mol⁻¹. In this case, CTMA-Cl ($M_w = 320 \text{ g mol}^{-1}$) could diffuse through the dialysis membrane into the aqueous dialysis medium while the Lutensol® AT25 ($M_w = 1,230 \text{ g mol}^{-1}$) was kept inside. Afterwards, the dialyzed dispersion was centrifuged at 12,000 g to remove the excess of Lutensol® surfactant. The pellet was redispersed in water and the dispersion was stirred at 1,000 rpm for 24 h. The samples were stored at room temperature and protected from light under constant agitation.

5.5.2 Synthesis of polystyrene nanoparticles (PS-NPs)

Polystyrene NPs were synthesized by Katja Klein (MPI-P) using the miniemulsion polymerization method as previously published.^{116, 117} Therefore, 200 mg of Lutensol AT25, 50, or 80 were dissolved in 24 mL deionized water. Simultaneously, 98 mg of the initiator V59 and 323 μ L of hexadecane were dissolved in 6.6 mL of purified styrene. After separate preparation of the two phases, they were combined and stirred for 1 h at room temperature for pre-emulsification. Afterwards, the mixture was homogenized by ultrasonication for 120 s at 90% intensity with a Branson W 450 digital sonifier (1/2'' tip) whilst cooled with an ice-water bath. The polymerization was then carried out for 16 h at 72 °C. Purification was achieved by centrifugation at 9,000 rpm for 1 h and resuspension in water for 3 times.

5.5.3 Protein corona analysis

The protein source of pooled or individual human citrate plasma was used for the experiments. For each sample, an aqueous NC suspension (0.05 m² of NC surface area in a total volume of 300 μ L) was mixed in an Eppendorf-tube with 1 mL of the respective plasma source. After an incubation period of 1 h, while shaking at a temperature of 37 °C, the remaining free proteins were removed using centrifugation (always 20,000 g, for 1 h at 4 °C). The supernatant was discarded, and the pellet was resuspended in 1 mL of PBS. The suspension was again centrifuged for 1 h at 20,000 g and 4 °C. These washing steps were repeated in total three times. Before the last washing step, the suspension was transferred into a new Eppendorf-tube.

After the last washing step of the corona preparation, the pellet was suspended in 100 μ L of a 0.0625 M Tris*HCl solution containing 2 wt% of SDS for protein detachment. The suspension was incubated at 95 °C for 5 min and was centrifuged again for 1 h at 20,000 g and 4 °C. The supernatant was further used for analysis.

5.5.4 FACS for protein corona analysis

To detect changes in the anti-PEG IgG concentration in the protein corona we used flow cytometry. The protein corona was formed as described above (chapter 5.5.3). PS-NPs with Lutensol® AT80 were used as NCs and the same plasma samples as described in chapter 5.6.1. After the last washing step, the suspension was redispersed in 1 mL PBS and the NC concentration was confirmed via fluorescence calibration. For the flow cytometry experiment, AF488 goat anti-human IgG secondary antibodies were used. The NC was diluted to $10 \mu\text{g mL}^{-1}$ and 20 μL mixed with 1 μg or 0.5 μg secondary antibody respectively analyzed with a 530 nm laser.

5.5.5 ELISA protein corona

For the measurement of protein corona samples, 120 μL of each sample was diluted with 240 μL of 2% (w/v) skim milk in PBS (33% dilution) and added to the wells as described.

5.6 Effect of anti-PEG antibodies in the protein corona on cell uptake

5.6.1 Protein corona preparation

For the protein corona preparation for cell uptake experiments, 5 plasma screening samples of similar anti-PEG IgG concentration were each pooled to obtain batches of low ($<0.5 \mu\text{g mL}^{-1}$), medium ($9.6 \mu\text{g mL}^{-1}$), and high ($110.5 \mu\text{g mL}^{-1}$) anti-PEG IgG concentration. The NC surface was normalized to a surface area of 0.0125 m^2 (in $75 \mu\text{L}$ volume) and incubated with $250 \mu\text{L}$ of plasma for 1 h at $37 \text{ }^\circ\text{C}$. The remaining free proteins were removed using centrifugation ($20,000 \text{ g}$, for 1 h at $4 \text{ }^\circ\text{C}$). The supernatant was discarded, and the pellet was resuspended in the appropriate cell culture medium with a resulting NC concentration of 0.5 mg mL^{-1} .

5.6.2 Cell culture

The murine macrophage cells from the cell line RAW 264.7 were cultured in Dulbecco Modified Eagle Medium (DMEM, Gibco, USA). The human cells from the cell line THP-1 were cultured in Roswell Park Memorial Institute (RPMI)-1640 medium. Both were supplemented with 10% fetal bovine serum (FBS), 100 U mL^{-1} penicillin, 100 mg mL^{-1} streptomycin, and 2 mM glutamine (all from Gibco, Germany) at $37 \text{ }^\circ\text{C}$ with 5% CO_2 in an incubator.

5.6.3 THP-1 macrophage differentiation

The human monocyte cell line THP-1 was differentiated into macrophages for 5 days prior to the experiments with the NCs. On day 0 the cells were stimulated with 100 ng mL^{-1} of phorbol-12-myristate-13-acetate (PMA) (Sigma-Aldrich, Germany) and seeded at a density of 200,000 cells per well in 24-well plates. After 2 days, the medium was changed to fresh RPMI without PMA and the cells rested for the following 3 days before the experiment.

5.6.4 Cell uptake experiments and flow cytometry measurements

For the cell uptake experiments, cells were seeded at a density of 150,000 cells per well in 24-well plates in cell culture medium with 10% FBS. After overnight incubation, the medium was changed to serum-free medium. The cells were incubated in fresh serum-free medium with the NC dispersions added at a concentration of $10 \mu\text{g mL}^{-1}$ to the cells for 2 h (RAW 264.7) or $75 \mu\text{g mL}^{-1}$ for 2 h (THP-1) at 37°C . RAW 264.7 macrophages tend to show a high uptake behavior. To not overload the cells and see differences in the uptake, a lower NC concentration was used as for THP-1 cells.

For flow cytometry experiments, adherent cells were washed with PBS, detached from the culture vessel with 2.5% trypsin (Gibco, Germany), and measured as described above.

5.6.5 Cell blocking experiments with antibodies

For the cell blocking experiments, purified anti-CD64, CD16, and/or CD32 (BioLegend, USA) were added to the cells at $1 \mu\text{g mL}^{-1}$ in fresh serum-free medium for 30 min at 4°C before the respective NC samples were added. After the incubation, the nanoparticles were added to the wells, and the cells were incubated for 1 h at 4°C .

5.6.6 Cytokine assay

For the cytokine assay, RAW 264.7 were seeded as described. After overnight incubation and change of medium, the samples were added at a concentration of $75 \mu\text{g mL}^{-1}$. As samples the NC dispersion with a low ($<0.5 \mu\text{g mL}^{-1}$), medium ($9.6 \mu\text{g mL}^{-1}$), and high ($110.5 \mu\text{g mL}^{-1}$) anti-PEG IgG concentration were used. As positive control diABZI (InvivoGen, France) was added. After 2 h incubation $5 \mu\text{L}$ per sample was used for cytokine quantification performed using a multiplex protein quantification assay.

6 Summary and Outlook

The objective of this thesis was to gain insights into the interaction of anti-PEG antibodies with PEG. In more detail, we aimed to find out whether the anti-PEG antibodies enrich in the protein corona of PEGylated nanocarriers and how their presence correlates with cellular uptake.

First, we evaluated the anti-PEG antibody prevalence and concentration in the German population. For this, we used ELISA, which has proven to be the most reliable method with high sensitivity and specificity that could be confirmed by a competition assay. The performed plasma screening on 500 plasma samples revealed a high prevalence of anti-PEG antibodies in the German population. Overall, 83% of the samples were found to be positive for either anti-PEG IgG, IgM, or both. The highest absolute concentration and most variation were detected in the age group between 21-30 years. Both the prevalence and concentration are inversely correlated with age. One explanation for the high prevalence might be the casual exposure to PEG compounds in everyday products. It is important to note that the plasma samples were from early 2019 before PEGylated Covid-19 vaccines were approved and applied. Nowadays, the abundance of anti-PEG antibodies might be even more widespread throughout the population.

To characterize the binding behavior of anti-PEG antibodies to free PEG, multiple methods were used. First, we used competitive ELISA for a qualitative comparison of the binding behavior of anti-PEG IgG to PEG with different chain lengths and end-groups. Our analysis revealed a stronger binding to PEG_{10k} as compared to PEG_{2k}. A more detailed analysis and quantification of the binding strength could be achieved with microscale thermophoresis. The K_d determined values were between 24-44 nM for the interaction with mPEG_{10k} or mPEG_{20k}, which represent a very strong binding. The analysis revealed a clear trend that binding strength decreased with decreasing PEG chain length. Additionally, the binding behavior for anti-PEG IgG to mPEG_{5k} was confirmed by FCS measurements.

After characterizing the binding of anti-PEG antibodies to soluble PEG, the influence on the protein corona was investigated. Therefore, SiNCs and PS-NPs were synthesized and PEGylated with the non-covalent PEG-based surfactant Lutensol®. The protein corona was formed using undiluted pooled human plasma and after detachment from the NCs analyzed

with multiple methods. Pierce assay and LC-MS were used to determine the overall protein content and composition. As expected, the PEGylated NCs showed an enrichment in stealth proteins like apolipoprotein A1 (SiNCs) and clusterin (PS-NPs). ELISA was used to quantify the anti-PEG IgG concentration in the detached protein corona. The analysis of the protein corona on SiNCs revealed enrichment of anti-PEG IgG on PEGylated SiNCs compared to non-PEGylated NCs. We expected the same results for PS-NPs, but here further investigation on the influence of the NC material is still needed.

To analyze the effect of anti-PEG antibodies in the protein corona, we monitored the cellular uptake of PEGylated SiNCs in murine and human macrophages. With increasing anti-PEG IgG concentration in the protein corona, the cellular uptake steadily increased in both cell lines. Most prominent, the uptake in human THP-1 macrophages doubled when the protein corona was formed only from anti-PEG IgG. This increased uptake is likely to be not anti-PEG antibody specific but a general immunoglobulin effect.

So far, the enrichment in the protein corona and the following effect on the cellular uptake was analyzed for anti-PEG IgG. We expect similar results also for other Ig classes. Especially the analysis regarding anti-PEG IgM and IgE would be interesting. IgM antibodies can effectively activate the complement system and promote phagocytosis, IgE causes anaphylactic reactions and might be responsible for some reported severe reactions to PEGylated NCs. We were not able to analyze their presence in the protein corona and their consequences for cellular uptake yet, due to sensitivity limits. As it can be seen from the results of the plasma screening, the concentration of anti-PEG IgM is one-tenth of that of anti-PEG IgG, and accordingly a more sensitive analysis is needed to detect small concentration differences in the protein corona. IgE is mainly cell bound and only in extremely small amounts in the serum. Zhou *et al.* recently developed a bead assay to determine anti-PEG IgG, IgM, and IgE.¹¹³ They reported PEGylated drug-associated anaphylaxis was due to specific anti-PEG IgE-mediated type 1 hypersensitivity. Due to the low concentration of anti-PEG IgE in the plasma and the limitation of the ELISA setup, it has not been possible to analyze anti-PEG IgE concentration so far. In the future, it would be extremely interesting to examine also IgE plasma levels and evaluate the interaction of IgE with PEGylated NCs.

In conclusion, our results show that anti-PEG antibodies can accumulate in the protein corona of PEGylated NCs and promote their uptake into macrophages. Thus, the stealth effect of PEG is mitigated. These findings have significant implications regarding the use and design of nanomedicines and contribute to further our understanding of nano-bio interactions.

According to our results, it is important to monitor anti-PEG antibody prevalence in the bloodstream and account for their existence in patients' blood when designing new nanocarrier-based therapeutics. Various strategies could be envisaged to minimize the impact of anti-PEG antibodies in the protein corona. On the one hand, one strategy could be to find solutions that do not require PEGylation or functionalization with other polymers and create stealth behavior in other ways. One approach for a successful NC-based therapy might be precoating the NC with stealth proteins. Precoating NC with clusterin can successfully prevent IgG-adsorption and additionally reduces cellular internalization.⁴⁸ Therefore, precoating NCs may be utilized as a powerful method to reduce the influence of an increased anti-PEG IgG adsorption on PEGylated NCs.

On the other hand, finding alternatives to PEG in terms of polymer functionalization could be a promising approach. Multiple possible alternatives are already under investigation. For example, polyphosphoesters^{50, 118}, polysaccharides^{119, 120}, or poly(2-oxazoline)s^{121, 122} have already proven a similar stealth behavior. Additionally, by incorporating a co-monomer into PEG, it might be possible to retain the qualities of PEGylation but prevent anti-PEG antibody binding. If and how PEG alternatives can prevent the accumulation of anti-PEG antibodies or possibly newly formed antibodies in the protein corona needs to be further evaluated.

7 List of Abbreviations

ABTS	2,2'-azino-bis(3-ethylbenzothiazoline-6-sulfonic acid)
BSA	bovine serum albumin
ELISA	enzyme-linked immunosorbent assay
EPR	enhanced-permeation-and-retention
ESI	electrospray ionization
PRRs	pattern recognition receptors
F _{ab}	antigen-binding fragment
F _c	crystallizable fragment
FCS	fluorescence correlation spectroscopy
FITC	fluorescein isothiocyanate
HPLC	high-performance liquid chromatography
HRP	Horseradish peroxidase
D _h	hydrodynamic diameter
Ig	immunoglobulins
IR	infrared
LC-MS	liquid chromatography–mass spectrometry
LNP	lipid nanoparticles
LOD	limit of detection
LOQ	limit of quantification
MFI	median fluorescence intensity
MST	microscale thermophoresis
NNI	National Nanotechnology Initiative of the U.S. Government
NC	nanocarrier
PEG	poly(ethylene glycol)

PS-NP	polystyrene nanoparticle
R_h	hydrodynamic radius
SDS	sodium dodecyl sulfate
SiNC	silica nanocapsule
TI-2	thymus independent
TRIC	temperature related intensity change

8 References

1. I. H. Plenderleith. Treating the treatment: toxicity of cancer chemotherapy. *Can Fam Physician* **1990**, *36*, 1827-1830.
2. V. Jain, S. Jain and S. C. Mahajan. Nanomedicines based drug delivery systems for anti-cancer targeting and treatment. *Curr Drug Deliv* **2015**, *12* (2), 177-191. DOI: 10.2174/1567201811666140822112516
3. R. R. Wakaskar. Promising effects of nanomedicine in cancer drug delivery. *Journal of Drug Targeting* **2018**, *26* (4), 319-324. DOI: 10.1080/1061186X.2017.1377207
4. Y. Matsumura and K. Kataoka. Preclinical and clinical studies of anticancer agent-incorporating polymer micelles. *Cancer Science* **2009**, *100* (4), 572-579. DOI: 10.1111/j.1349-7006.2009.01103.x
5. H. Maeda, J. Wu, T. Sawa, Y. Matsumura and K. Hori. Tumor vascular permeability and the EPR effect in macromolecular therapeutics: a review. *Journal of Controlled Release* **2000**, *65* (1-2), 271-284. DOI: [http://dx.doi.org/10.1016/S0168-3659\(99\)00248-5](http://dx.doi.org/10.1016/S0168-3659(99)00248-5)
6. T. Cedervall, I. Lynch, S. Lindman, T. Berggard, E. Thulin, H. Nilsson, K. A. Dawson and S. Linse. Understanding the nanoparticle-protein corona using methods to quantify exchange rates and affinities of proteins for nanoparticles. *Proc Natl Acad Sci U S A* **2007**, *104* (7), 2050-2055. DOI: 10.1073/pnas.0608582104
7. I. Lynch, A. Salvati and K. A. Dawson. Protein-nanoparticle interactions: What does the cell see? *Nat Nanotechnol* **2009**, *4* (9), 546-547. DOI: 10.1038/nnano.2009.248
8. E. Allard-Vannier, S. Cohen-Jonathan, J. Gautier, K. Herve-Aubert, E. Munnier, M. Souce, P. Legras, C. Passirani and I. Chourpa. Pegylated magnetic nanocarriers for doxorubicin delivery: a quantitative determination of stealthiness in vitro and in vivo. *Eur J Pharm Biopharm* **2012**, *81* (3), 498-505. DOI: 10.1016/j.ejpb.2012.04.002
9. K. Knop, R. Hoogenboom, D. Fischer and U. S. Schubert. Poly(ethylene glycol) in drug delivery: pros and cons as well as potential alternatives. *Angew Chem Int Ed Engl* **2010**, *49* (36), 6288-6308. DOI: 10.1002/anie.200902672
10. P. Aggarwal, J. B. Hall, C. B. McLeland, M. A. Dobrovolskaia and S. E. McNeil. Nanoparticle interaction with plasma proteins as it relates to particle biodistribution, biocompatibility and therapeutic efficacy. *Adv Drug Deliv Rev* **2009**, *61* (6), 428-437. DOI: 10.1016/j.addr.2009.03.009
11. L. Hong, Z. Wang, X. Wei, J. Shi and C. Li. Antibodies against polyethylene glycol in human blood: A literature review. *Journal of Pharmacological and Toxicological Methods* **2020**, *102*, 106678. DOI: <https://doi.org/10.1016/j.vascn.2020.106678>
12. A. W. Richter and E. Akerblom. Antibodies against polyethylene glycol produced in animals by immunization with monomethoxy polyethylene glycol modified proteins. *Int Arch Allergy Appl Immunol* **1983**, *70* (2), 124-131. DOI: 10.1159/000233309
13. J. M. Harris and R. B. Chess. Effect of pegylation on pharmaceuticals. *Nature Reviews Drug Discovery* **2003**, *2* (3), 214-221. DOI: 10.1038/nrd1033

-
14. J. Armstrong, R. Leger, R. Wenby, H. Meiselman, G. Garratty and T. Fisher, 2003.
 15. R. P. Garay, R. El-Gewely, J. K. Armstrong, G. Garratty and P. Richette. Antibodies against polyethylene glycol in healthy subjects and in patients treated with PEG-conjugated agents. *Expert Opin Drug Deliv* **2012**, 9 (11), 1319-1323. DOI: 10.1517/17425247.2012.720969
 16. Q. Yang and S. K. Lai. Anti-PEG immunity: emergence, characteristics, and unaddressed questions. *Wiley Interdiscip Rev Nanomed Nanobiotechnol* **2015**, 7 (5), 655-677. DOI: 10.1002/wnan.1339
 17. B. M. Chen, Y. C. Su, C. J. Chang, P. A. Burnouf, K. H. Chuang, C. H. Chen, T. L. Cheng, Y. T. Chen, J. Y. Wu and S. R. Roffler. Measurement of Pre-Existing IgG and IgM Antibodies against Polyethylene Glycol in Healthy Individuals. *Anal Chem* **2016**, 88 (21), 10661-10666. DOI: 10.1021/acs.analchem.6b03109
 18. Q. Yang, T. M. Jacobs, J. D. McCallen, D. T. Moore, J. T. Huckaby, J. N. Edelstein and S. K. Lai. Analysis of Pre-existing IgG and IgM Antibodies against Polyethylene Glycol (PEG) in the General Population. *Anal Chem* **2016**, 88 (23), 11804-11812. DOI: 10.1021/acs.analchem.6b03437
 19. J. T. Huckaby, T. M. Jacobs, Z. Li, R. J. Perna, A. Wang, N. I. Nicely and S. K. Lai. Structure of an anti-PEG antibody reveals an open ring that captures highly flexible PEG polymers. *Communications Chemistry* **2020**, 3 (1). DOI: 10.1038/s42004-020-00369-y
 20. C. Fruijtjer-Polloth. Safety assessment on polyethylene glycols (PEGs) and their derivatives as used in cosmetic products. *Toxicology* **2005**, 214 (1-2), 1-38. DOI: 10.1016/j.tox.2005.06.001
 21. S. M. Moghimi. Allergic Reactions and Anaphylaxis to LNP-Based COVID-19 Vaccines. *Mol Ther* **2021**, 29 (3), 898-900. DOI: 10.1016/j.ymthe.2021.01.030
 22. P. Laverman, M. G. Carstens, O. C. Boerman, E. Th. M. Dams, W. J. G. Oyen, N. van Rooijen, F. H. M. Corstens and G. Storm. Factors Affecting the Accelerated Blood Clearance of Polyethylene Glycol-Liposomes upon Repeated Injection. *Journal of Pharmacology and Experimental Therapeutics* **2001**, 298 (2), 607-612.
 23. T. J. Povsic, M. G. Lawrence, A. M. Lincoff, R. Mehran, C. P. Rusconi, S. L. Zelenkofske, Z. Huang, J. Sailstad, P. W. Armstrong, P. G. Steg, C. Bode, R. C. Becker, J. H. Alexander, N. F. Adkinson, A. I. Levinson and R.-P. Investigators. Pre-existing anti-PEG antibodies are associated with severe immediate allergic reactions to pegnivacogin, a PEGylated aptamer. *J Allergy Clin Immunol* **2016**, 138 (6), 1712-1715. DOI: 10.1016/j.jaci.2016.04.058
 24. A. Chanan-Khan, J. Szebeni, S. Savay, L. Liebes, N. M. Rafique, C. R. Alving and F. M. Muggia. Complement activation following first exposure to pegylated liposomal doxorubicin (Doxil): possible role in hypersensitivity reactions. *Ann Oncol* **2003**, 14 (9), 1430-1437. DOI: 10.1093/annonc/mdg374
 25. P. Grenier, I. M. O. Viana, E. M. Lima and N. Bertrand. Anti-polyethylene glycol antibodies alter the protein corona deposited on nanoparticles and the physiological pathways regulating their fate in vivo. *J Control Release* **2018**, 287, 121-131. DOI: 10.1016/j.jconrel.2018.08.022

26. S. E. McNeil. Nanotechnology for the biologist. *J Leukoc Biol* **2005**, 78 (3), 585-594. DOI: 10.1189/jlb.0205074
27. H. M. E. Azzazy and M. M. H. Mansour. In vitro diagnostic prospects of nanoparticles. *Clinica Chimica Acta* **2009**, 403 (1-2), 1-8. DOI: <http://dx.doi.org/10.1016/j.cca.2009.01.016>
28. M. Zhang and K. Kataoka. Nano-structured composites based on calcium phosphate for cellular delivery of therapeutic and diagnostic agents. *Nano Today* **2009**, 4 (6), 508-517. DOI: <http://dx.doi.org/10.1016/j.nantod.2009.10.009>
29. H. Ringsdorf, 1975.
30. R. Duncan. Polymer conjugates as anticancer nanomedicines. *Nat Rev Cancer* **2006**, 6 (9), 688-701, 10.1038/nrc1958.
31. M. D. Howard, M. Jay, T. D. Dziubla and X. Lu. PEGylation of Nanocarrier Drug Delivery Systems: State of the Art. *Journal of Biomedical Nanotechnology* **2008**, 4 (2), 133-148. DOI: 10.1166/jbn.2008.021
32. K. Strebhardt and A. Ullrich. Paul Ehrlich's magic bullet concept: 100 years of progress. *Nat Rev Cancer* **2008**, 8 (6), 473-480. DOI: 10.1038/nrc2394
33. K. S. Soppimath, T. M. Aminabhavi, A. R. Kulkarni and W. E. Rudzinski. Biodegradable polymeric nanoparticles as drug delivery devices. *J Control Release* **2001**, 70 (1-2), 1-20. DOI: 10.1016/s0168-3659(00)00339-4
34. C. D. Walkey and W. C. Chan. Understanding and controlling the interaction of nanomaterials with proteins in a physiological environment. *Chem Soc Rev* **2012**, 41 (7), 2780-2799. DOI: 10.1039/c1cs15233e
35. D. Walczyk, F. B. Bombelli, M. P. Monopoli, I. Lynch and K. A. Dawson. What the cell "sees" in bionanoscience. *J Am Chem Soc* **2010**, 132 (16), 5761-5768. DOI: 10.1021/ja910675v
36. R. M. Pearson, V. V. Juettner and S. Hong. Biomolecular corona on nanoparticles: a survey of recent literature and its implications in targeted drug delivery. *Front Chem* **2014**, 2, 108. DOI: 10.3389/fchem.2014.00108
37. L. Vroman. Effect of absorbed proteins on the wettability of hydrophilic and hydrophobic solids. *Nature* **1962**, 196, 476-477. DOI: 10.1038/196476a0
38. H. Noh and E. A. Vogler. Volumetric interpretation of protein adsorption: competition from mixtures and the Vroman effect. *Biomaterials* **2007**, 28 (3), 405-422. DOI: 10.1016/j.biomaterials.2006.09.006
39. M. Lundqvist, J. Stigler, T. Cedervall, T. Berggard, M. B. Flanagan, I. Lynch, G. Elia and K. Dawson. The evolution of the protein corona around nanoparticles: a test study. *ACS Nano* **2011**, 5 (9), 7503-7509. DOI: 10.1021/nn202458g

-
40. S. Winzen, S. Schoettler, G. Baier, C. Rosenauer, V. Mailaender, K. Landfester and K. Mohr. Complementary analysis of the hard and soft protein corona: sample preparation critically effects corona composition. *Nanoscale* **2015**, 7 (7), 2992-3001. DOI: 10.1039/c4nr05982d
 41. I. Lynch, T. Cedervall, M. Lundqvist, C. Cabaleiro-Lago, S. Linse and K. Dawson. The nanoparticle-protein complex as a biological entity; a complex fluids and surface science challenge for the 21st century. *Advances in colloid and interface science* **2007**, 134-135, 167-174. DOI: 10.1016/j.cis.2007.04.021
 42. D. E. Owens, 3rd and N. A. Peppas. Opsonization, biodistribution, and pharmacokinetics of polymeric nanoparticles. *Int J Pharm* **2006**, 307 (1), 93-102. DOI: 10.1016/j.ijpharm.2005.10.010
 43. D. A. Tyrrell, V. J. Richardson and B. E. Ryman. The effect of serum protein fractions on liposome-cell interactions in cultured cells and the perfused rat liver. *Biochim Biophys Acta* **1977**, 497 (2), 469-480. DOI: 10.1016/0304-4165(77)90204-5
 44. S. Ritz, S. Schöttler, N. Kotman, G. Baier, A. Musyanovych, J. Kuharev, K. Landfester, H. Schild, O. Jahn, S. Tenzer and V. Mailänder. Protein Corona of Nanoparticles: Distinct Proteins Regulate the Cellular Uptake. *Biomacromolecules* **2015**, 16 (4), 1311-1321. DOI: 10.1021/acs.biomac.5b00108
 45. H. Spreen, M. Behrens, D. Mulac, H.-U. Humpf and K. Langer. Identification of main influencing factors on the protein corona composition of PLGA and PLA nanoparticles. *European Journal of Pharmaceutics and Biopharmaceutics* **2021**, 163, 212-222. DOI: <https://doi.org/10.1016/j.ejpb.2021.04.006>
 46. S. M. Pustulka, K. Ling, S. L. Pish and J. A. Champion. Protein Nanoparticle Charge and Hydrophobicity Govern Protein Corona and Macrophage Uptake. *ACS Appl Mater Interfaces* **2020**, 12 (43), 48284-48295. DOI: 10.1021/acsami.0c12341
 47. D. Prozeller, C. Rosenauer, S. Morsbach and K. Landfester. Immunoglobulins on the surface of differently charged polymer nanoparticles. *Biointerphases* **2020**, 15 (3), 031009. DOI: 10.1116/6.0000139
 48. D. Prozeller, J. Pereira, J. Simon, V. Mailander, S. Morsbach and K. Landfester. Prevention of Dominant IgG Adsorption on Nanocarriers in IgG-Enriched Blood Plasma by Clusterin Precoating. *Adv Sci* **2019**, 6 (10), 1802199. DOI: 10.1002/advs.201802199
 49. N. Singh, C. Marets, J. Boudon, N. Millot, L. Saviot and L. Maurizi. In vivo protein corona on nanoparticles: does the control of all material parameters orient the biological behavior? *Nanoscale Adv* **2021**, 3 (5), 1209-1229. DOI: 10.1039/d0na00863j
 50. S. Schottler, G. Becker, S. Winzen, T. Steinbach, K. Mohr, K. Landfester, V. Mailander and F. R. Wurm. Protein adsorption is required for stealth effect of poly(ethylene glycol)- and poly(phosphoester)-coated nanocarriers. *Nat Nanotechnol* **2016**, 11 (4), 372-377. DOI: 10.1038/nnano.2015.330
 51. M. A. Dobrovolskaia, P. Aggarwal, J. B. Hall and S. E. McNeil. Preclinical studies to understand nanoparticle interaction with the immune system and its potential effects on nanoparticle biodistribution. *Mol Pharm* **2008**, 5 (4), 487-495. DOI: 10.1021/mp800032f

-
52. F. M. Veronese and G. Pasut. PEGylation, successful approach to drug delivery. *Drug Discovery Today* **2005**, *10* (21), 1451-1458. DOI: 10.1016/s1359-6446(05)03575-0
53. S. N. S. Alconcel, A. S. Baas and H. D. Maynard. FDA-approved poly(ethylene glycol)–protein conjugate drugs. *Polymer Chemistry* **2011**, *2* (7). DOI: 10.1039/c1py00034a
54. P. Bailon and W. Berthold. Polyethylene glycol-conjugated pharmaceutical proteins. *Pharmaceutical Science & Technology Today* **1998**, *1* (8), 352-356. DOI: 10.1016/s1461-5347(98)00086-8
55. L. Shi, J. Zhang, M. Zhao, S. Tang, X. Cheng, W. Zhang, W. Li, X. Liu, H. Peng and Q. Wang. Effects of polyethylene glycol on the surface of nanoparticles for targeted drug delivery. *Nanoscale* **2021**, *13* (24), 10748-10764. DOI: 10.1039/d1nr02065j
56. A. Abuchowski, T. van Es, N. C. Palczuk and F. F. Davis. Alteration of immunological properties of bovine serum albumin by covalent attachment of polyethylene glycol. *Journal of Biological Chemistry* **1977**, *252* (11), 3578-3581. DOI: 10.1016/s0021-9258(17)40291-2
57. M. L. Nucci, R. Shorr and A. Abuchowski. The therapeutic value of poly(ethylene glycol)-modified proteins. *Advanced Drug Delivery Reviews* **1991**, *6* (2), 133-151. DOI: 10.1016/0169-409x(91)90037-d
58. J. M. Harris, N. E. Martin and M. Modi. Pegylation: a novel process for modifying pharmacokinetics. *Clin Pharmacokinet* **2001**, *40* (7), 539-551. DOI: 10.2165/00003088-200140070-00005
59. A. Kozłowski and J. Milton Harris. Improvements in protein PEGylation: pegylated interferons for treatment of hepatitis C. *Journal of Controlled Release* **2001**, *72* (1), 217-224. DOI: [https://doi.org/10.1016/S0168-3659\(01\)00277-2](https://doi.org/10.1016/S0168-3659(01)00277-2)
60. A. V. Kabanov, V. P. Chekhonin, V. Y. Alakhov, E. V. Batrakova, A. S. Lebedev, N. S. Melik-Nubarov, S. A. Arzhakov, A. V. Levashov, G. V. Morozov, E. S. Severin and V. A. Kabanov. The neuroleptic activity of haloperidol increases after its solubilization in surfactant micelles: Micelles as microcontainers for drug targeting. *FEBS Letters* **1989**, *258* (2), 343-345. DOI: [https://doi.org/10.1016/0014-5793\(89\)81689-8](https://doi.org/10.1016/0014-5793(89)81689-8)
61. M. S. Hershfield. PEG-ADA replacement therapy for adenosine deaminase deficiency: an update after 8.5 years. *Clinical Immunology and Immunopathology* **1995**, *76* (3, Part 2), S228-S232. DOI: [https://doi.org/10.1016/S0090-1229\(95\)90306-2](https://doi.org/10.1016/S0090-1229(95)90306-2)
62. D. Łażewski, M. Murias and M. Wierzchowski. Pegylation – in search of balance and enhanced bioavailability. *Journal of Medical Science* **2022**, *91*, e761. DOI: 10.20883/medical.e761
63. D. A. Herold, K. Keil and D. E. Bruns. Oxidation of polyethylene glycols by alcohol dehydrogenase. *Biochemical Pharmacology* **1989**, *38* (1), 73-76. DOI: [https://doi.org/10.1016/0006-2952\(89\)90151-2](https://doi.org/10.1016/0006-2952(89)90151-2)

-
64. D. Pozzi, V. Colapicchioni, G. Caracciolo, S. Piovesana, A. L. Capriotti, S. Palchetti, S. De Grossi, A. Riccioli, H. Amenitsch and A. Lagana. Effect of polyethyleneglycol (PEG) chain length on the bio-nano-interactions between PEGylated lipid nanoparticles and biological fluids: from nanostructure to uptake in cancer cells. *Nanoscale* **2014**, 6 (5), 2782-2792. DOI: 10.1039/c3nr05559k
65. L. Hong, Z. Wang, X. Wei, J. Shi and C. Li. Antibodies against polyethylene glycol in human blood: A literature review. *J Pharmacol Toxicol Methods* **2020**, 102, 106678. DOI: 10.1016/j.vascn.2020.106678
66. B. Alberts., A. Johnson., J. Lewis., M. Raff., K. Roberts. and P. Walter., *Molecular Biology of the Cell*, Garland Science, New York, 2002.
67. B. Bröker, C. Schütt and B. Fleischer, in *Grundwissen Immunologie*, eds. B. Bröker, C. Schütt and B. Fleischer, Springer Berlin Heidelberg, Berlin, Heidelberg, 2019, DOI: 10.1007/978-3-662-58330-2_1, pp. 3-25.
68. S. Dübel, F. Breitling, A. Frenzel, T. Jostock, A. L. J. Marschall, T. Schirrmann and M. Hust, *Rekombinante Antikörper*, 2019.
69. A. W. Richter and E. Akerblom. Polyethylene glycol reactive antibodies in man: titer distribution in allergic patients treated with monomethoxy polyethylene glycol modified allergens or placebo, and in healthy blood donors. *Int Arch Allergy Appl Immunol* **1984**, 74 (1), 36-39. DOI: 10.1159/000233512
70. M. Mohamed, A. S. Abu Lila, T. Shimizu, E. Alaaeldin, A. Hussein, H. A. Sarhan, J. Szebeni and T. Ishida. PEGylated liposomes: immunological responses. *Sci Technol Adv Mater* **2019**, 20 (1), 710-724. DOI: 10.1080/14686996.2019.1627174
71. J. J. Verhoef, J. F. Carpenter, T. J. Anchordoquy and H. Schellekens. Potential induction of anti-PEG antibodies and complement activation toward PEGylated therapeutics. *Drug Discov Today* **2014**, 19 (12), 1945-1952. DOI: 10.1016/j.drudis.2014.08.015
72. H. Wang, S. Lin, X. Wu, K. Jiang, H. Lu and C. Zhan. Interplay between Liposomes and IgM: Principles, Challenges, and Opportunities. *Adv Sci (Weinh)* **2023**, DOI: 10.1002/advs.202301777, e2301777. DOI: 10.1002/advs.202301777
73. N. J. Ganson, T. J. Povsic, B. A. Sullenger, J. H. Alexander, S. L. Zelenkofske, J. M. Sailstad, C. P. Rusconi and M. S. Hershfield. Pre-existing anti-polyethylene glycol antibody linked to first-exposure allergic reactions to pegnivacogin, a PEGylated RNA aptamer. *J Allergy Clin Immunol* **2016**, 137 (5), 1610-1613 e1617. DOI: 10.1016/j.jaci.2015.10.034
74. H. Schellekens, W. E. Hennink and V. Brinks. The immunogenicity of polyethylene glycol: facts and fiction. *Pharm Res* **2013**, 30 (7), 1729-1734. DOI: 10.1007/s11095-013-1067-7
75. R. M. Lequin. Enzyme immunoassay (EIA)/enzyme-linked immunosorbent assay (ELISA). *Clin Chem* **2005**, 51 (12), 2415-2418. DOI: 10.1373/clinchem.2005.051532
76. J. R. Crowther, in *ELISA: Theory and Practice*, ed. J. R. Crowther, Humana Press, Totowa, NJ, 1995, DOI: 10.1385/0-89603-279-5:1, pp. 1-34.
-

-
77. A. J. Gupta, S. Duhr and P. Baaske, in *Encyclopedia of Biophysics*, 2018, DOI: 10.1007/978-3-642-35943-9_10063-1, ch. Chapter 10063-1, pp. 1-5.
78. S. Duhr and D. Braun. Why molecules move along a temperature gradient. *Proc Natl Acad Sci U S A* **2006**, *103* (52), 19678-19682. DOI: 10.1073/pnas.0603873103
79. M. Jerabek-Willemsen, T. André, R. Wanner, H. M. Roth, S. Duhr, P. Baaske and D. Breitsprecher. MicroScale Thermophoresis: Interaction analysis and beyond. *Journal of Molecular Structure* **2014**, *1077*, 101-113. DOI: 10.1016/j.molstruc.2014.03.009
80. B. S. Antharavally, K. A. Mallia, P. Rangaraj, P. Haney and P. A. Bell. Quantitation of proteins using a dye-metal-based colorimetric protein assay. *Anal Biochem* **2009**, *385* (2), 342-345. DOI: 10.1016/j.ab.2008.11.024
81. L. Monaci and A. Visconti. Mass spectrometry-based proteomics methods for analysis of food allergens. *TrAC Trends in Analytical Chemistry* **2009**, *28* (5), 581-591. DOI: 10.1016/j.trac.2009.02.013
82. J. M. Burkhardt, C. Schumbrutzki, S. Wortelkamp, A. Sickmann and R. P. Zahedi. Systematic and quantitative comparison of digest efficiency and specificity reveals the impact of trypsin quality on MS-based proteomics. *J Proteomics* **2012**, *75* (4), 1454-1462. DOI: 10.1016/j.jprot.2011.11.016
83. W. Bittremieux, D. L. Tabb, F. Impens, A. Staes, E. Timmerman, L. Martens and K. Laukens. Quality control in mass spectrometry-based proteomics. *Mass Spectrom Rev* **2018**, *37* (5), 697-711. DOI: 10.1002/mas.21544
84. G. T. Kozma, T. Shimizu, T. Ishida and J. Szebeni. Anti-PEG antibodies: Properties, formation, testing and role in adverse immune reactions to PEGylated nanobiopharmaceuticals. *Adv Drug Deliv Rev* **2020**, DOI: 10.1016/j.addr.2020.07.024. DOI: 10.1016/j.addr.2020.07.024
85. T. L. Cheng, C. M. Cheng, B. M. Chen, D. A. Tsao, K. H. Chuang, S. W. Hsiao, Y. H. Lin and S. R. Roffler. Monoclonal antibody-based quantitation of poly(ethylene glycol)-derivatized proteins, liposomes, and nanoparticles. *Bioconjug Chem* **2005**, *16* (5), 1225-1231. DOI: 10.1021/bc050133f
86. P. J. Linton and K. Dorshkind. Age-related changes in lymphocyte development and function. *Nat Immunol* **2004**, *5* (2), 133-139. DOI: 10.1038/ni1033
87. P. Zhang, F. Sun, S. Liu and S. Jiang. Anti-PEG antibodies in the clinic: Current issues and beyond PEGylation. *J Control Release* **2016**, *244* (Pt B), 184-193. DOI: 10.1016/j.jconrel.2016.06.040
88. J. McCallen, J. Prybylski, Q. Yang and S. K. Lai. Cross-Reactivity of Select PEG-Binding Antibodies to Other Polymers Containing a C-C-O Backbone. *ACS Biomaterials Science & Engineering* **2017**, *3* (8), 1605-1615. DOI: 10.1021/acsbmaterials.7b00147
89. M. R. Sherman, L. D. Williams, M. A. Sobczyk, S. J. Michaels and M. G. P. Saifer. Role of the Methoxy Group in Immune Responses to mPEG-Protein Conjugates. *Bioconjugate Chemistry* **2012**, *23* (3), 485-499. DOI: 10.1021/bc200551b
-

-
90. M. T. Nguyen, Y. C. Shih, M. H. Lin, S. R. Roffler, C. Y. Hsiao, T. L. Cheng, W. W. Lin, E. C. Lin, Y. J. Jong, C. Y. Chang and Y. C. Su. Structural determination of an antibody that specifically recognizes polyethylene glycol with a terminal methoxy group. *Commun Chem* **2022**, 5 (1), 88. DOI: 10.1038/s42004-022-00709-0
91. C. C. Lee, Y. C. Su, T. P. Ko, L. L. Lin, C. Y. Yang, S. S. Chang, S. R. Roffler and A. H. Wang. Structural basis of polyethylene glycol recognition by antibody. *J Biomed Sci* **2020**, 27 (1), 12. DOI: 10.1186/s12929-019-0589-7
92. Y. C. Su, P. A. Burnouf, K. H. Chuang, B. M. Chen, T. L. Cheng and S. R. Roffler. Conditional internalization of PEGylated nanomedicines by PEG engagers for triple negative breast cancer therapy. *Nat Commun* **2017**, 8, 15507. DOI: 10.1038/ncomms15507
93. J. K. Armstrong, R. B. Wenby, H. J. Meiselman and T. C. Fisher. The hydrodynamic radii of macromolecules and their effect on red blood cell aggregation. *Biophys J* **2004**, 87 (6), 4259-4270. DOI: 10.1529/biophysj.104.047746
94. S. Tenzer, D. Docter, S. Rosfa, A. Wlodarski, J. Kuharev, A. Rekić, S. K. Knauer, C. Bantz, T. Nawroth, C. Bier, J. Sirirattanapan, W. Mann, L. Treuel, R. Zellner, M. Maskos, H. Schild and R. H. Stauber. Nanoparticle size is a critical physicochemical determinant of the human blood plasma corona: a comprehensive quantitative proteomic analysis. *ACS Nano* **2011**, 5 (9), 7155-7167. DOI: 10.1021/nn201950e
95. X. Zhang, H. Wang, Z. Ma and B. Wu. Effects of pharmaceutical PEGylation on drug metabolism and its clinical concerns. *Expert Opinion on Drug Metabolism & Toxicology* **2014**, 10 (12), 1691-1702. DOI: 10.1517/17425255.2014.967679
96. S. Jiang, D. Prozeller, J. Pereira, J. Simon, S. Han, S. Wirsching, M. Fichter, M. Mottola, I. Lieberwirth, S. Morsbach, V. Mailänder, S. Gehring, D. Crespy and K. Landfester. Controlling protein interactions in blood for effective liver immunosuppressive therapy by silica nanocapsules. *Nanoscale* **2020**, 12 (4), 2626-2637. DOI: 10.1039/c9nr09879h
97. S. Schöttler, K. Landfester and V. Mailänder. Controlling the Stealth Effect of Nanocarriers through Understanding the Protein Corona. *Angewandte Chemie International Edition* **2016**, 55 (31), 8806-8815. DOI: 10.1002/anie.201602233
98. X. Zhang, H. Wang, Z. Ma and B. Wu. Effects of pharmaceutical PEGylation on drug metabolism and its clinical concerns. *Expert Opin Drug Metab Toxicol* **2014**, 10 (12), 1691-1702. DOI: 10.1517/17425255.2014.967679
99. C. Zhou, J.-M. Friedt, A. Angelova, K.-H. Choi, W. Laureyn, F. Frederix, L. A. Francis, A. Campitelli, Y. Engelborghs and G. Borghs. Human Immunoglobulin Adsorption Investigated by Means of Quartz Crystal Microbalance Dissipation, Atomic Force Microscopy, Surface Acoustic Wave, and Surface Plasmon Resonance Techniques. *Langmuir* **2004**, 20 (14), 5870-5878. DOI: 10.1021/la036251d
100. P. D. Benech, K. Sastry, R. R. Iyer, Q. G. Eichbaum, D. P. Raveh and R. A. Ezekowitz. Definition of interferon gamma-response elements in a novel human Fc gamma receptor gene (Fc gamma RIb) and characterization of the gene structure. *J Exp Med* **1992**, 176 (4), 1115-1123. DOI: 10.1084/jem.176.4.1115

101. R. C. van Schie and M. E. Wilson. Evaluation of human Fcγ₂RIIA (CD32) and Fcγ₂RIIIB (CD16) polymorphisms in Caucasians and African-Americans using salivary DNA. *Clin Diagn Lab Immunol* **2000**, 7 (4), 676-681. DOI: 10.1128/cdli.7.4.676-681.2000
102. B. Bröker, C. Schütt and B. Fleischer, in *Grundwissen Immunologie*, eds. B. Bröker, C. Schütt and B. Fleischer, Springer Berlin Heidelberg, Berlin, Heidelberg, 2019, DOI: 10.1007/978-3-662-58330-2_10, pp. 115-141.
103. S. H. E. Kaufmann, in *Basiswissen Immunologie*, ed. S. H. E. Kaufmann, Springer Berlin Heidelberg, Berlin, Heidelberg, 2014, DOI: 10.1007/978-3-642-40325-5_8, pp. 63-83.
104. H. H. Gustafson, D. Holt-Casper, D. W. Grainger and H. Ghandehari. Nanoparticle Uptake: The Phagocyte Problem. *Nano Today* **2015**, 10 (4), 487-510. DOI: 10.1016/j.nantod.2015.06.006
105. H. Ma, K. Shiraishi, T. Minowa, K. Kawano, M. Yokoyama, Y. Hattori and Y. Maitani. Accelerated Blood Clearance Was Not Induced for a Gadolinium-Containing PEG-poly(L-lysine)-Based Polymeric Micelle in Mice. *Pharmaceutical Research* **2010**, 27 (2), 296-302, journal article. DOI: 10.1007/s11095-009-0018-9
106. C. Li, J. Cao, Y. Wang, X. Zhao, C. Deng, N. Wei, J. Yang and J. Cui. Accelerated blood clearance of pegylated liposomal topotecan: influence of polyethylene glycol grafting density and animal species. *J Pharm Sci* **2012**, 101 (10), 3864-3876. DOI: 10.1002/jps.23254
107. R. Saadati, S. Dadashzadeh, Z. Abbasian and H. Soleimanjahi. Accelerated Blood Clearance of PEGylated PLGA Nanoparticles Following Repeated Injections: Effects of Polymer Dose, PEG Coating, and Encapsulated Anticancer Drug. *Pharmaceutical Research* **2013**, 30 (4), 985-995, journal article. DOI: 10.1007/s11095-012-0934-y
108. X. Wang, T. Ishida and H. Kiwada. Anti-PEG IgM elicited by injection of liposomes is involved in the enhanced blood clearance of a subsequent dose of PEGylated liposomes. *J Control Release* **2007**, 119 (2), 236-244. DOI: 10.1016/j.jconrel.2007.02.010
109. T. Ishida, M. Ichihara, X. Wang, K. Yamamoto, J. Kimura, E. Majima and H. Kiwada. Injection of PEGylated liposomes in rats elicits PEG-specific IgM, which is responsible for rapid elimination of a second dose of PEGylated liposomes. *J Control Release* **2006**, 112 (1), 15-25. DOI: 10.1016/j.jconrel.2006.01.005
110. K. Shiraishi, M. Hamano, H. Ma, K. Kawano, Y. Maitani, T. Aoshi, K. J. Ishii and M. Yokoyama. Hydrophobic blocks of PEG-conjugates play a significant role in the accelerated blood clearance (ABC) phenomenon. *J Control Release* **2013**, 165 (3), 183-190. DOI: 10.1016/j.jconrel.2012.11.016
111. H. Freire Haddad, J. A. Burke, E. A. Scott and G. A. Ameer. Clinical Relevance of Pre-Existing and Treatment-Induced Anti-Poly(Ethylene Glycol) Antibodies. *Regen Eng Transl Med* **2022**, 8 (1), 32-42. DOI: 10.1007/s40883-021-00198-y
112. B. Bröker, C. Schütt and B. Fleischer, *Grundwissen Immunologie*, 2019.

-
113. Z. H. Zhou, C. A. Stone, Jr., B. Jakubovic, E. J. Phillips, G. Sussman, J. Park, U. Hoang, S. L. Kirshner, R. Levin and S. Kozłowski. Anti-PEG IgE in anaphylaxis associated with polyethylene glycol. *J Allergy Clin Immunol Pract* **2021**, 9 (4), 1731-1733 e1733. DOI: 10.1016/j.jaip.2020.11.011
114. F. Giulimondi, E. Vulpis, L. Digiacomio, M. V. Giuli, A. Mancusi, A. L. Capriotti, A. Lagana, A. Cerrato, R. Zenezini Chiozzi, C. Nicoletti, H. Amenitsch, F. Cardarelli, L. Masuelli, R. Bei, I. Screpanti, D. Pozzi, A. Zingoni, S. Checquolo and G. Caracciolo. Opsonin-Deficient Nucleoproteic Corona Endows UnPEGylated Liposomes with Stealth Properties In Vivo. *ACS Nano* **2022**, 16 (2), 2088-2100. DOI: 10.1021/acsnano.1c07687
115. J. Simon, T. Wolf, K. Klein, K. Landfester, F. R. Wurm and V. Mailander. Hydrophilicity Regulates the Stealth Properties of Polyphosphoester-Coated Nanocarriers. *Angew Chem Int Ed Engl* **2018**, 57 (19), 5548-5553. DOI: 10.1002/anie.201800272
116. L. L. Hecht, A. Schoth, R. Muñoz-Espí, A. Javadi, K. Köhler, R. Miller, K. Landfester and H. P. Schuchmann. Determination of the Ideal Surfactant Concentration in Miniemulsion Polymerization. *Macromolecular Chemistry and Physics* **2013**, 214 (7), 812-823. DOI: 10.1002/macp.201200583
117. K. Landfester, in *Colloid Chemistry II*, ed. M. Antonietti, Springer Berlin Heidelberg, Berlin, Heidelberg, 2003, DOI: 10.1007/3-540-36412-9_4, pp. 75-123.
118. K. N. Bauer, H. T. Tee, M. M. Velencoso and F. R. Wurm. Main-chain poly(phosphoester)s: History, syntheses, degradation, bio- and flame-retardant applications. *Progress in Polymer Science* **2017**, 73, 61-122. DOI: <https://doi.org/10.1016/j.progpolymsci.2017.05.004>
119. B. Kang, P. Okwieka, S. Schottler, S. Winzen, J. Langhanki, K. Mohr, T. Opatz, V. Mailander, K. Landfester and F. R. Wurm. Carbohydrate-Based Nanocarriers Exhibiting Specific Cell Targeting with Minimum Influence from the Protein Corona. *Angew Chem Int Ed Engl* **2015**, 54 (25), 7436-7440. DOI: 10.1002/anie.201502398
120. G. Baier, D. Baumann, J. M. Siebert, A. Musyanovych, V. Mailänder and K. Landfester. Suppressing Unspecific Cell Uptake for Targeted Delivery Using Hydroxyethyl Starch Nanocapsules. *Biomacromolecules* **2012**, 13 (9), 2704-2715. DOI: 10.1021/bm300653v
121. M. Bauer, C. Lautenschlaeger, K. Kempe, L. Tauhardt, U. S. Schubert and D. Fischer. Poly(2-ethyl-2-oxazoline) as Alternative for the Stealth Polymer Poly(ethylene glycol): Comparison of in vitro Cytotoxicity and Hemocompatibility. *Macromolecular Bioscience* **2012**, 12 (7), 986-998. DOI: <https://doi.org/10.1002/mabi.201200017>
122. H. Bludau, A. E. Czapar, A. S. Pitek, S. Shukla, R. Jordan and N. F. Steinmetz. POxylation as an alternative stealth coating for biomedical applications. *European Polymer Journal* **2017**, 88, 679-688. DOI: <https://doi.org/10.1016/j.eurpolymj.2016.10.041>

Appendix

Acknowledgments

Curriculum Vitae
